High-energy astrophysics and black holes.

Gustavo E. Romero

Instituto Argentino de Radioastronomía (IAR) and University of La Plata

March 3rd, 2019; ISAPP school 2019 @ the Pierre Auger Observatory.

General relativity: gravitation is a manifestation of the curvature of spacetime

Einstein's equations

Curvature of space

Distribution of mass/energy

$$G_{\alpha\beta} = \frac{8\pi G}{c^4} T_{\alpha\beta}$$

Some constants

$$G_{\alpha\beta} = R_{\alpha\beta} - \frac{1}{2} g_{\alpha\beta} R$$

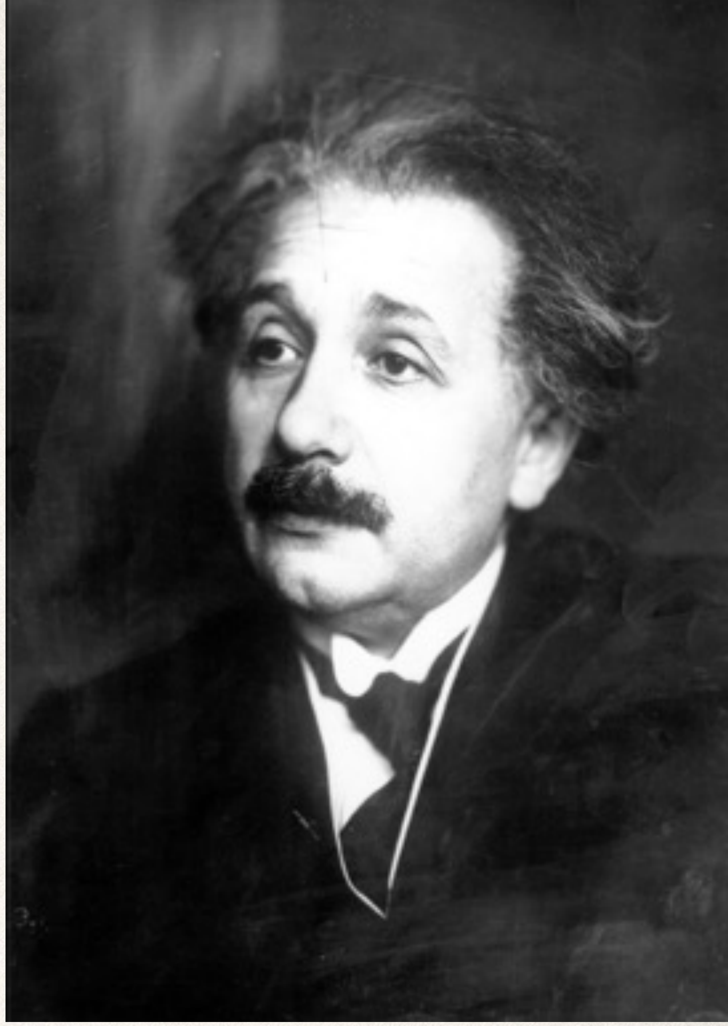

$$R_{\alpha\beta} - \frac{1}{2} g_{\alpha\beta} R = \frac{8\pi G}{c^4} T_{\alpha\beta}$$

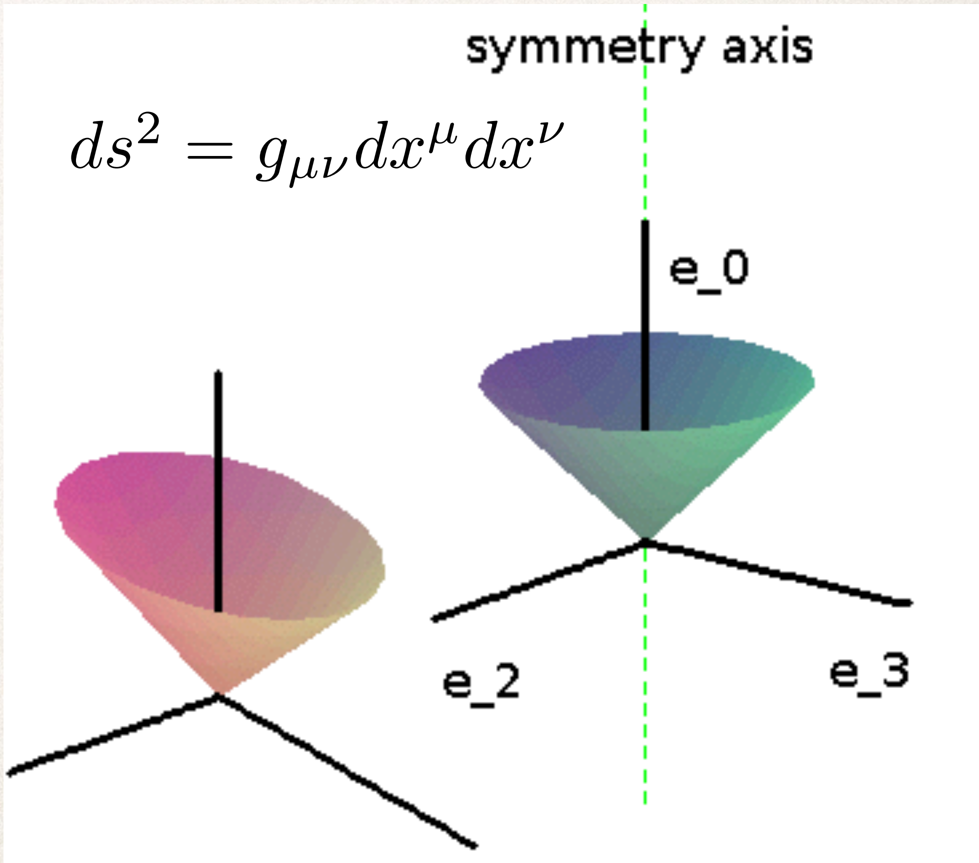

$$T_{\alpha\ ;\beta}^{\ \beta} = 0$$

dynamics of matter

A **black hole** is a spacetime region, i.e. what characterizes the black hole is its metric and its curvature. What is peculiar of this spacetime region is that it is causally disconnected from the rest of the spacetime: no events in this region cannot affect events outside the region.

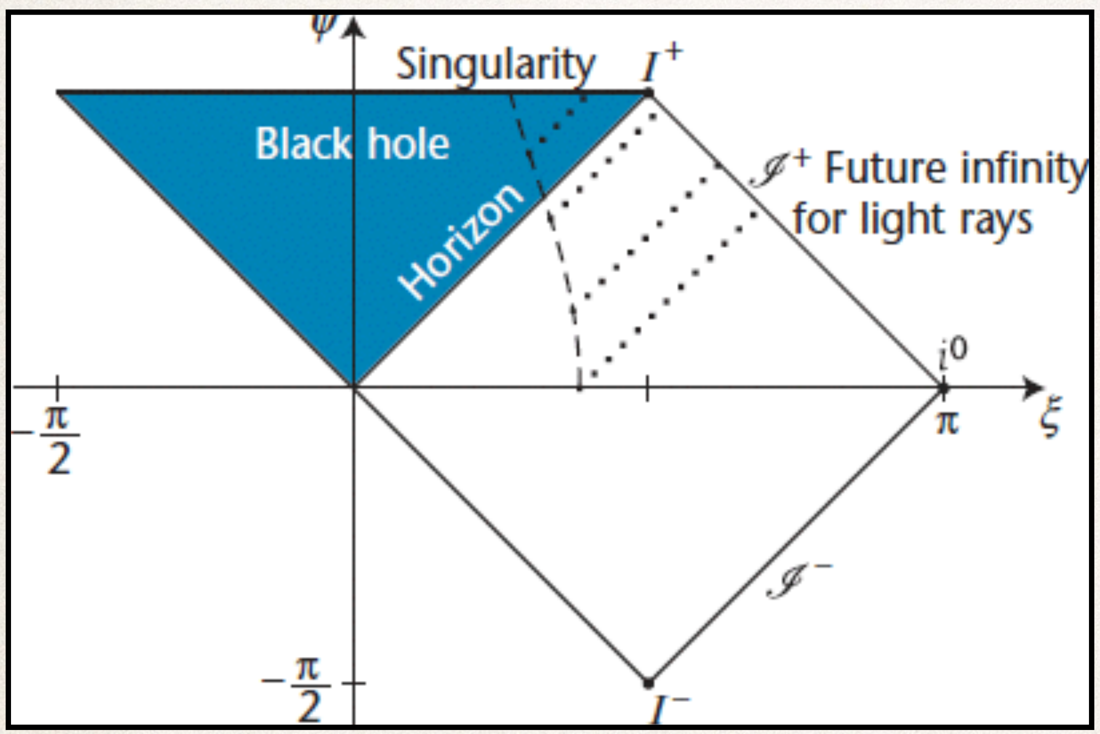

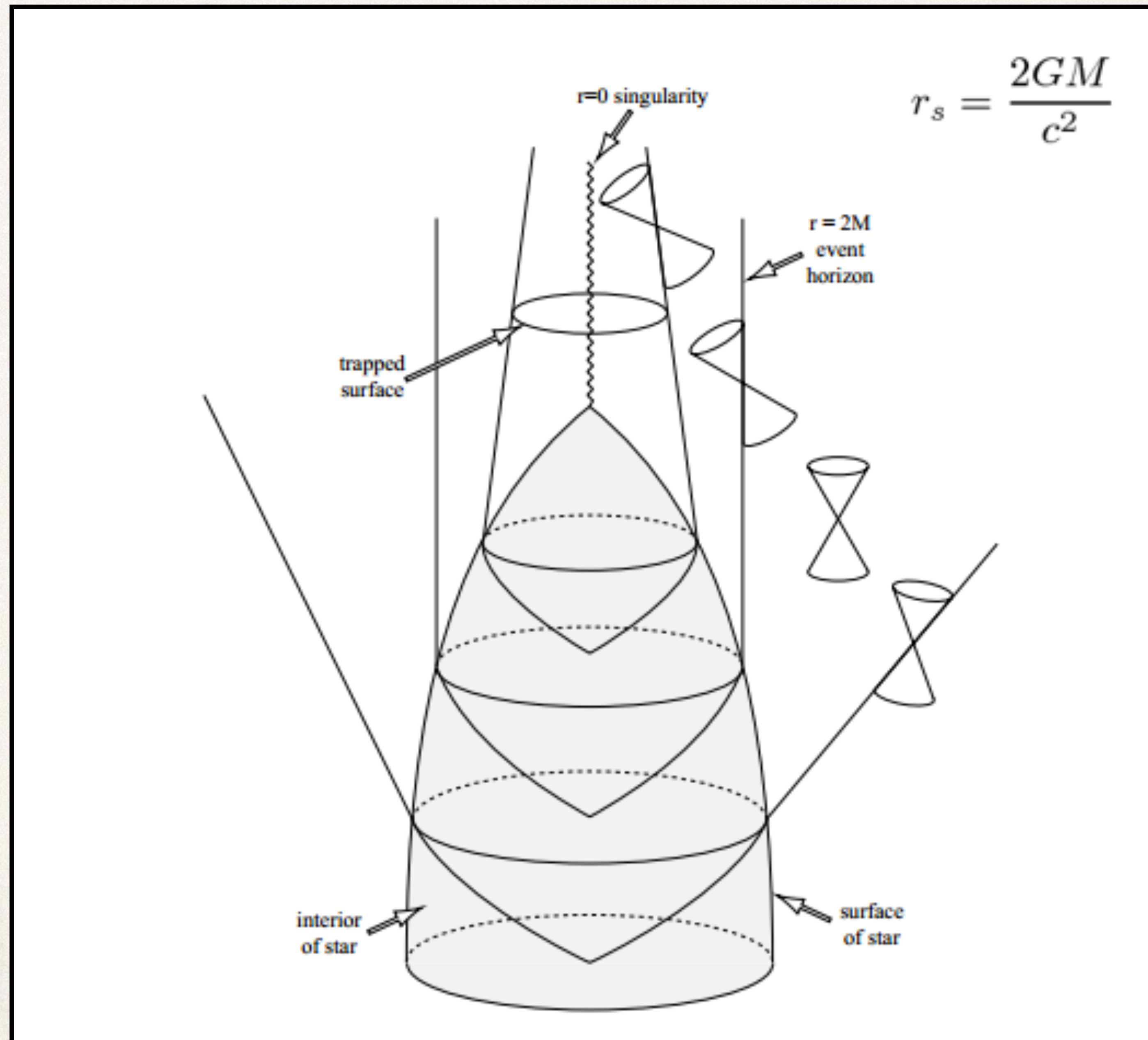

$$ds^2 = \left(1 - \frac{2GM}{rc^2}\right)c^2dt^2 - \left(1 - \frac{2GM}{rc^2}\right)^{-1}dr^2 - r^2(d\theta^2 + \sin^2\theta d\phi^2).$$

Axially symmetric black hole (Kerr)

$$
\begin{aligned}
ds^2 &= g_{tt}dt^2 + 2g_{t\phi}dtd\phi - g_{\phi\phi}d\phi^2 - \Sigma\Delta^{-1}dr^2 - \Sigma d\theta^2 \\
g_{tt} &= (c^2 - 2GMr\Sigma^{-1}) \\
g_{t\phi} &= 2GMac^{-2}\Sigma^{-1}r\sin^2\theta \\
g_{\phi\phi} &= [(r^2 + a^2c^{-2})^2 - a^2c^{-2}\Delta\sin^2\theta]\Sigma^{-1}\sin^2\theta \\
\Sigma &\equiv r^2 + a^2c^{-2}\cos^2\theta \\
\Delta &\equiv r^2 - 2GMc^{-2}r + a^2c^{-2}. \qquad a = J/M
\end{aligned}
$$

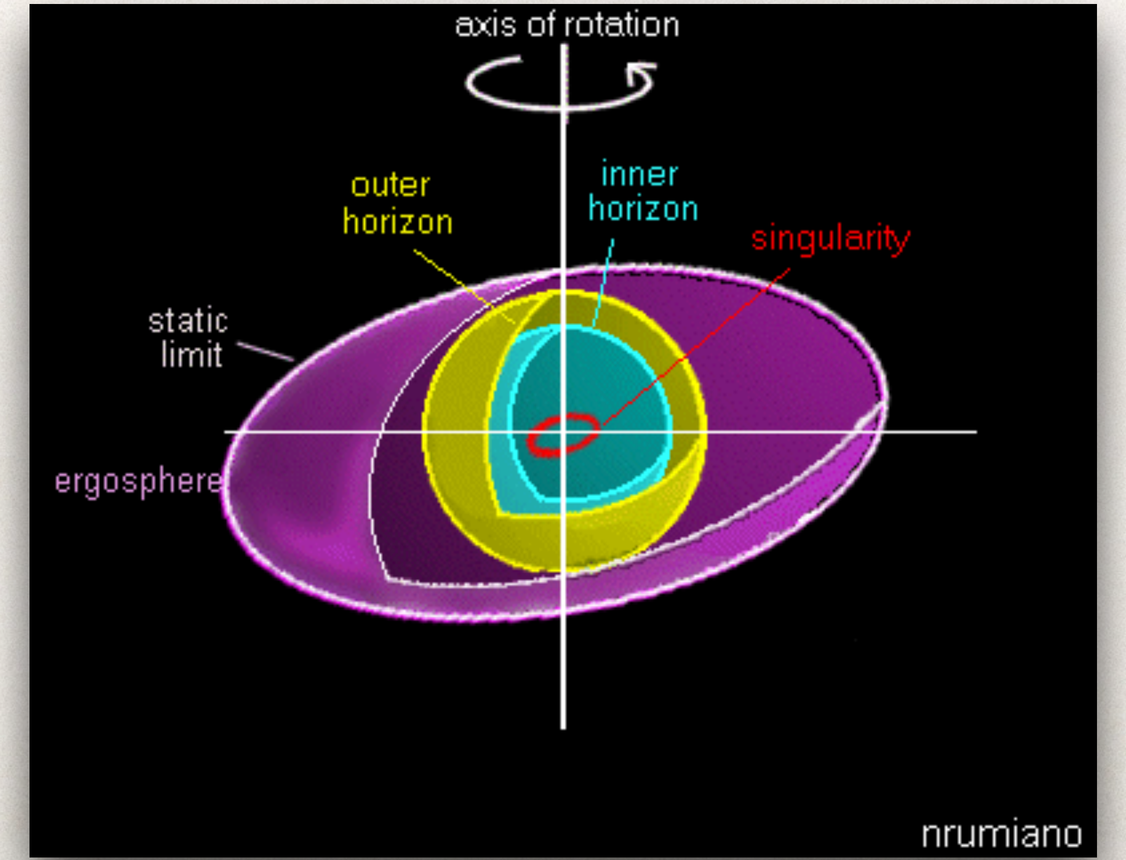

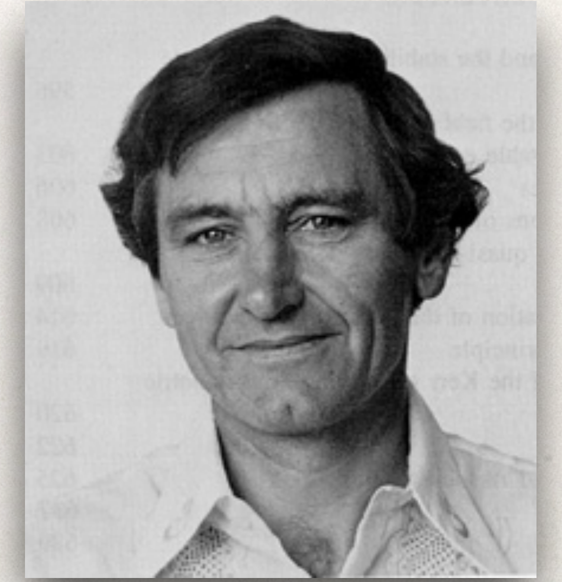

Roy Kerr

Kerr black hole

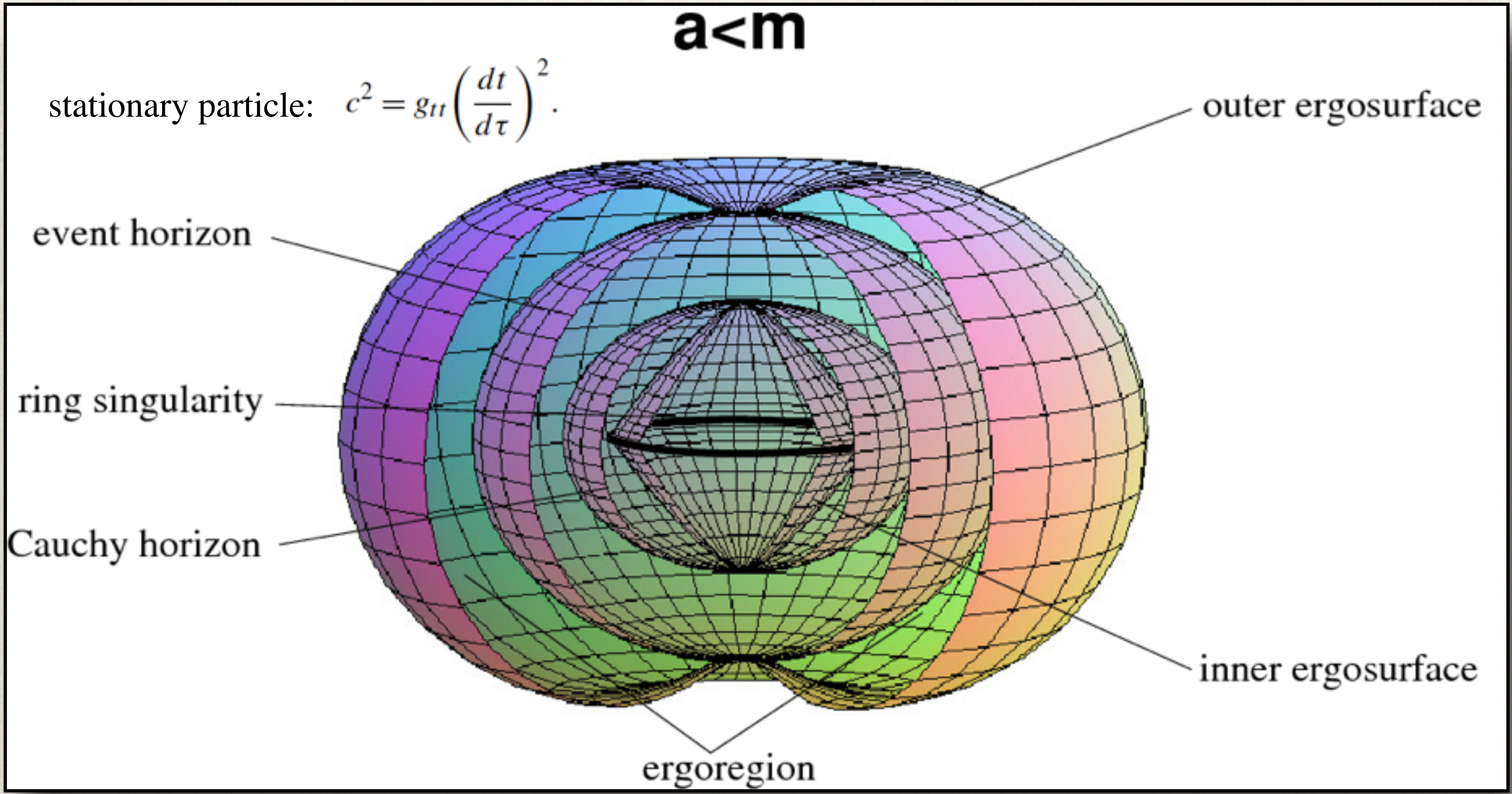

When $g_{tt} \leq 0$ the stationary condition cannot be fulfilled, and hence a massive particle cannot be stationary inside the surface defined by $g_{tt} = 0$ —> ergosphere

Back holes, nevertheless, can act on the external medium. This action can be done through the effects of gravitation. We distinguish several forms in which such action might occur:

- Accretion of matter and fields onto the black hole.
- Effects of the ergosphere.
- Tidal disruptions.
- Perturbation of spacetime (generation of gravitational waves).
- Generation of bow-shocks.
- Effects on background light.
- Effects on the CMB.
- Evaporation.

The idea of BH was not widely accepted until Lynden-Bell paper (1969) and the interpretation of the X-ray emission of binaries by accretion onto collapsed objects.

Standard disk model (Shakura & Sunyaev 1973): conservation of angular momentum leads to the formation of a disk around the BH. Energy is dissipated through radiation created by viscosity. Then angular momentum is removed and there is an inflow. If the disk is optically thick each ring radiates as a blackbody of different temperature.

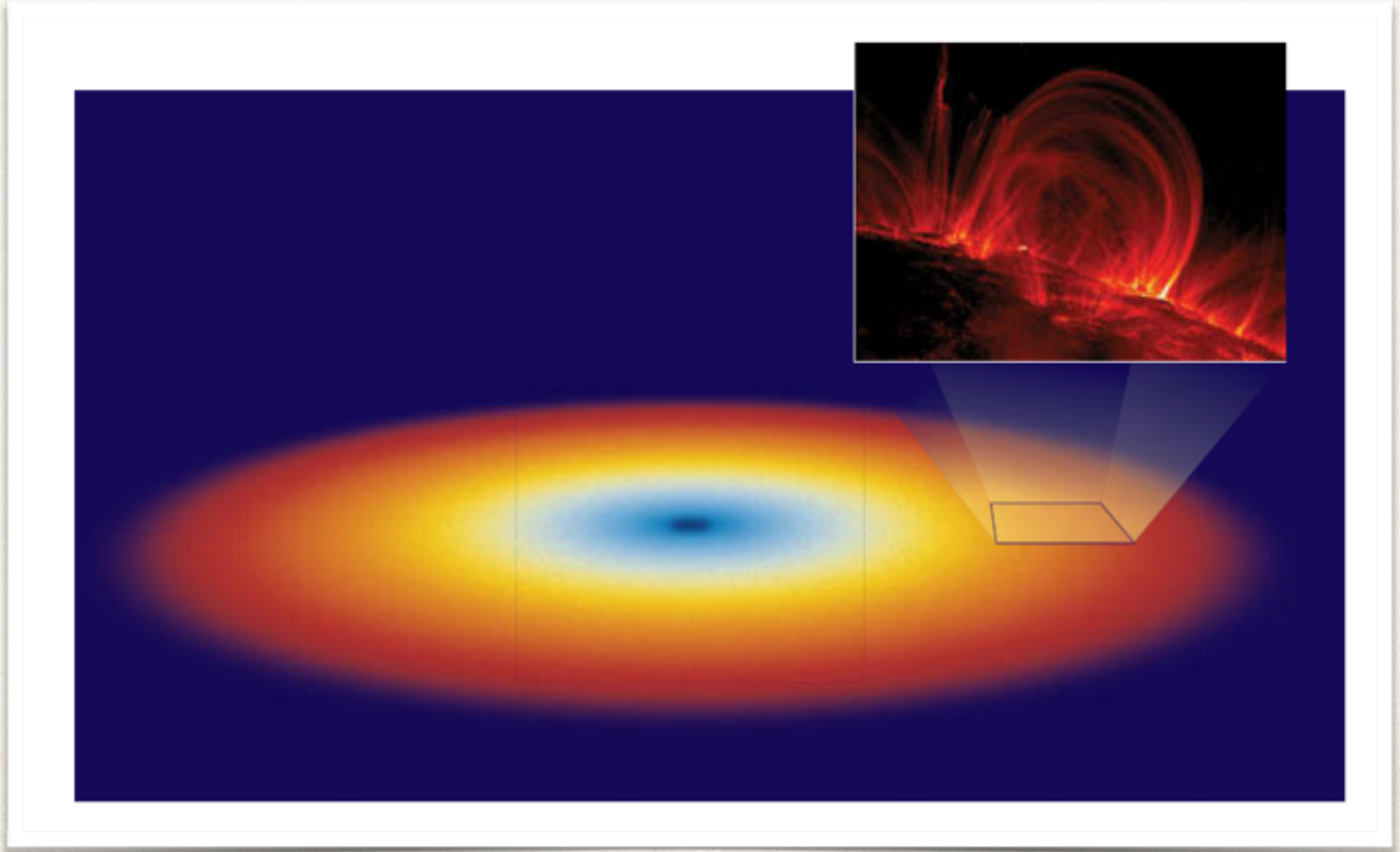

Basic equations for (thin) accretion disks

Simplifying assumptions:

1. The disk is axisymmetric, i.e. $\partial/\partial\varphi = 0$.
2. The disk is thin, i.e. its characteristic size scale in the z - axis is $H << R$.
3. The matter in the disk is in hydrostatic equilibrium in the z-direction.
4. The self-gravitation of the disk is negligible.

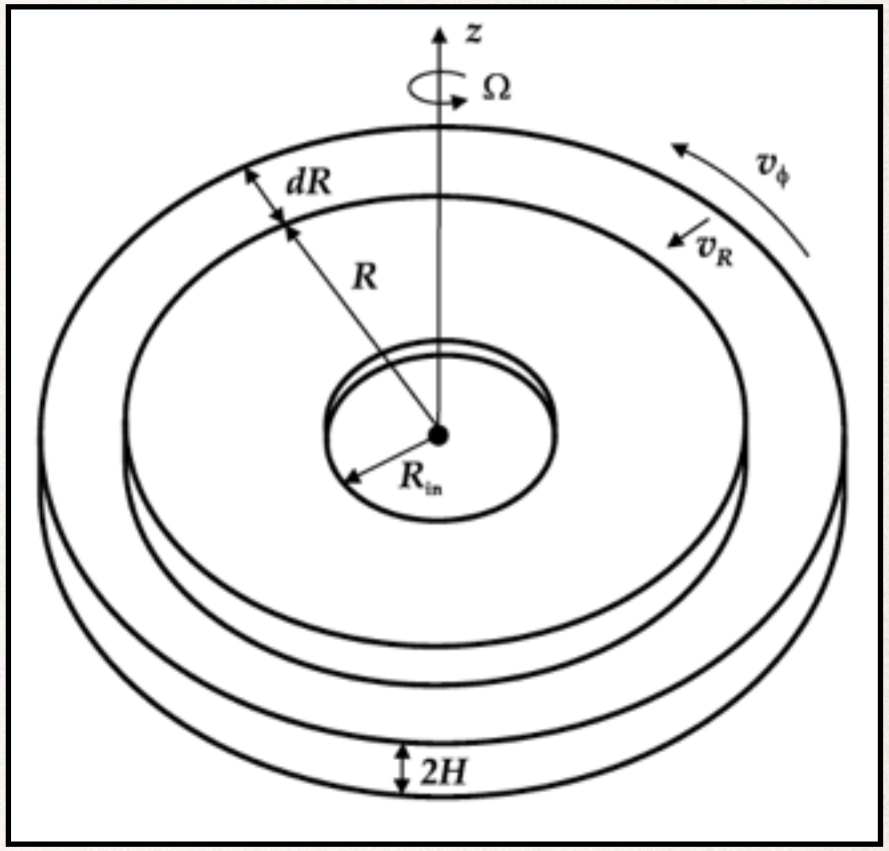

- Equation of continuity
- Equation of momentum transfer
- Energy dissipation in the disk
- Viscous stresses $\nu = \alpha a_{\rm s} H.$
- Equation of state $P = P_{\rm gas} + P_{\rm rad} = \frac{\rho k T}{\mu m_p} + \frac{4\sigma_{\rm SB}}{3c} T.$
- Opacity law $\kappa = \kappa\left(\rho, T\right).$
- Relation between electron and proton temperature.

Structure of the thin disks

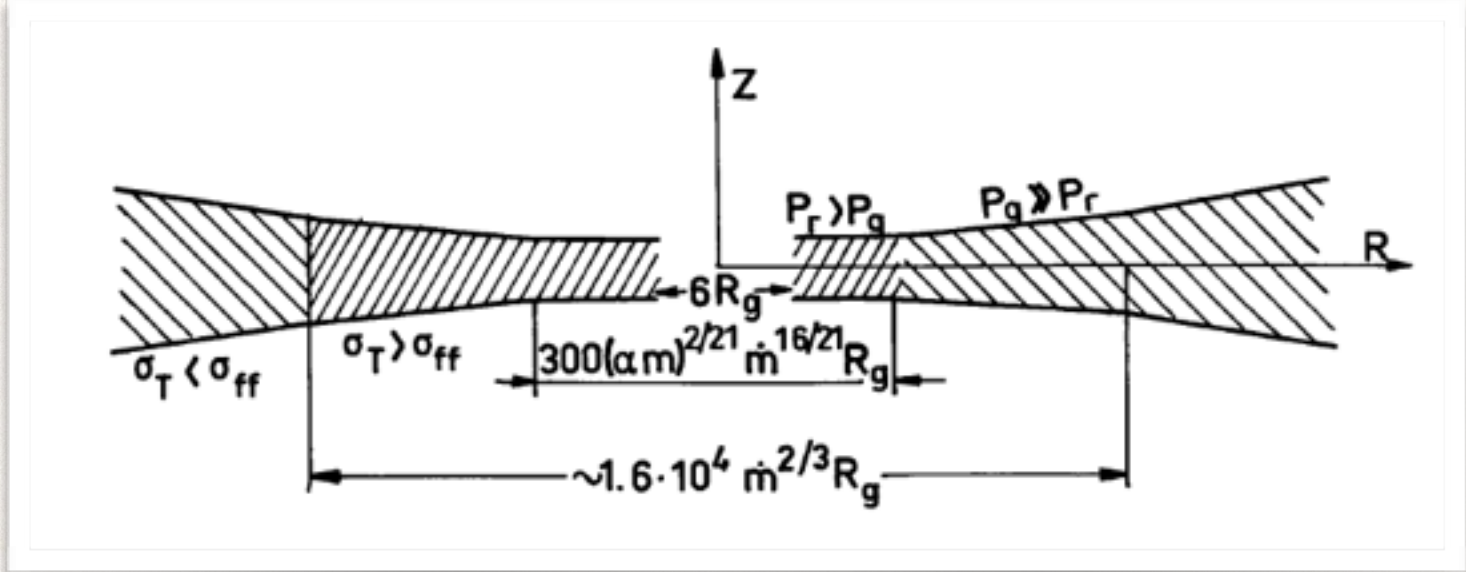

1. An outer region (large R) in which gas pressure dominates over radiation pressure and the opacity is due to free-free absorption.

2. A middle region (smaller R) in which gas pressure dominates over radiation pressure but opacity is due to Thomson scattering off electrons.

3. An inner region (small R) in which radiation pressure dominates over gas pressure and opacity is mainly due to scattering.

Thin accretion disk

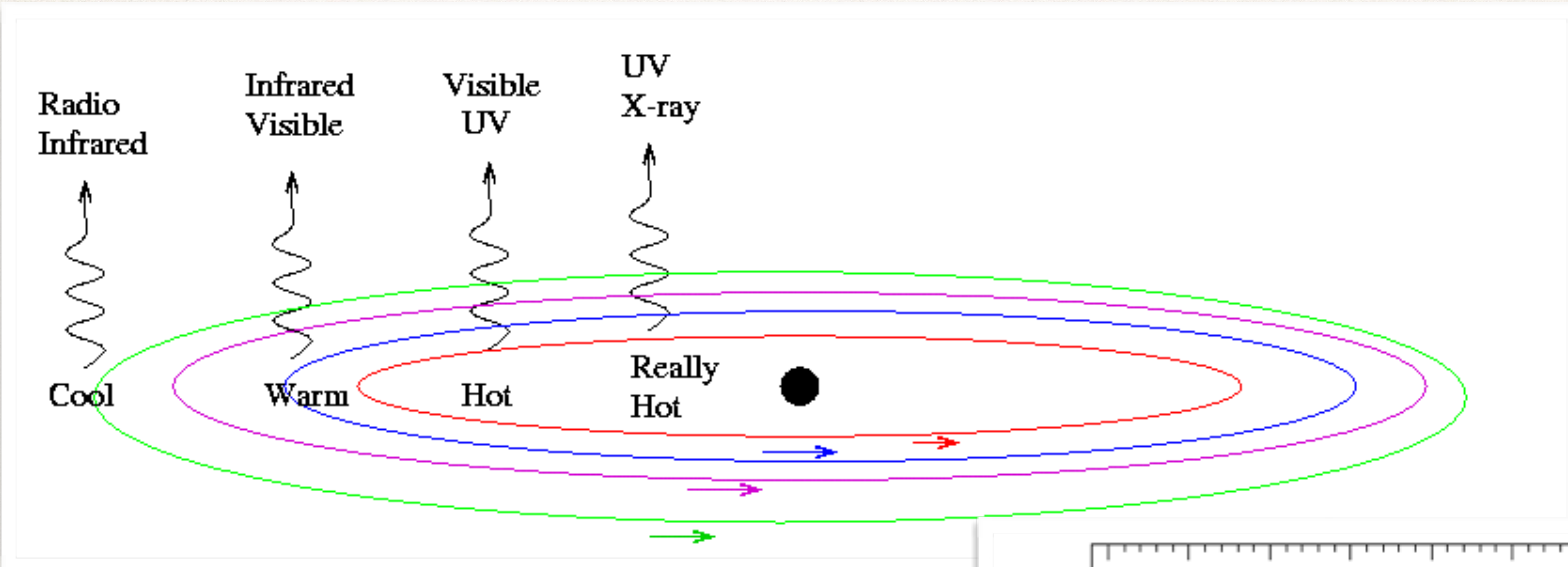

$$T(R) = \left[\frac{Q^+(R)}{\sigma_{SB}}\right]^{1/4} = \left(\frac{3GM\dot{M}}{8\pi\sigma_{SB}R^3}\right)^{1/4}\left(1-\sqrt{\frac{R_{in}}{R}}\right)^{1/4}.$$

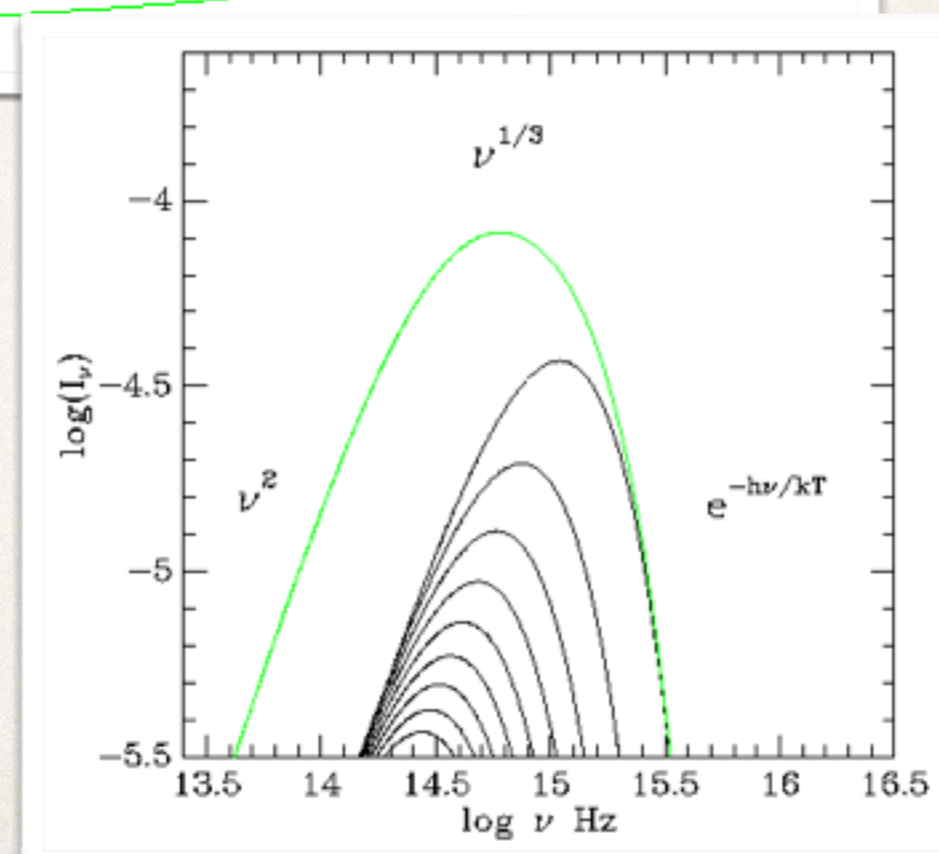

Spectrum

$$I_\nu(\nu,R) = B_\nu(\nu,R) \equiv \frac{2h\nu^3}{c^2[\exp(h\nu/kT)-1]}.$$

The total flux at frequency ν detected by an observer at a distance d whose line of sight forms and angle $\theta_{\rm d}$ with the normal to the disk is:

$$F_\nu(\nu) = \frac{\cos\theta_{\rm d}}{d^2}\int_{R_{\rm in}}^{R_{\rm out}} 2\pi\, R\, I_\nu\, dR.$$

The flux grows as $F_\nu \propto \nu^2$ for photon energies $h\nu \ll kT(R_{\rm out})$, and decreases exponentially for $h\nu \gg kT(R_{\rm in})$. For intermediate energies the spectrum has the characteristic dependence $F_\nu \propto \nu^{1/3}$. As $T(R_{\rm out})$ approaches $T(R_{\rm in})$ this part of the spectrum narrows, and it becomes similar to that of a simple blackbody.

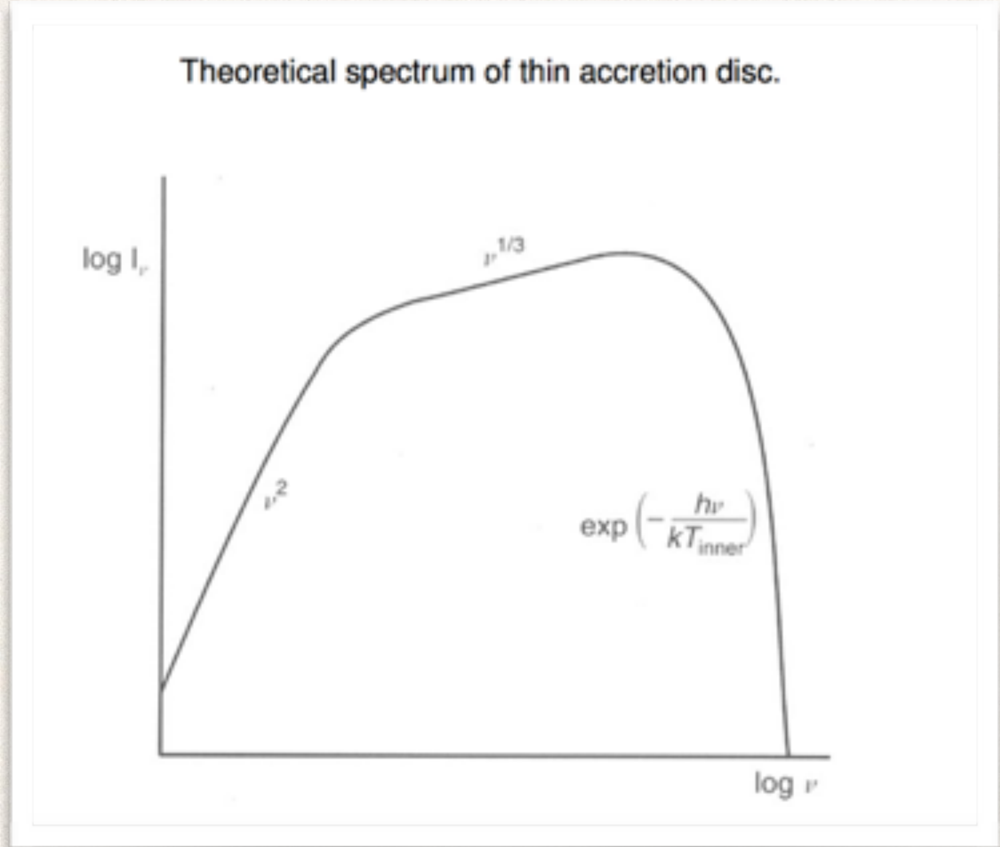

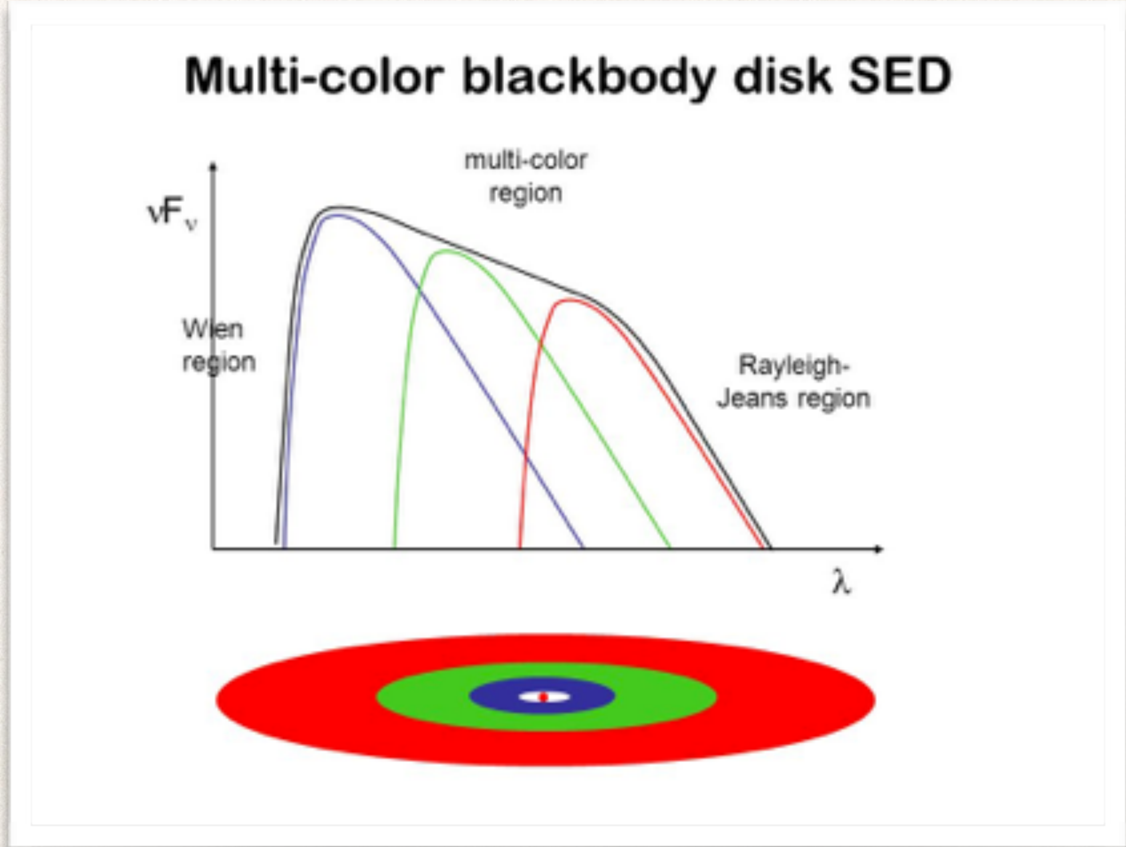

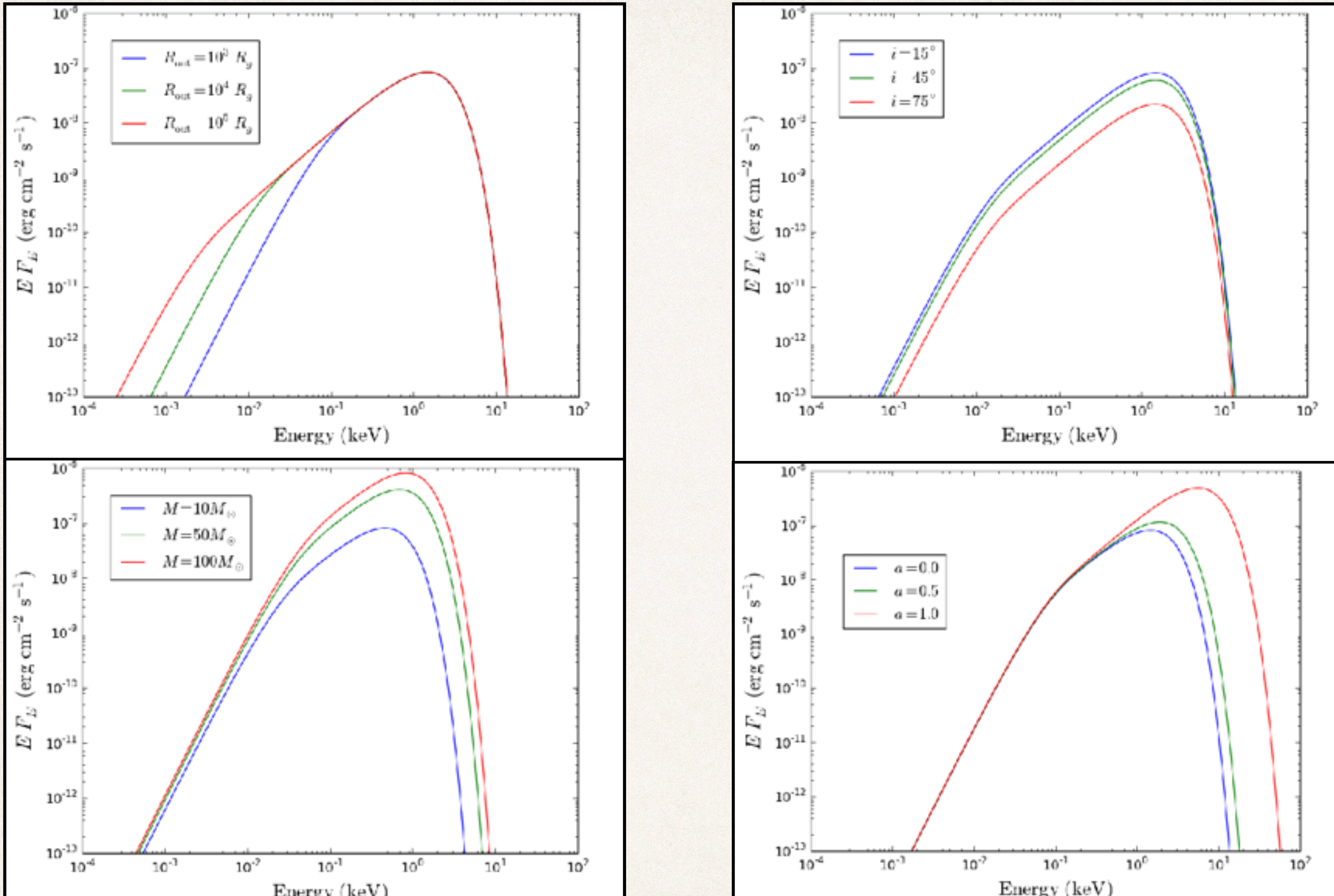

Changes in the accretion disk spectrum with different parameters

Diagnostics through Fe K-alpha lines

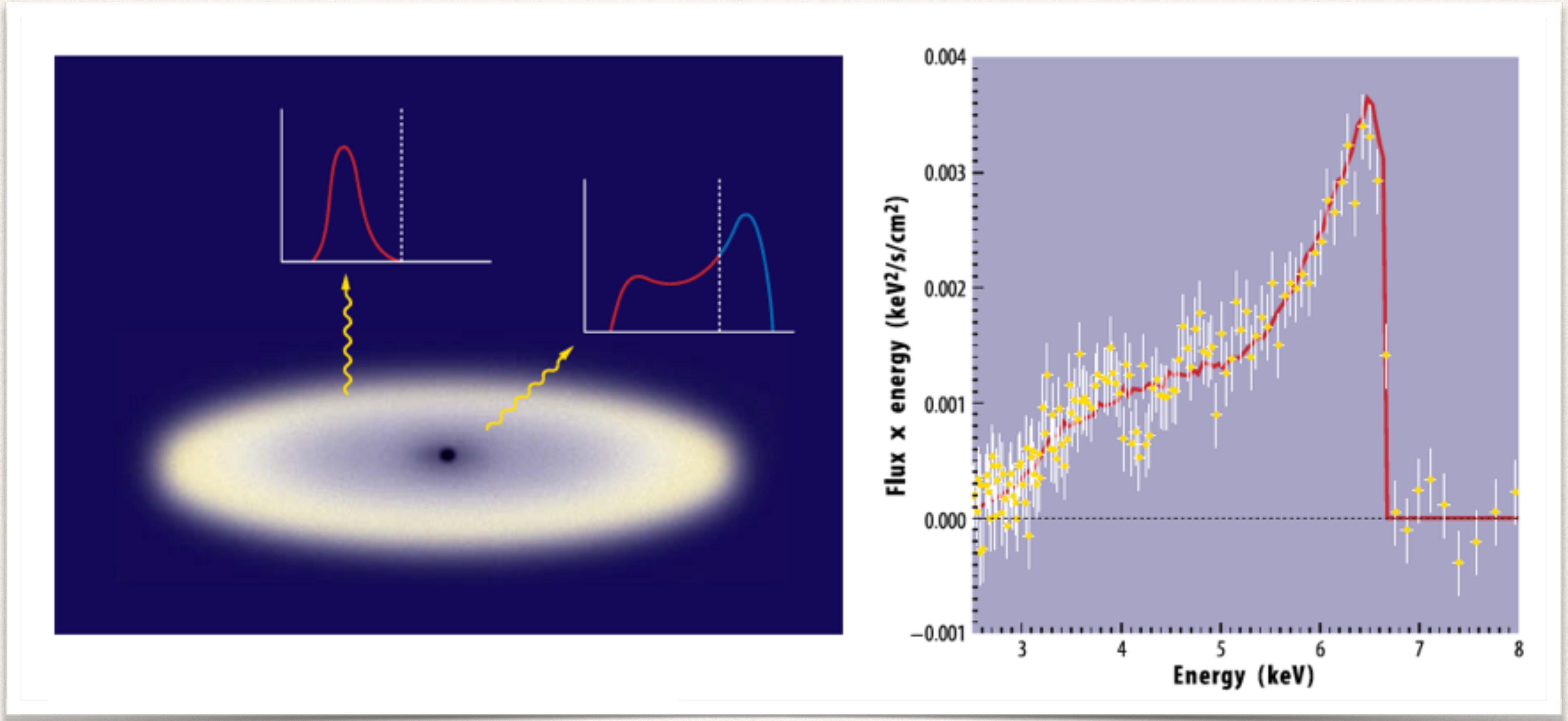

It is possible to determine the spin parameter *a*

$$r_{\rm isco} = \frac{GM}{c^2}\left(3 + Z_2 \pm \sqrt{(3 - Z_1)(3 + Z_1 + 2Z_2)}\right)$$

$$Z_1 = 1 + (1 - x^2)^{1/3}\left[(1+x)^{1/3} + (1-x)^{1/3}\right]$$

$$Z_2 = \sqrt{3x^2 + Z_1^2} \qquad x = a/M$$

The spectrum of X-ray binaries is more complex: more components

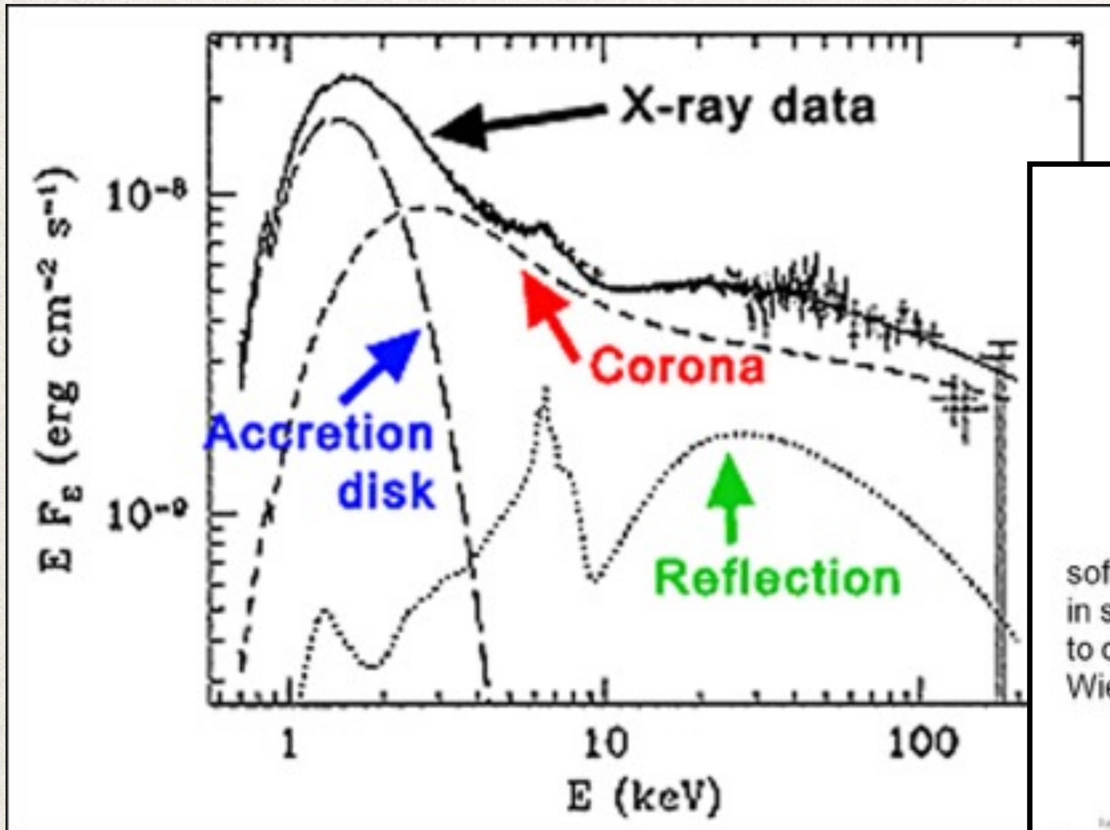

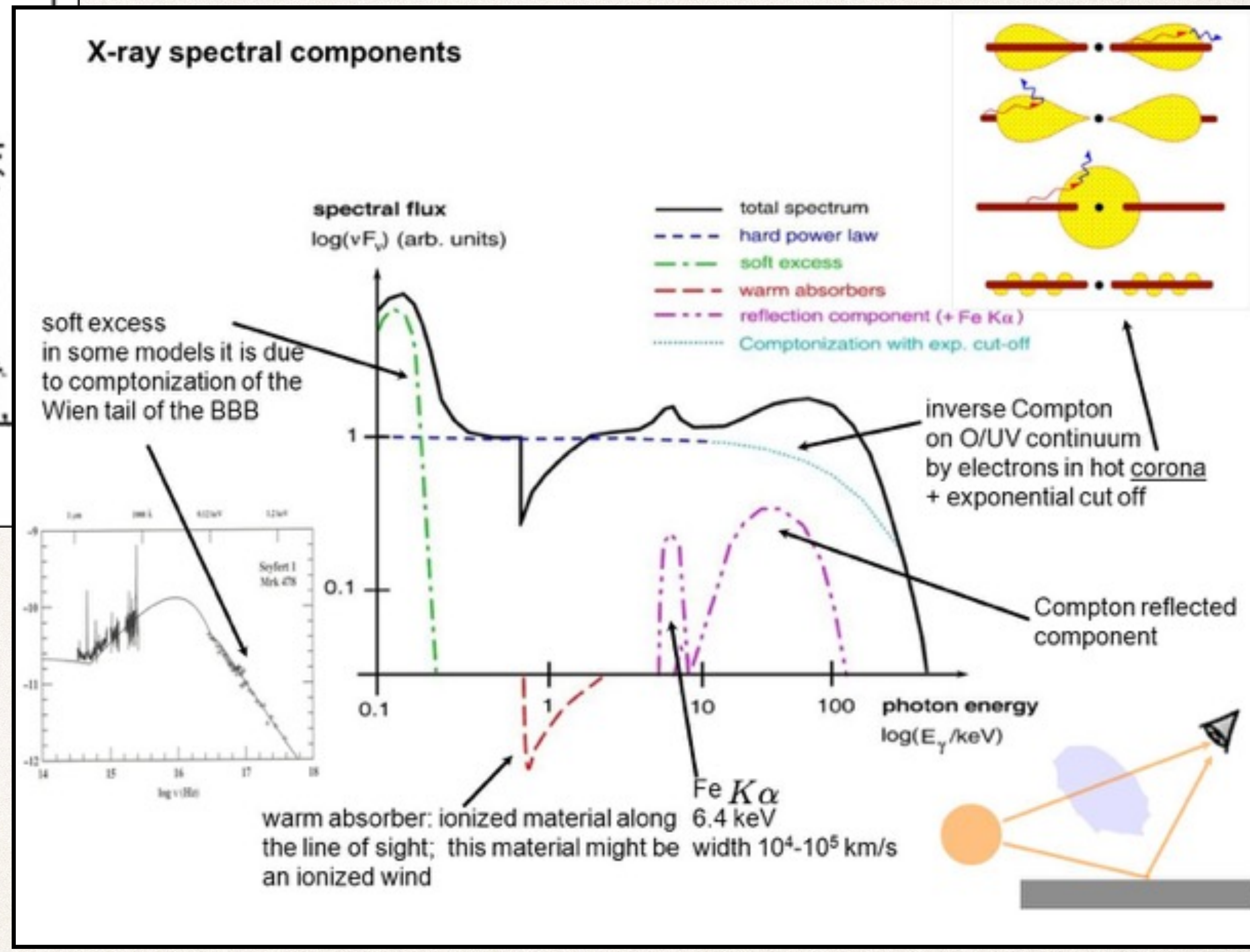

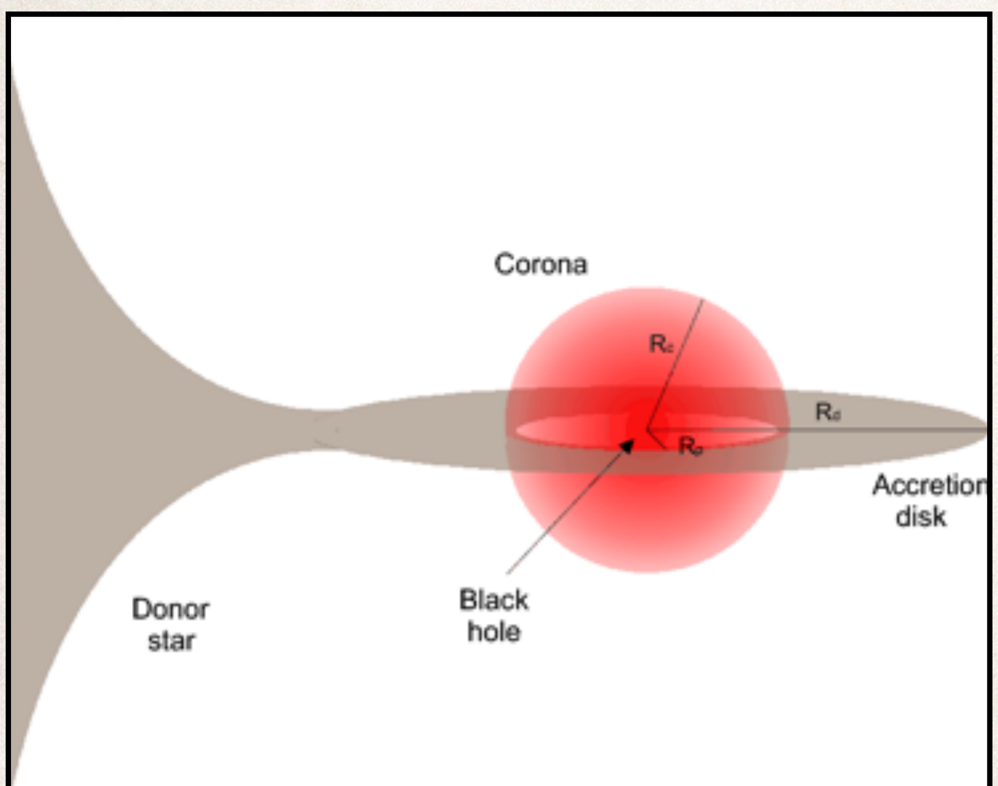

Eddington limits

The Eddington luminosity, also referred to as the Eddington limit, is the maximum luminosity that can be achieved when there is balance between the force of radiation acting outward and the gravitational force acting inward. The state of balance is called hydrostatic equilibrium.

$$L_{\rm Edd} = \frac{4\pi G M m_{\rm p} c}{\sigma_{\rm T}}$$
$$\cong 1.26\times 10^{31}\left(\frac{M}{M_\odot}\right)\,{\rm W} = 1.26\times 10^{38}\left(\frac{M}{M_\odot}\right)\,{\rm erg/s} = 3.2\times 10^{4}\left(\frac{M}{M_\odot}\right) L_\odot$$

$$\dot{M}_{\rm Edd} = \frac{L_{\rm Edd}}{c^2} \approx 0.2\times 10^{-8}\left(\frac{M}{M_\odot}\right)\; M_\odot\;{\rm yr}^{-1}.$$

$$T_{\rm Edd} = \left(\frac{L_{\rm Edd}}{4\pi\sigma_{\rm SB} R^2_{\rm Schw}}\right) \approx 6.6\times 10^{7}\left(\frac{M}{M_\odot}\right)^{-1/4}\;{\rm K}.$$

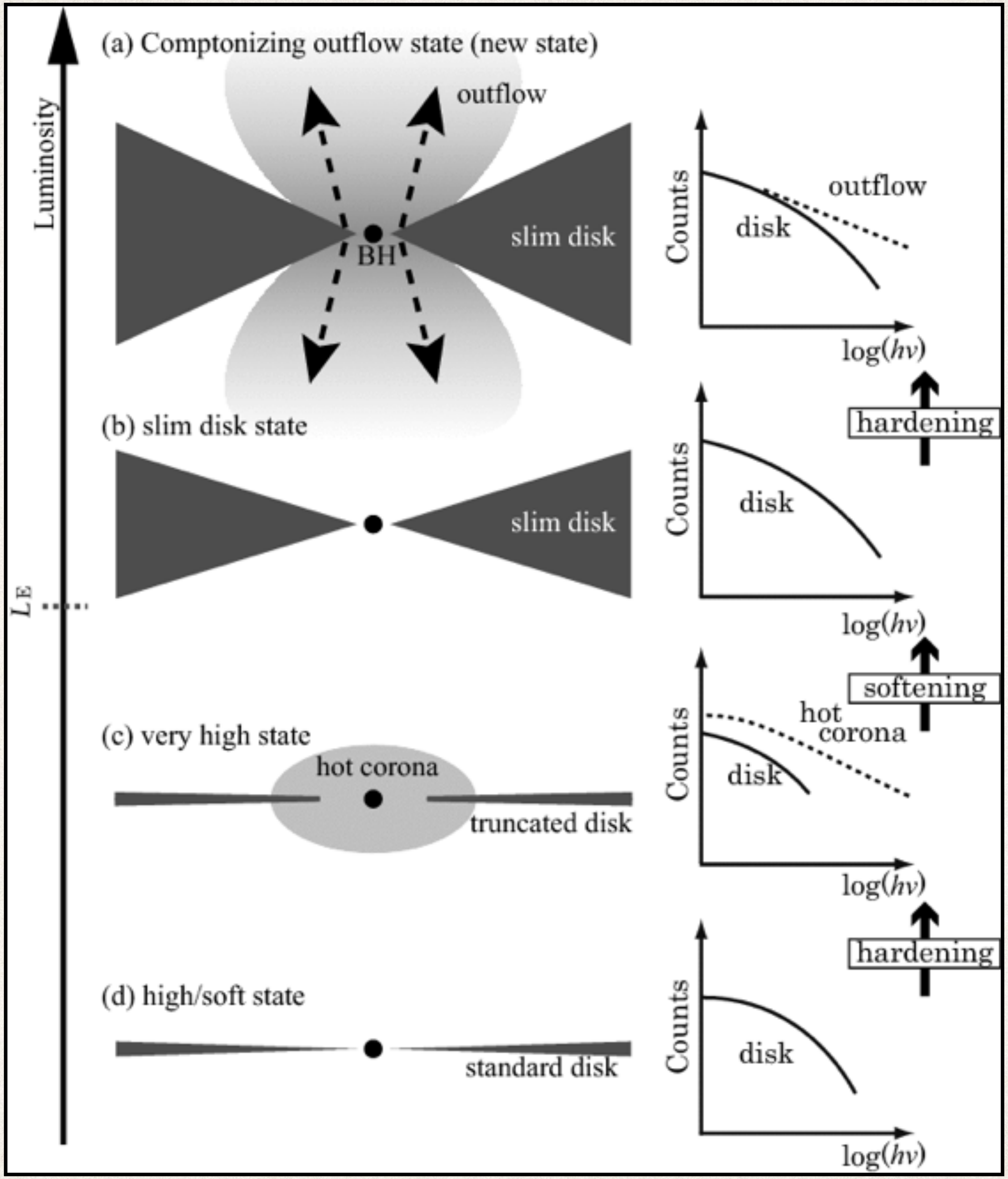

The super-Eddington wind is driven by radiation pressure.

ADAF

The assumption that all the heat generated by viscosity is radiated away does not hold for all accretion rates. Under some conditions the radial velocity of the accretion flow becomes large and the heat cannot be transformed into radiation and emitted fast enough. A significant fraction of the heat is stored as kinetic energy in the flow and advected onto the accretor. At the same time the disk "inflates", so that the thin disk assumption breaks down. This regime is known as "Advected Dominated Accretion Flow" (ADAF).

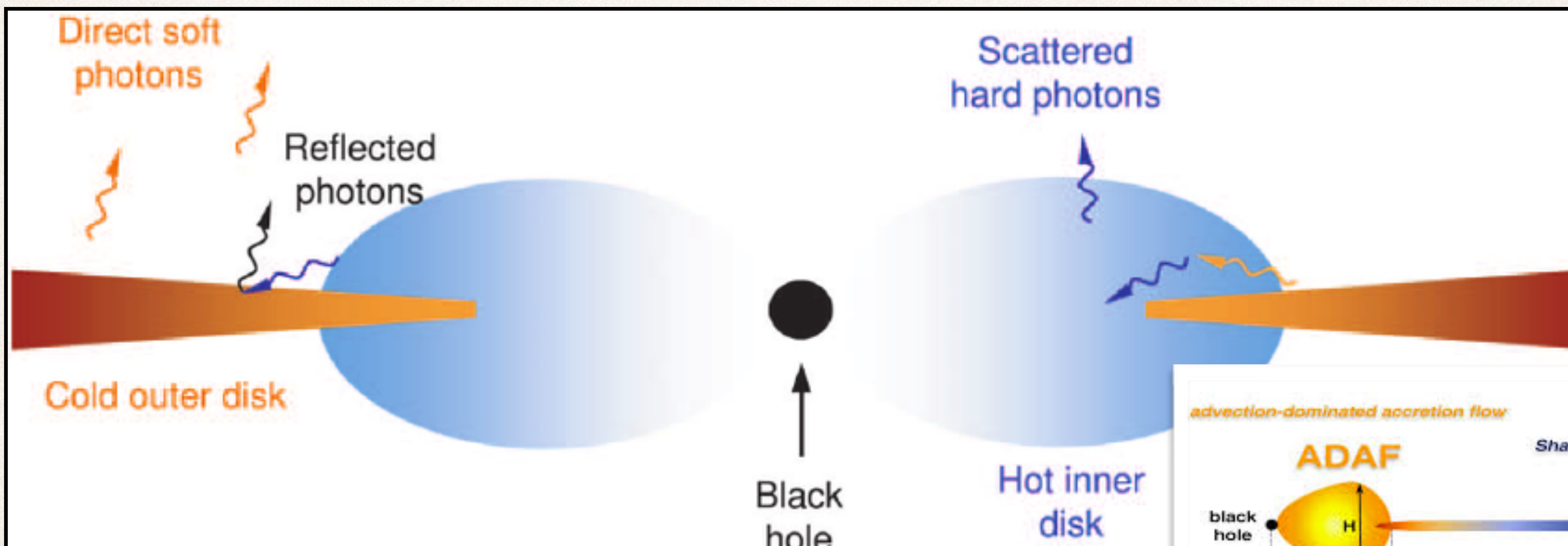

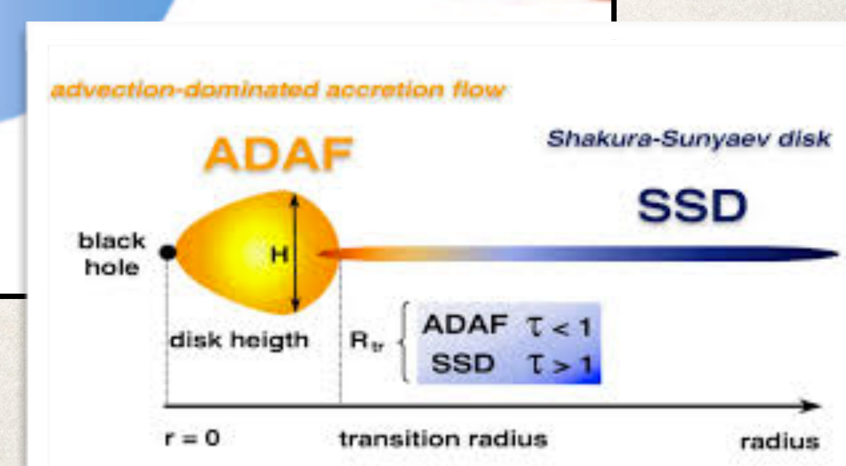

ADAF

There are two types of advection-dominated accretion flows. Optically thick ADAFs develop at very high accretion rates, typically larger than the Eddington value. In this limit the radiation gets trapped in the accretion flow and is advected because the optical depth is very large.

Optically thin ADAFs occur in the opposite limit of sufficiently low accretion rates. In this regime the cooling timescale of the flow is longer than the accretion timescale, resulting again in a significant fraction of the energy being advected. These models are similar to the disk + corona models.

Super-Eddignton

Sub-Eddignton

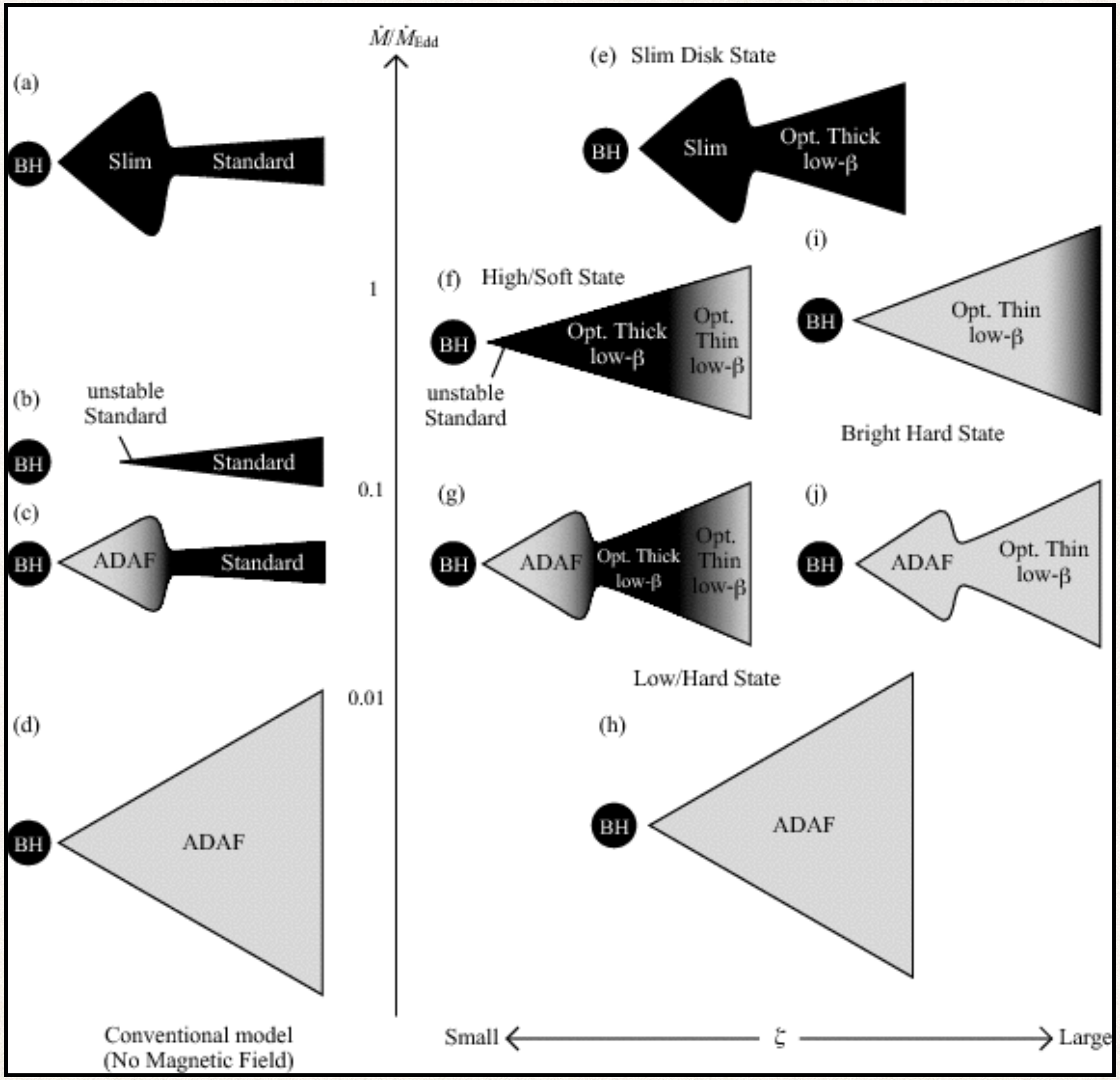

Main ADAF assumptions:

- The total pressure is considered as the sum of the pressure of a two-temperature gas and the magnetic pressure.
- The heat generated by viscosity is preferably transferred to ions. Hence, $T_i >> T_e$
- Electrons cool completely.

$$q_e^- = q_{\rm Br}^- + q_{\rm synchr}^- + q_{\rm IC}^-.$$

$$q_{\rm IC}^- = q_{\rm IC,Br}^- + q_{\rm IC,\ synchr}^- + q_{\rm IC,ext}^-.$$

→

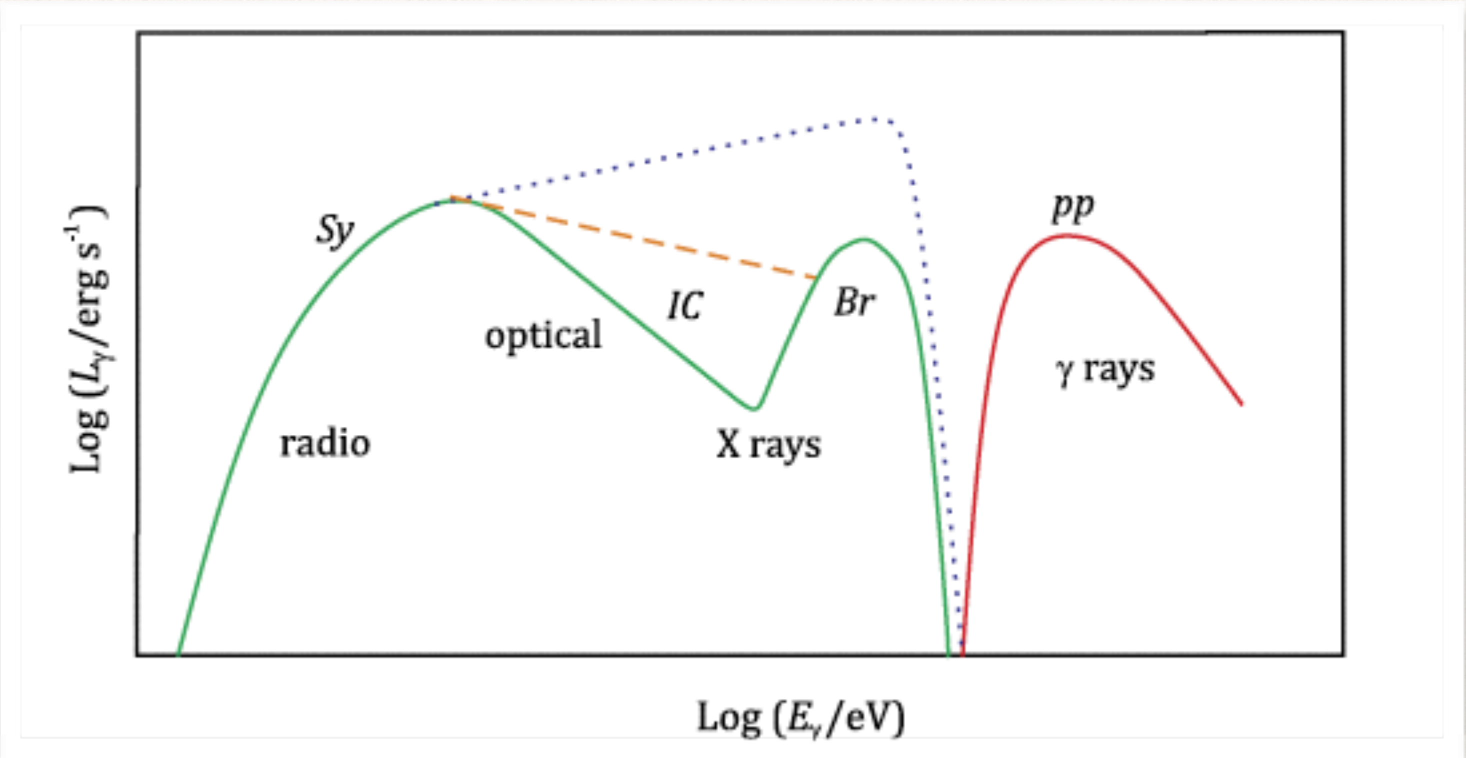

The spectrum of AGNs extends along the whole e.m. range: there is non-thermal emission

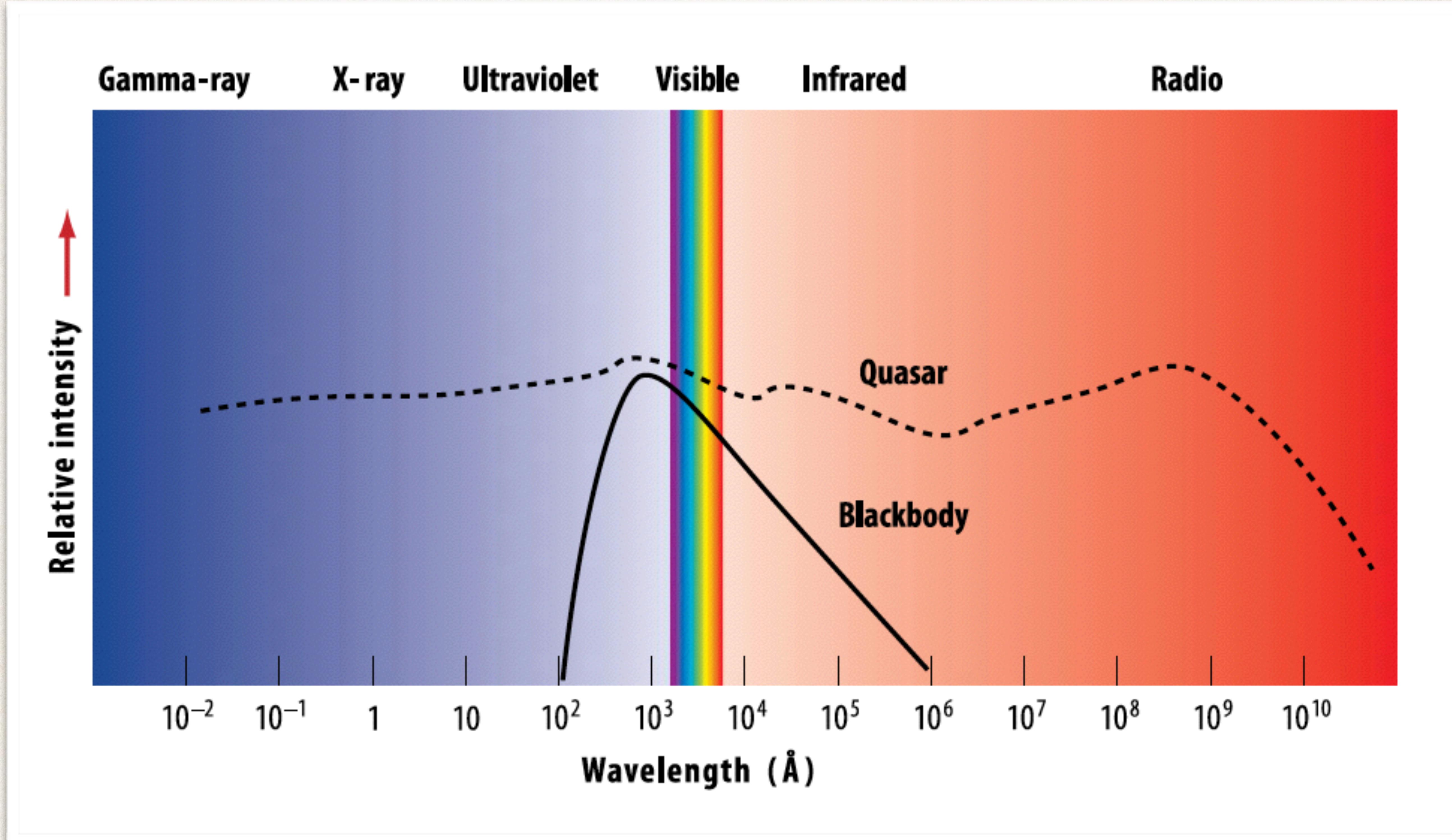

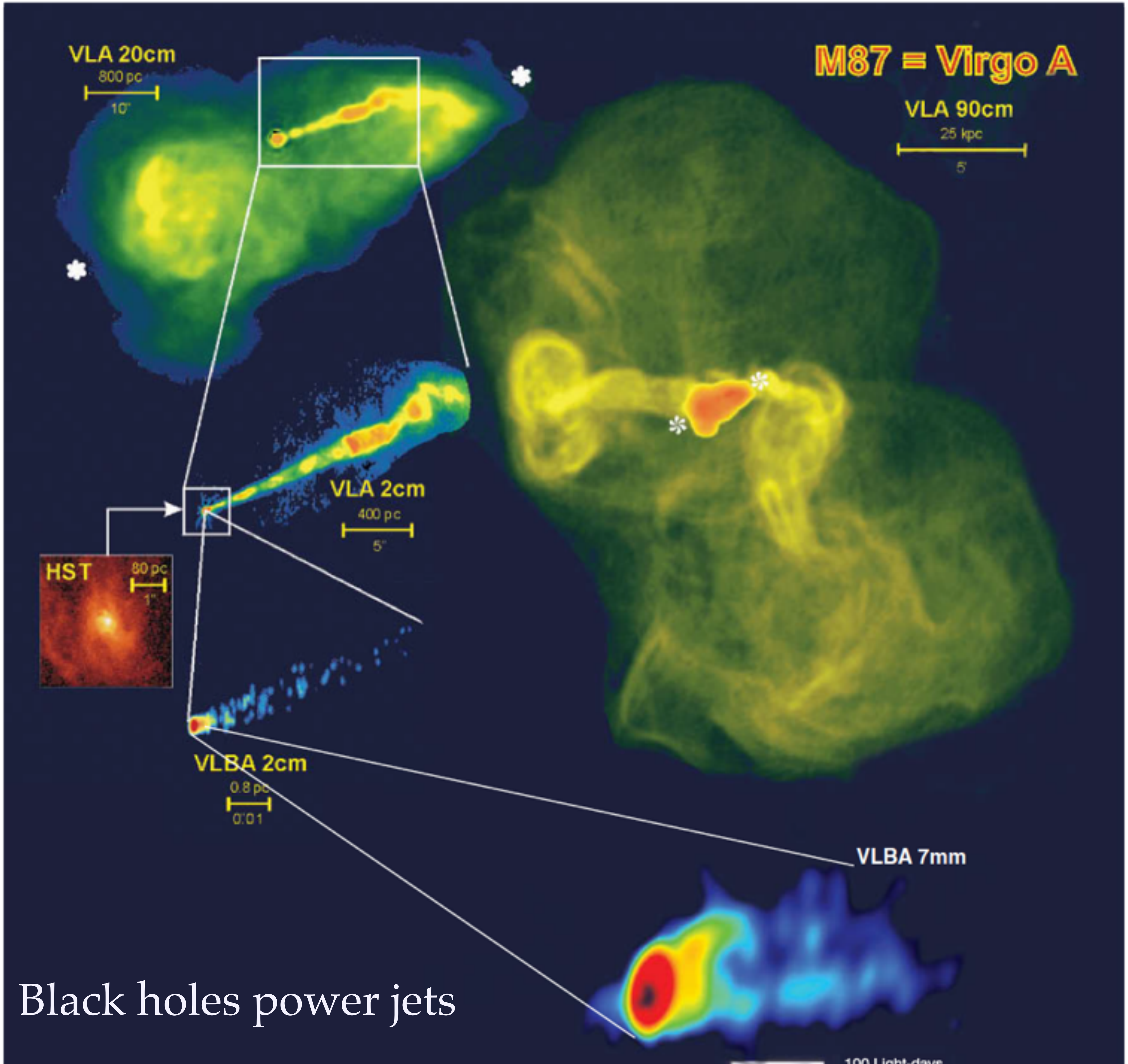

Black holes power jets

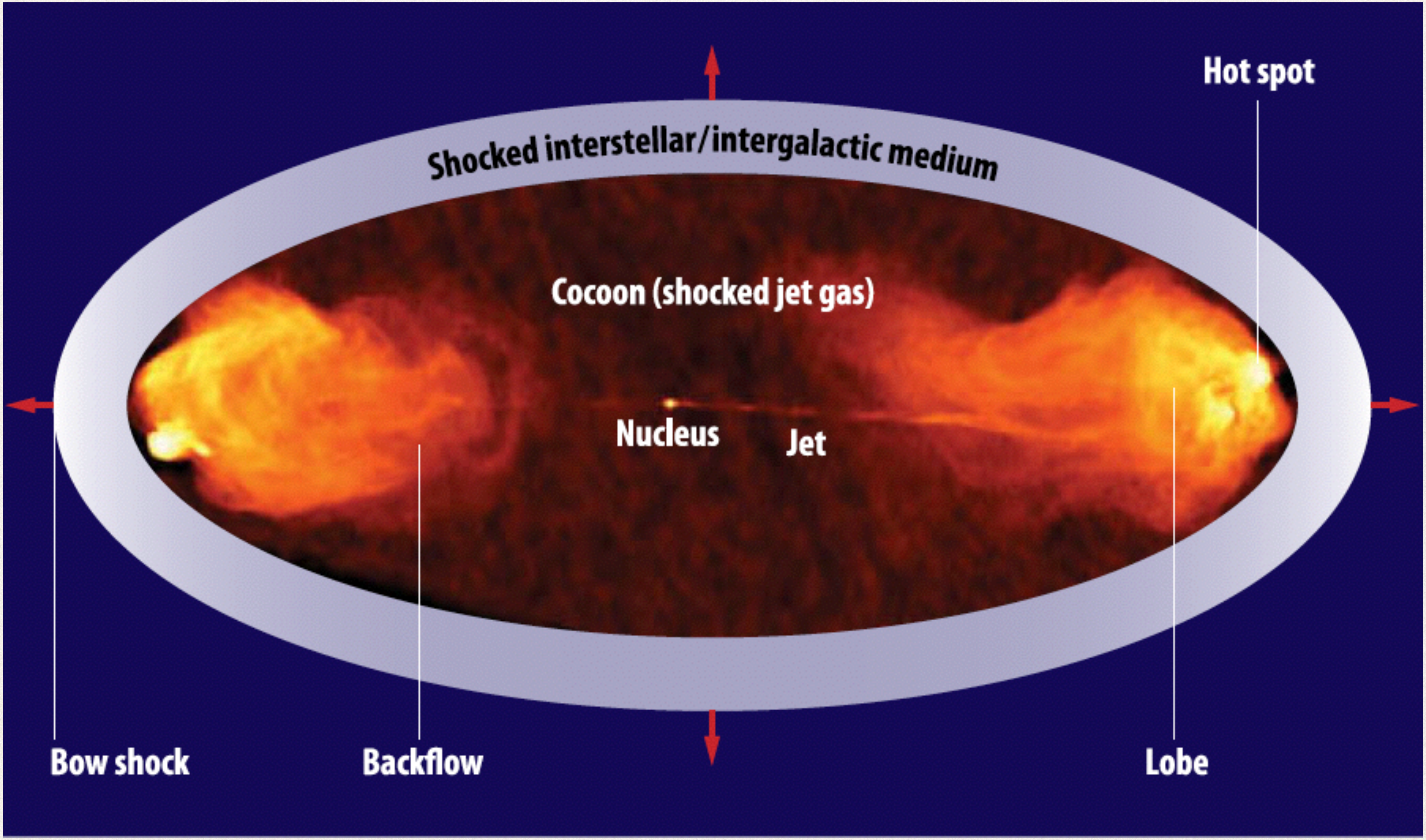
Hot spot
Shocked interstellar/intergalactic medium
Cocoon (shocked jet gas)
Nucleus
Jet
Bow shock
Backflow
Lobe

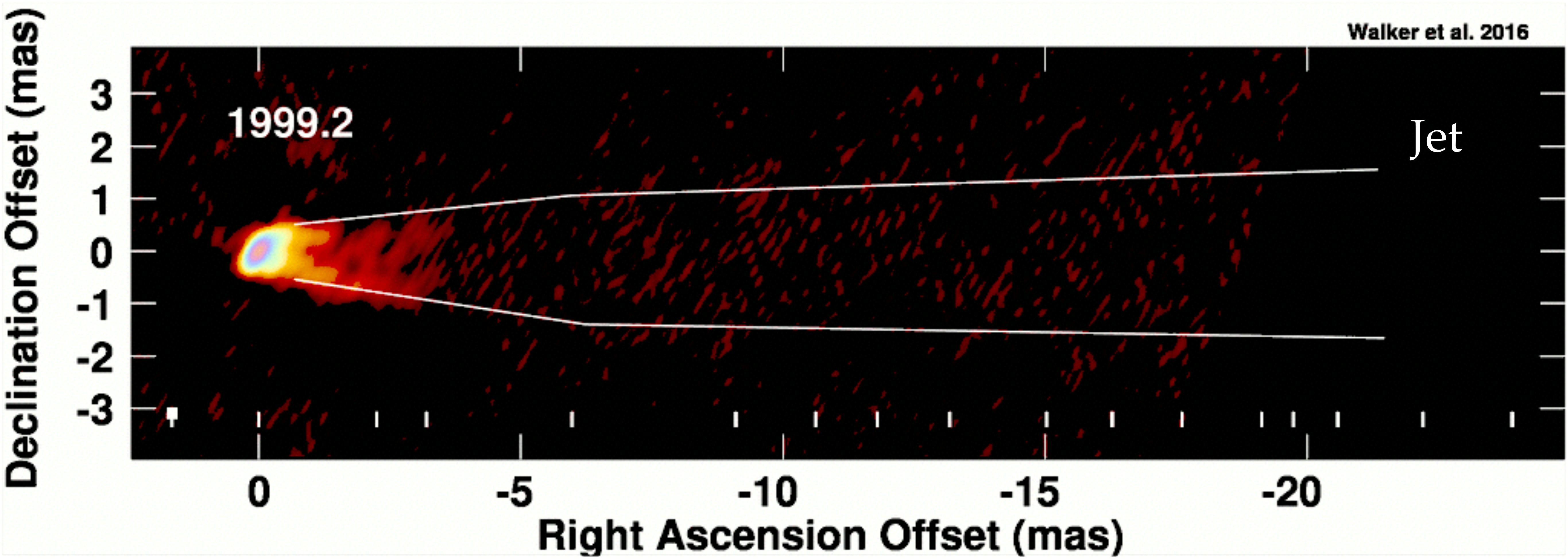
Walker et al. 2016
1999.2
Jet
Declination Offset (mas)
3
2
1
0
-1
-2
-3
0
-5
-10
-15
-20
Right Ascension Offset (mas)

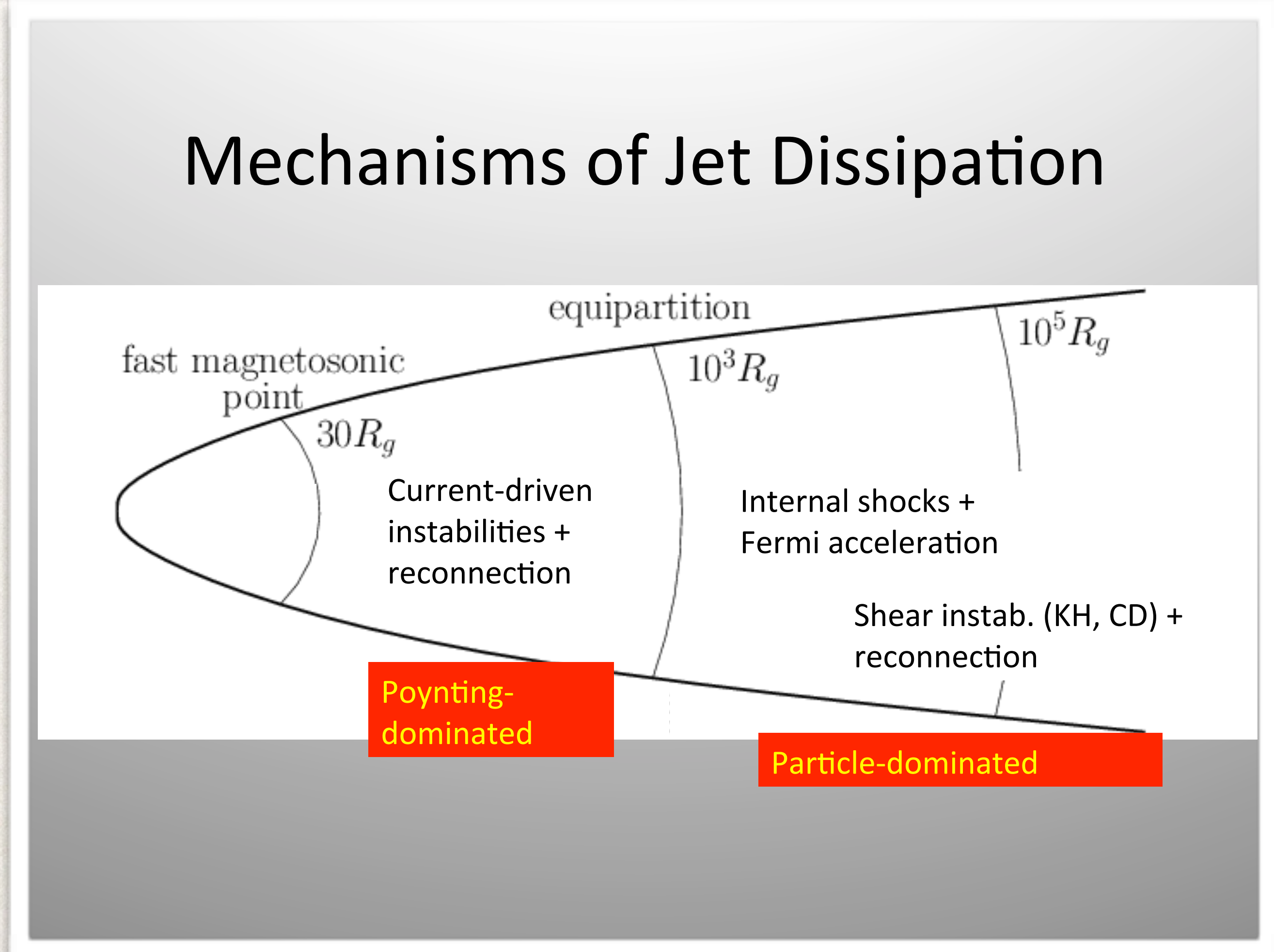
Mechanisms of Jet Dissipation
equipartition
fast magnetosonic point
$30R_g$
10^3R_g
10^5R_g
Current-driven instabilities + reconnection
Internal shocks + Fermi acceleration
Shear instab. (KH, CD) + reconnection
Poynting-dominated
Particle-dominated

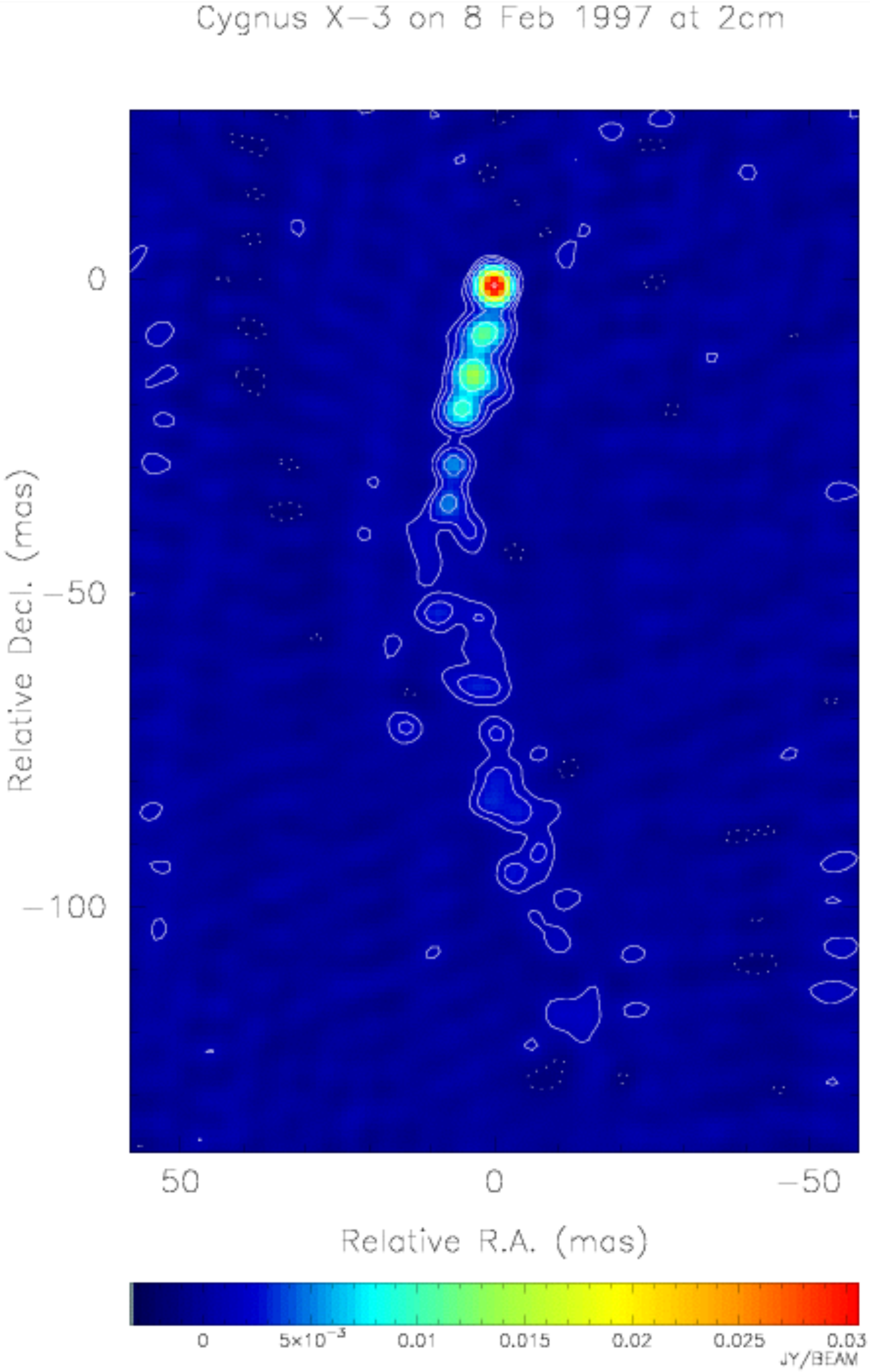

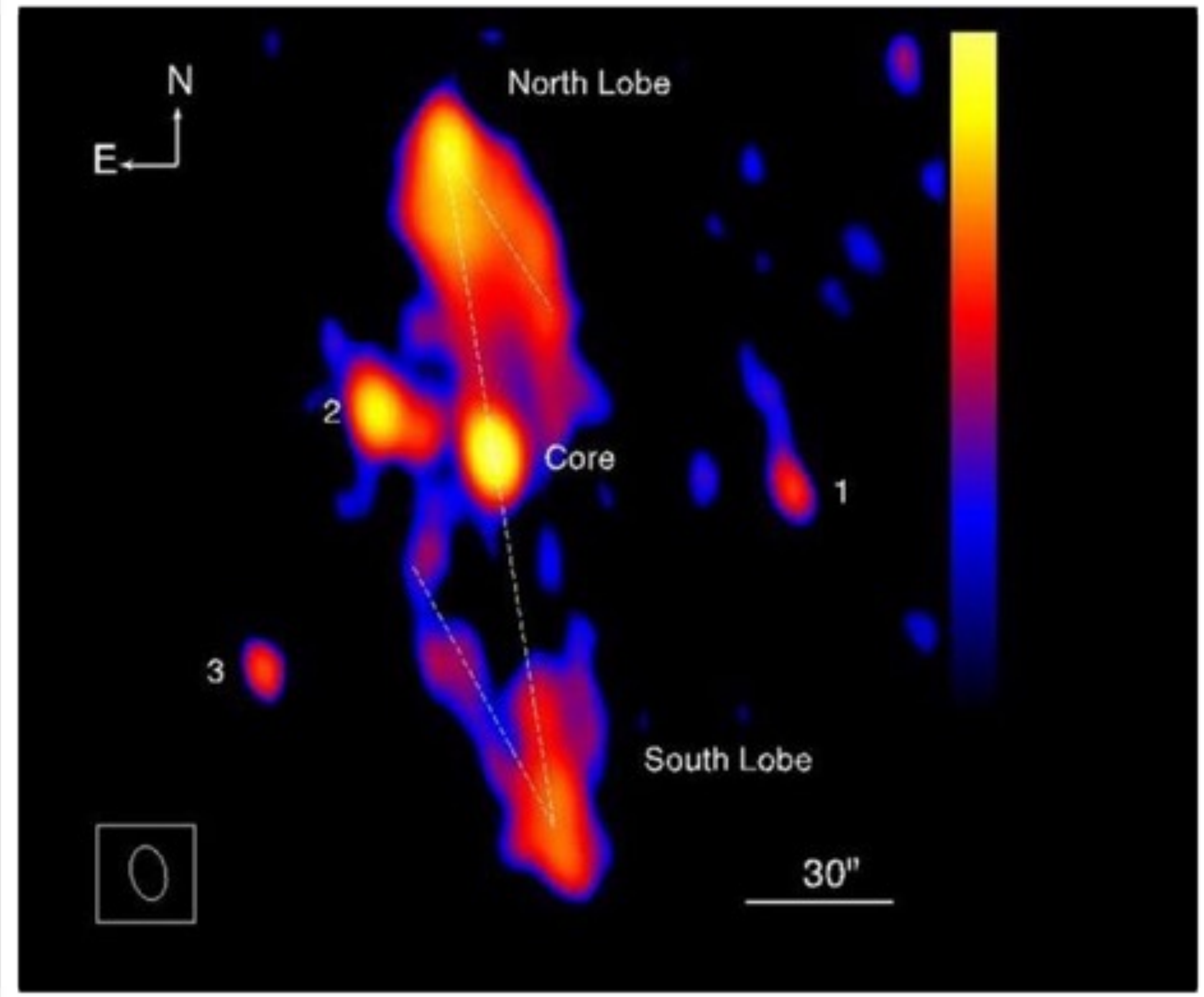

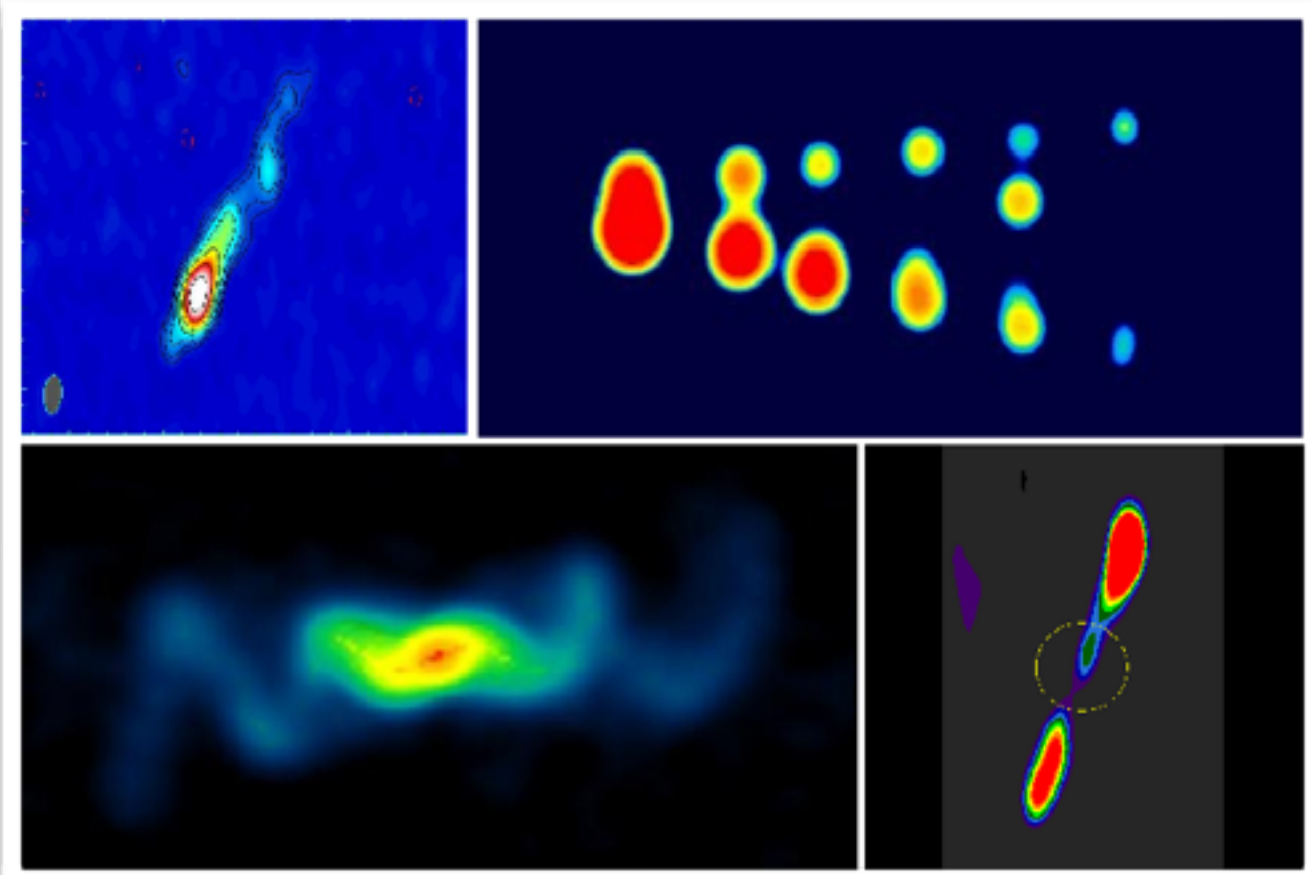

Also observed in micoquasars

Basic equations that rule the outflow (ideal MHD)

$$\nabla \times \vec{B} = \frac{4\pi}{c}\vec{J},$$

$$\nabla \cdot \vec{B} = 0,$$

$$\nabla \times \vec{E} = 0,$$

$$\nabla \cdot \vec{E} = 4\pi\rho_{\rm e},$$

Maxwell

(steady state and conductivity of the plasma is very large).

$$\vec{E} + \frac{1}{c}\vec{v} \times \vec{B} = 0,$$

Ohm

$$\nabla \times \left(\vec{v} \times \vec{B}\right) = 0,$$

Induction

$$\nabla \cdot (\rho\vec{v}) = 0,$$

Continuity

$$\rho\left(\vec{v} \cdot \nabla\right)\vec{v} = -\nabla P - \rho\nabla\Phi + \frac{1}{4\pi}\left(\nabla \times \vec{B}\right) \times \vec{B}.$$

Euler

$$\vec{B} = \vec{B}_{\rm p} + B_\phi\hat{\phi}.$$

$$\vec{B}_{\rm p} \equiv B_r\hat{r} + B_z\hat{z}$$

$$B_r = -\frac{1}{r}\frac{\partial\Psi}{\partial z} \qquad B_z = \frac{1}{r}\frac{\partial\Psi}{\partial r}.$$

The poloidal component is given by the ***flux function***

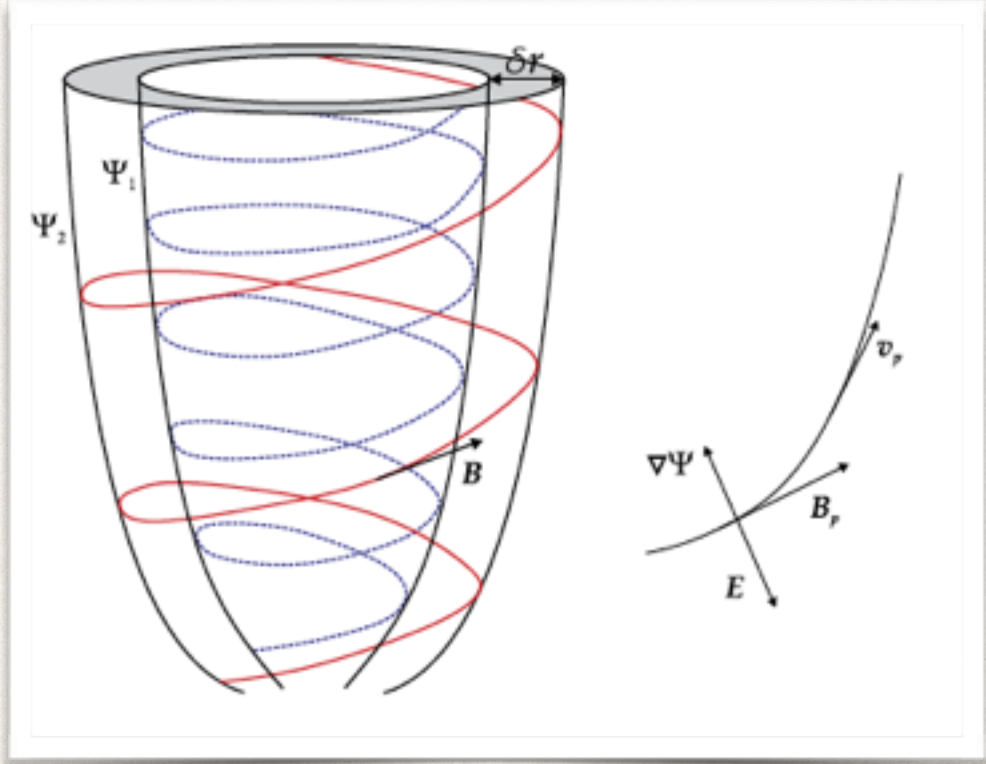

The jet structure and evolution is determined by the *Grad-Shafranov* or *transfield equation* and the Euler equation.

$$\rho(\mathbf{v}\cdot\nabla)\mathbf{v} = -\nabla P - \rho\nabla\Phi + \frac{1}{4\pi}(\nabla\times\mathbf{B})\times\mathbf{B}.$$

$$\nabla\cdot\left[(M_\mathrm{A}-1)\frac{\nabla\Psi}{4\pi r^2}\right] - \left(B_\phi^2 + M_\mathrm{A}^2 B_\mathrm{p}^2\right)\frac{\eta'}{4\pi\eta}$$
$$= \rho\left[E' - \Omega_\mathrm{m}(\Omega r_\mathrm{A})' - \left(\Omega_\mathrm{m} r^2 - \Omega r_\mathrm{A}^2\right)\Omega' - \frac{a_\mathrm{s}^2}{\gamma(\gamma-1)}K'\right].$$

Axisymmetric flows are nested magnetic surfaces of constant magnetic flux.
These surfaces are equipotential.
Plasma flows along these surfaces.

$$\mathbf{v} = r\Omega(\Psi)\hat{\phi} + \frac{1}{\rho}\eta(\Psi)\mathbf{B}.$$

$$M_\mathrm{A}^2 \equiv \frac{v_\mathrm{p}^2}{v_\mathrm{Ap}^2},$$

$$\mathbf{v}_\mathrm{A} \equiv \frac{\mathbf{B}}{\sqrt{4\pi\rho}}.$$

$$\eta(\Psi) = \frac{d\Psi_\mathrm{m}}{d\Psi},$$

The origin of jets is related to the central compact object

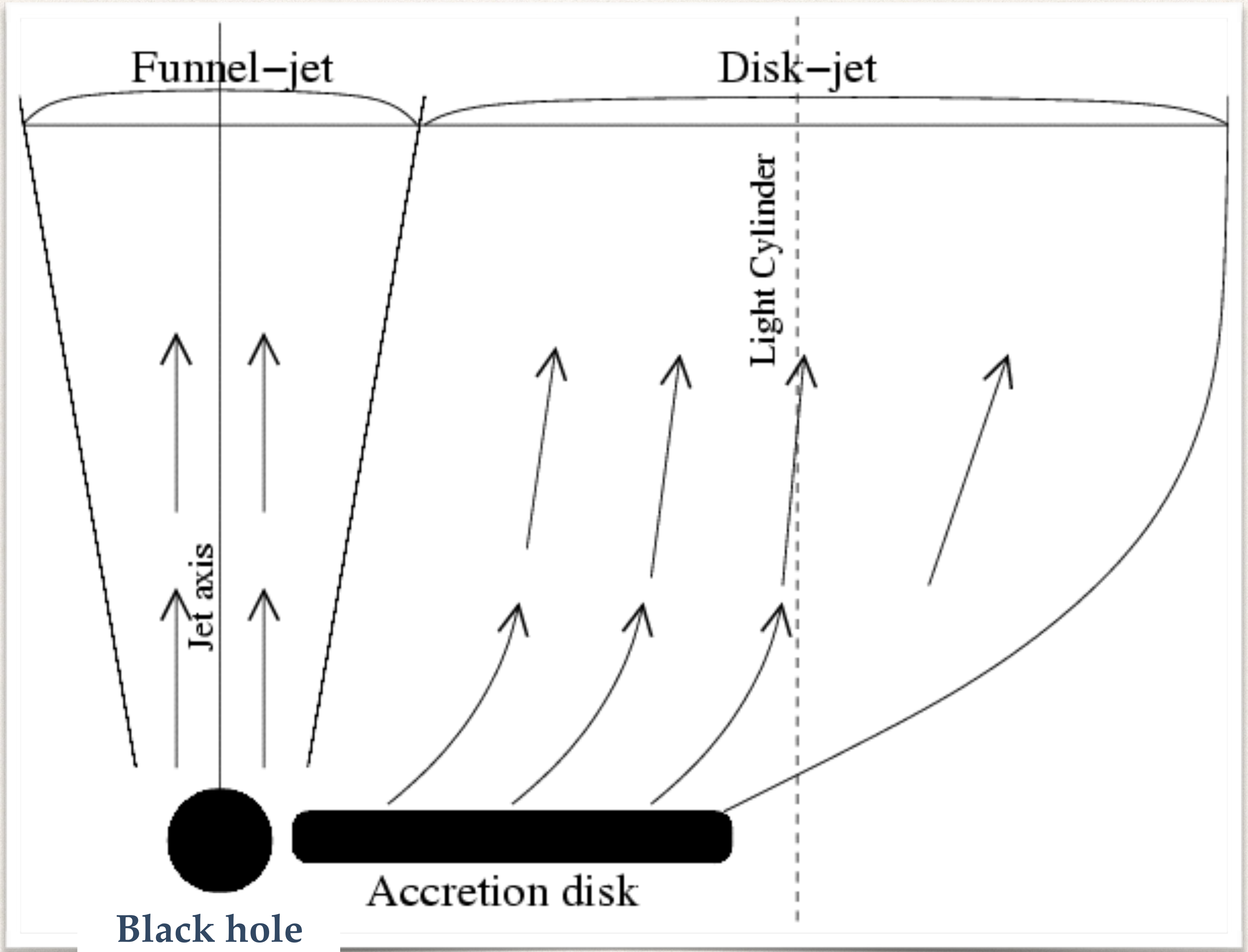

Both the black hole itself and the accretion disk can launch outflows

Rotation + poloidal field —> outflow

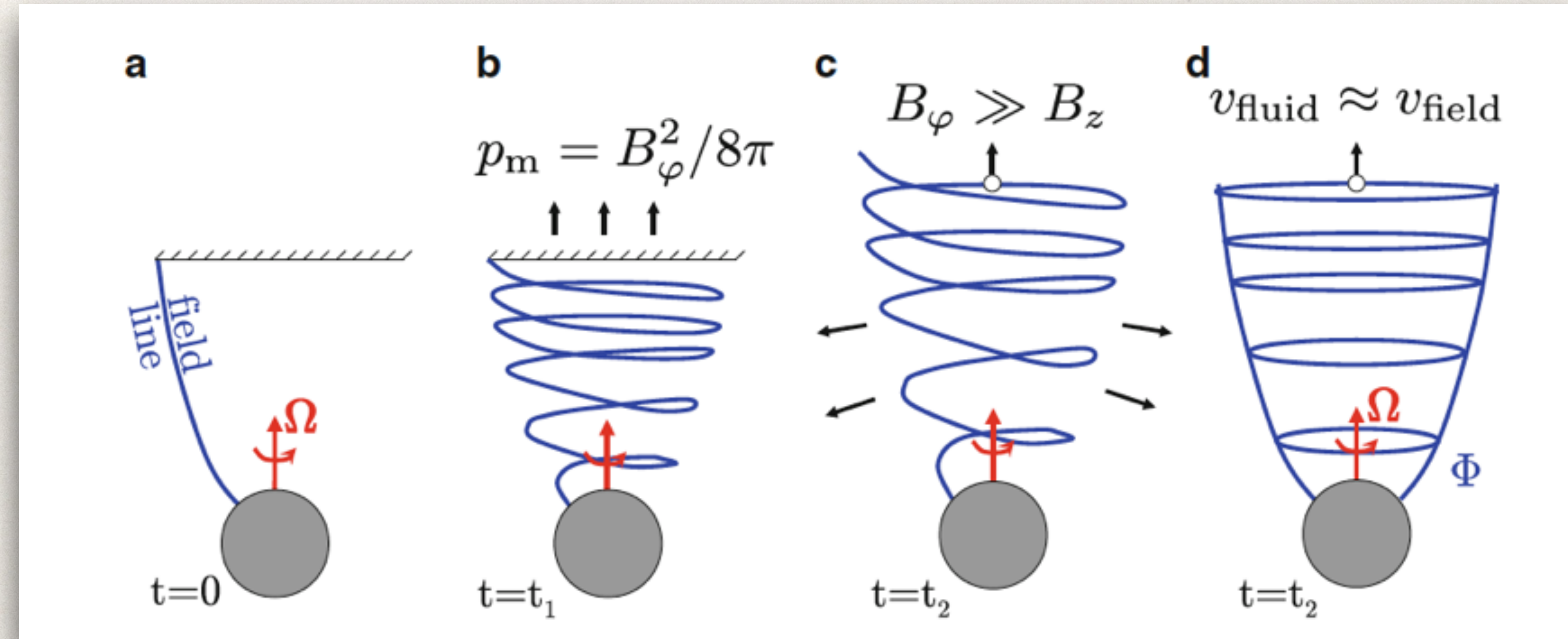

A. Tchekhovskoy

Magnetic model of jets

- Jets are produced by rapidly rotating BHs with magnetized accretion disks.
- Power source - the rotational energy.
- The energy is extracted via magnetic torque as Poynting flux.
- Jet collimation is due to external medium.
- Jet acceleration is via conversion of the electromagnetic energy into the bulk kinetic energy.
- Jet emission is via energy dissipation at shocks (kinetic energy) and/or reconnection sites (magnetic energy).

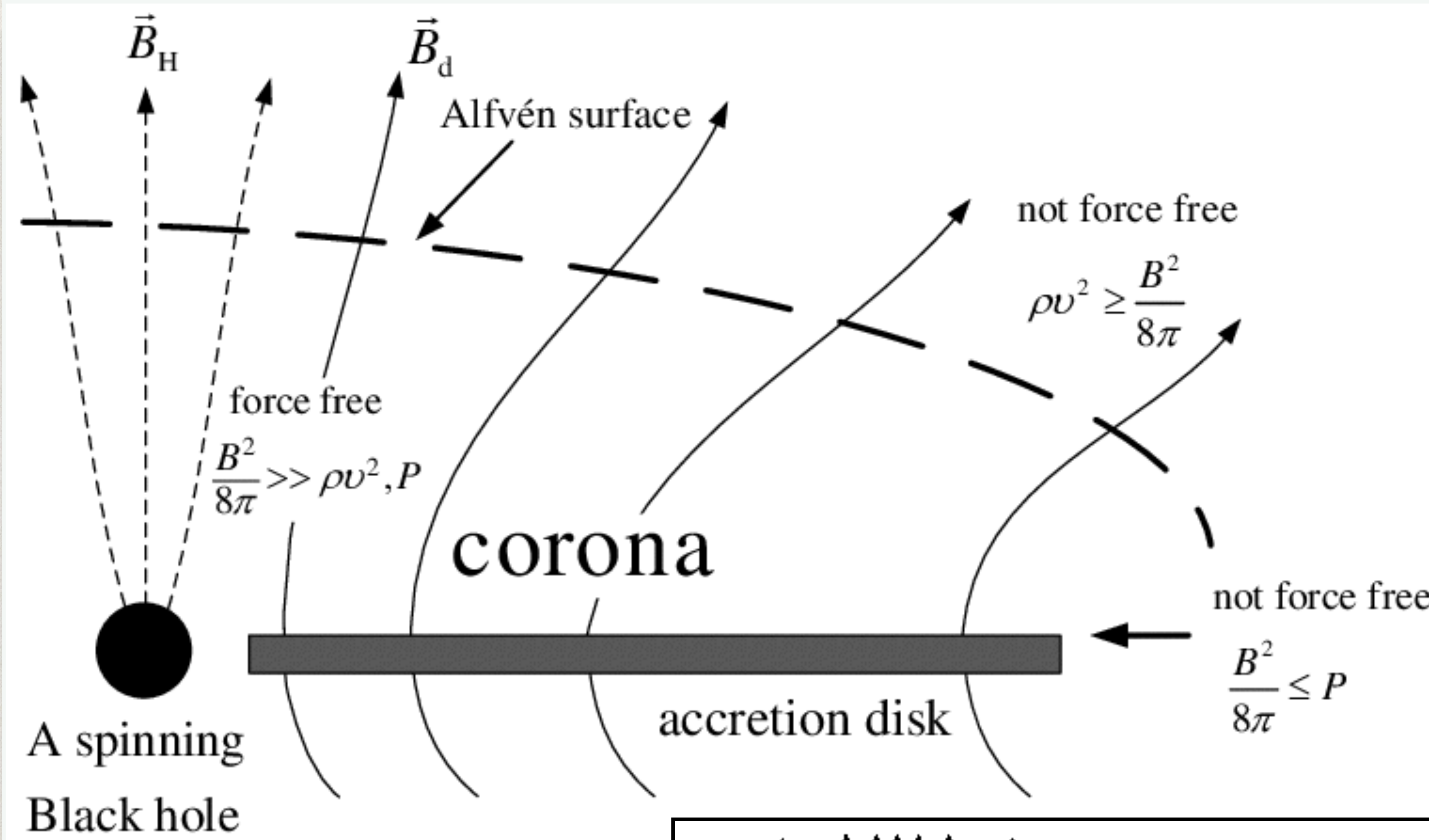
$\vec{B}_H$
$\vec{B}_d$
Alfvén surface
not force free
$\rho\upsilon^2 \geq \frac{B^2}{8\pi}$
force free
$\frac{B^2}{8\pi} >> \rho\upsilon^2, P$
corona
not force free
$\frac{B^2}{8\pi} \leq P$
accretion disk
A spinning
Black hole

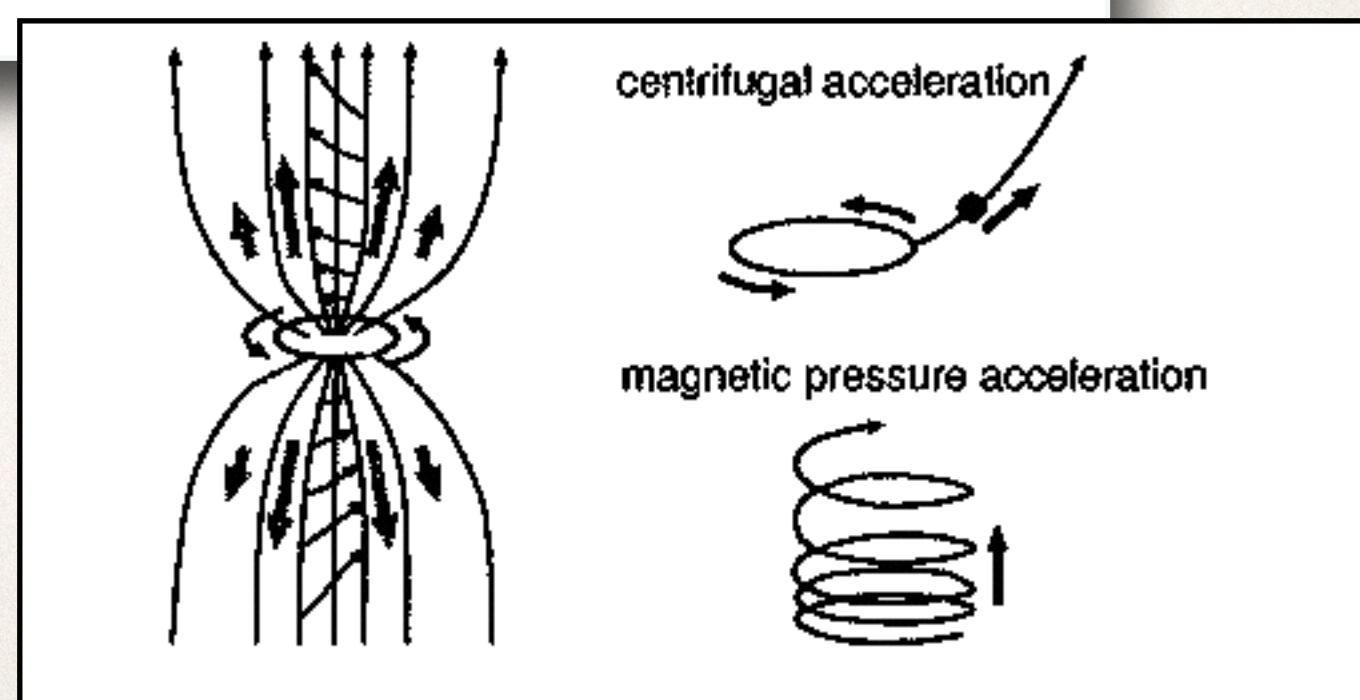
centrifugal acceleration
magnetic pressure acceleration

Accretion-disk driven jets

$$\Phi_{\rm off} = -\frac{GM_{\rm BH}}{\sqrt{r^2+z^2}} - \frac{1}{2}\Omega_{\rm m}^2 r^2.$$

$$\Phi_{\rm off} = -GM_{\rm BH}\left[\frac{r_0}{\sqrt{r^2+z^2}} + \frac{1}{2}\left(\frac{r}{r_0}\right)^2\right].$$

$$\frac{\partial^2\Phi_{\rm off}}{\partial s^2}(r_0,0) = -\frac{GM_{\rm BH}}{r_0^3}\left(3\sin\theta^2 - \cos\theta^2\right) < 0.$$

$$\theta > 30^\circ$$

$$\Omega_{\rm K}(R) = \left(\frac{GM}{R^3}\right)^{1/2}.$$

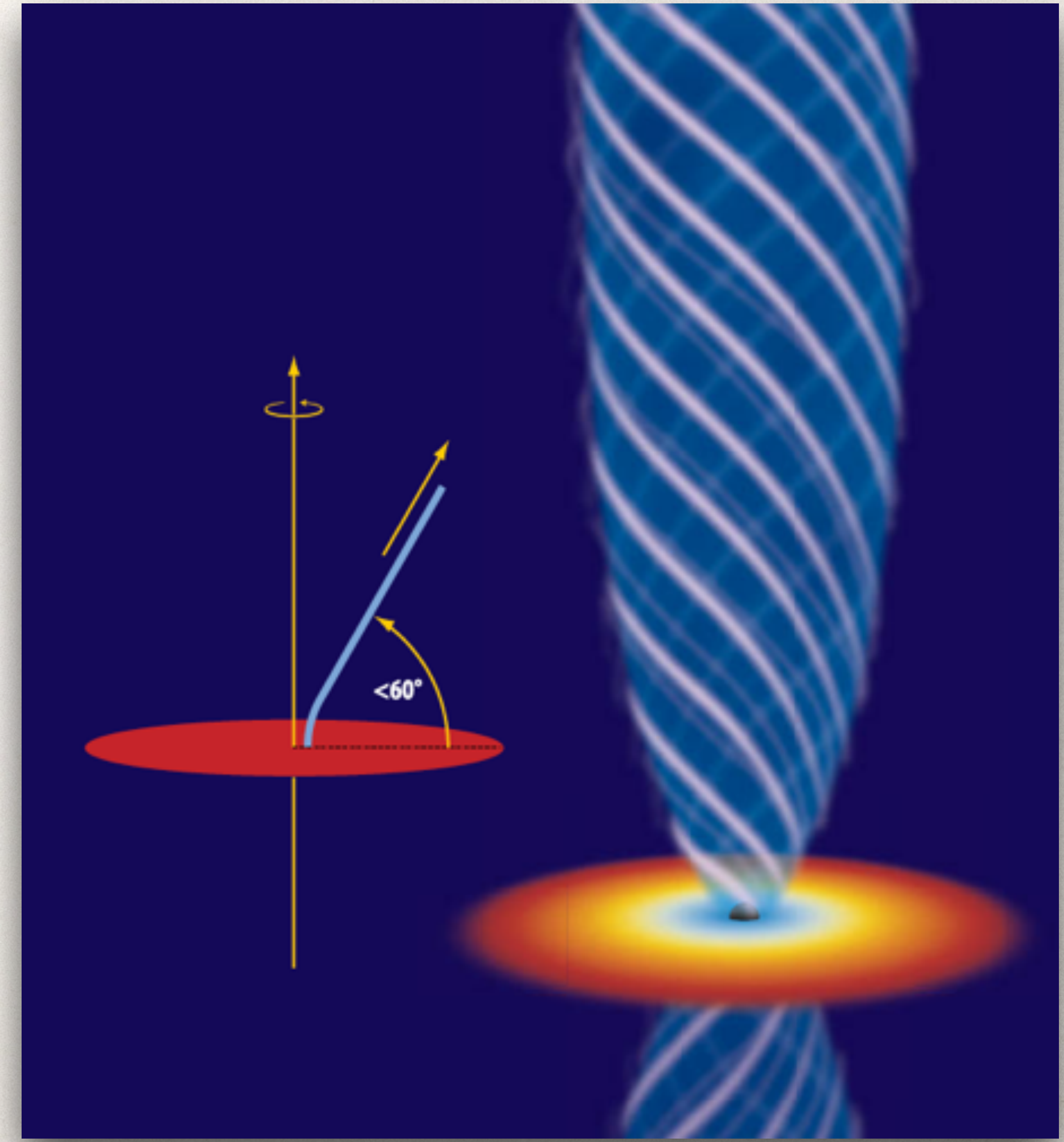

Mass loading argument favours BH over accretion disk

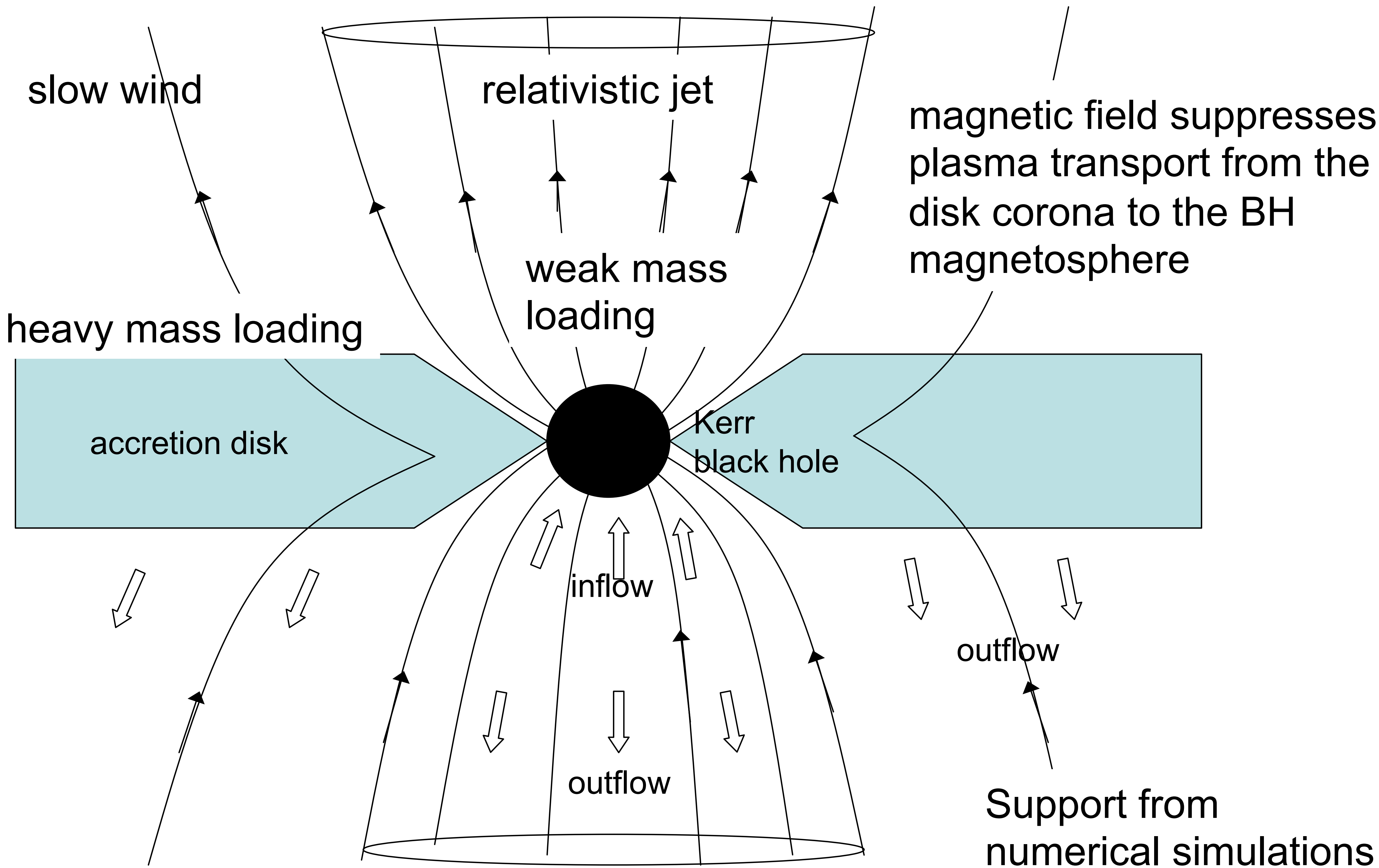

Ergospheric jets

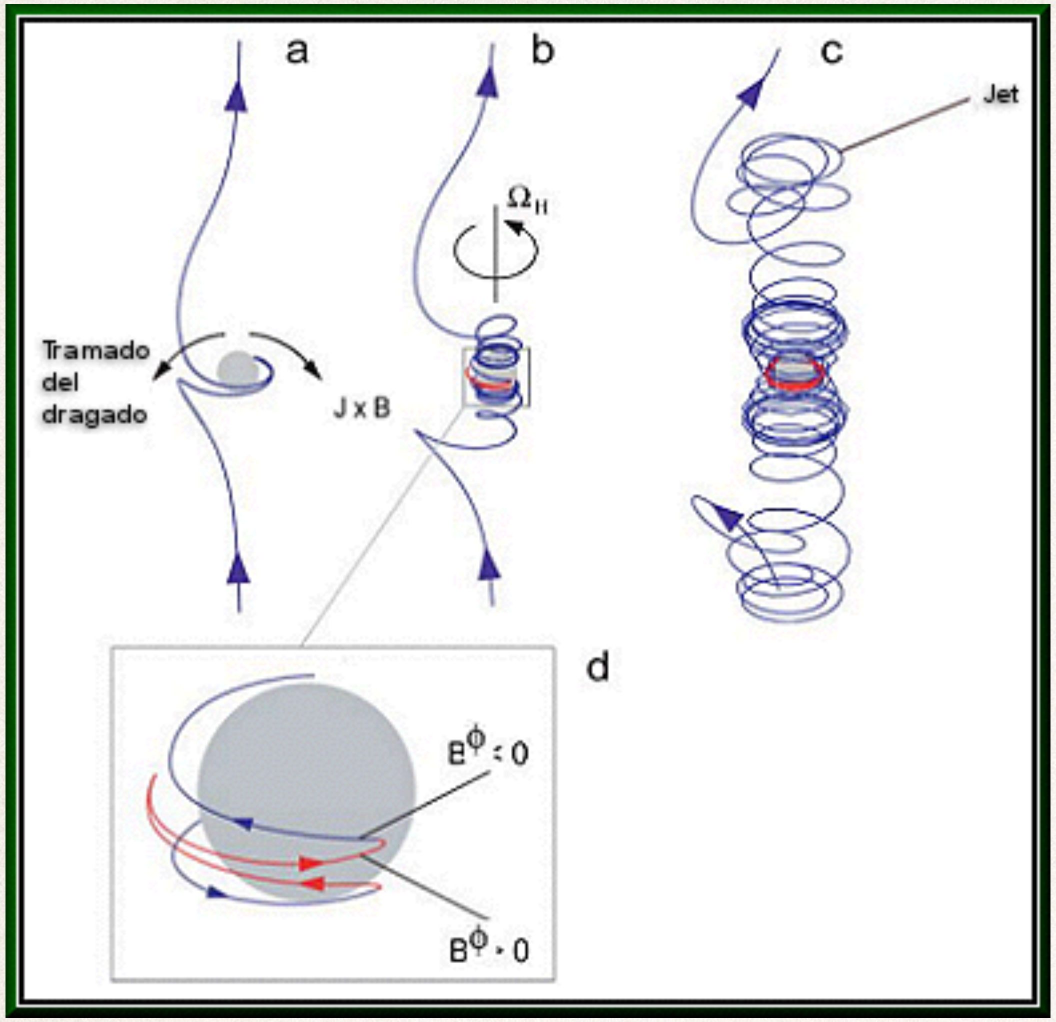

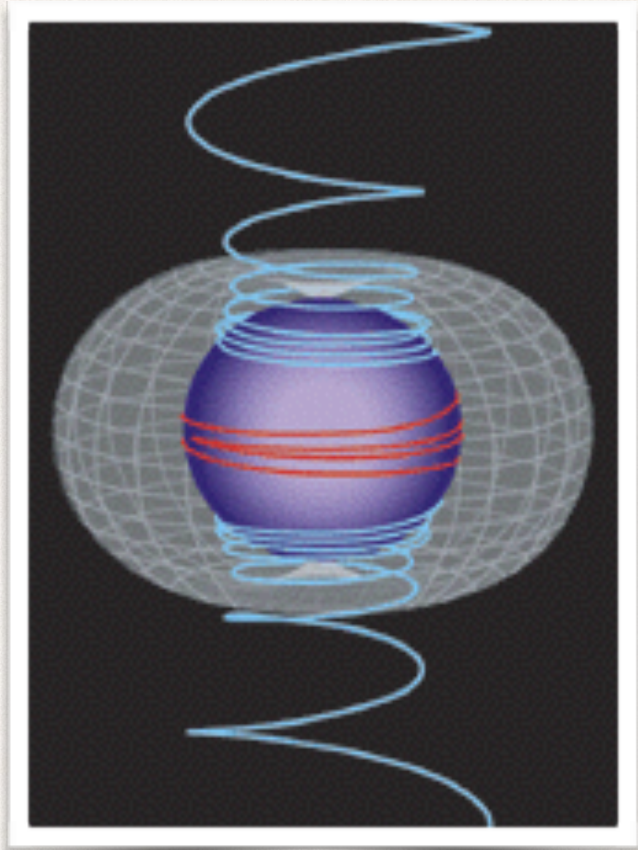

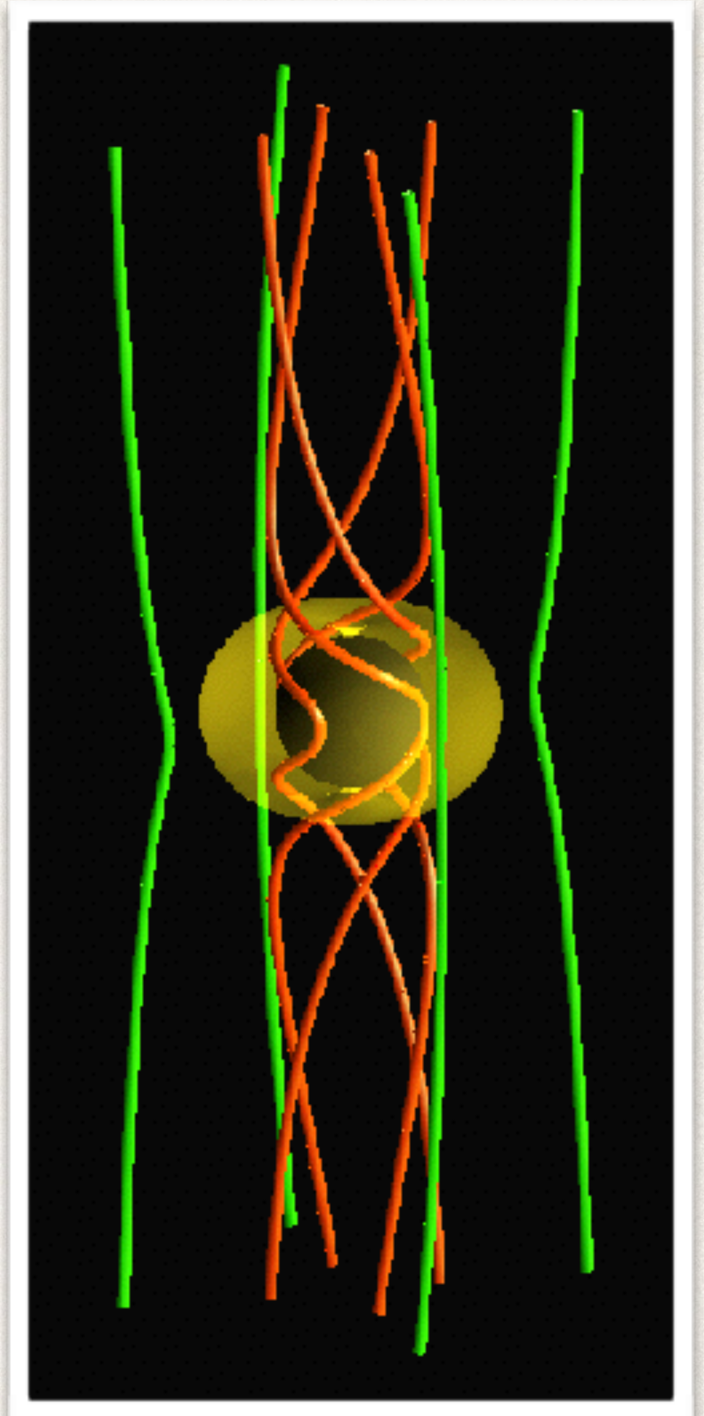

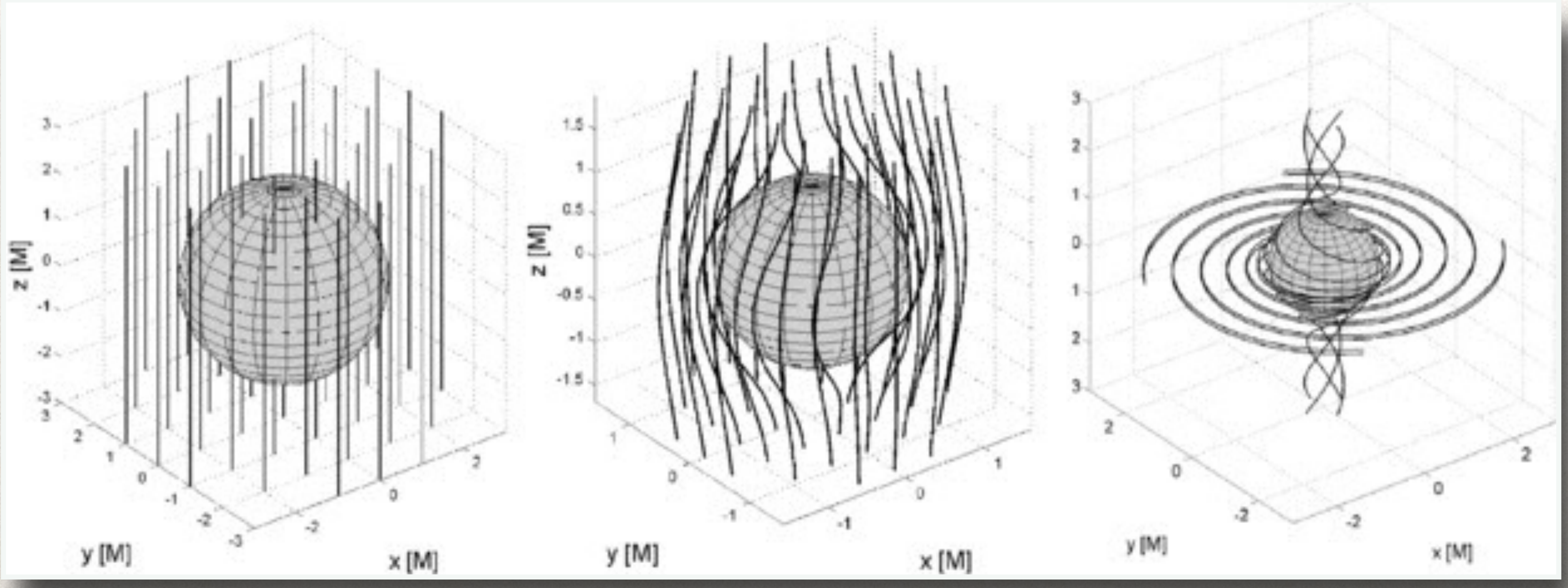

- While plasma is carried into the hole only (not ejected), electromagnetic power is ejected along the rotation axis.

- This Poynting power should eventually be turned into particles and a very fast jet.

- Magnetic field is tied to infalling plasma, not horizon.

- Frame dragging in the ergosphere twists up the field lines just as in the non-relativistic accretion disk case.

- Back-reaction of the magnetic field accelerates the ergospheric plasma to relativistic speeds counter to the hole's rotation: negative energy plasma.

- Accretion of negative energy plasma spins down the hole

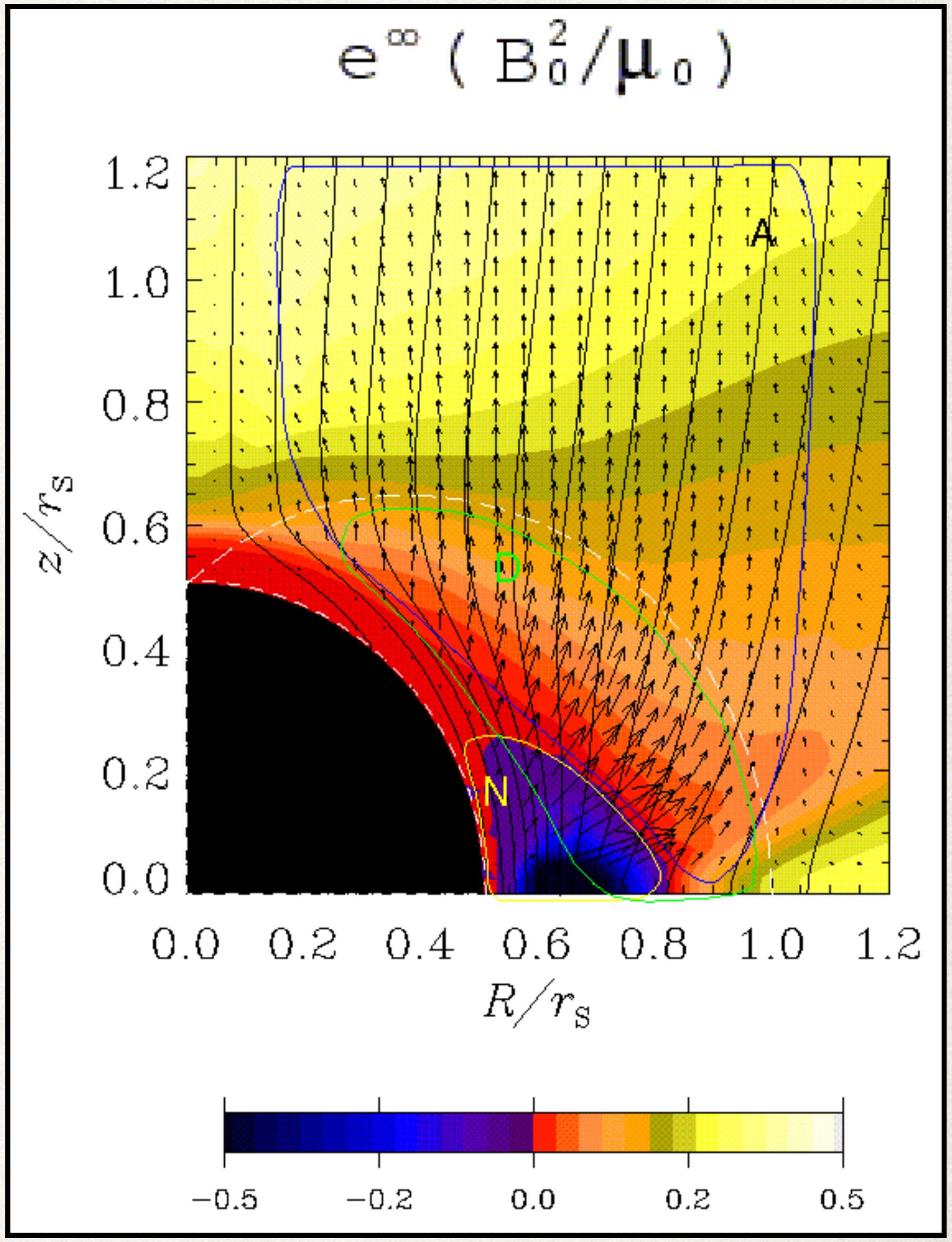

Relativistic Outflow driven by Magnetic Field from Ergosphere

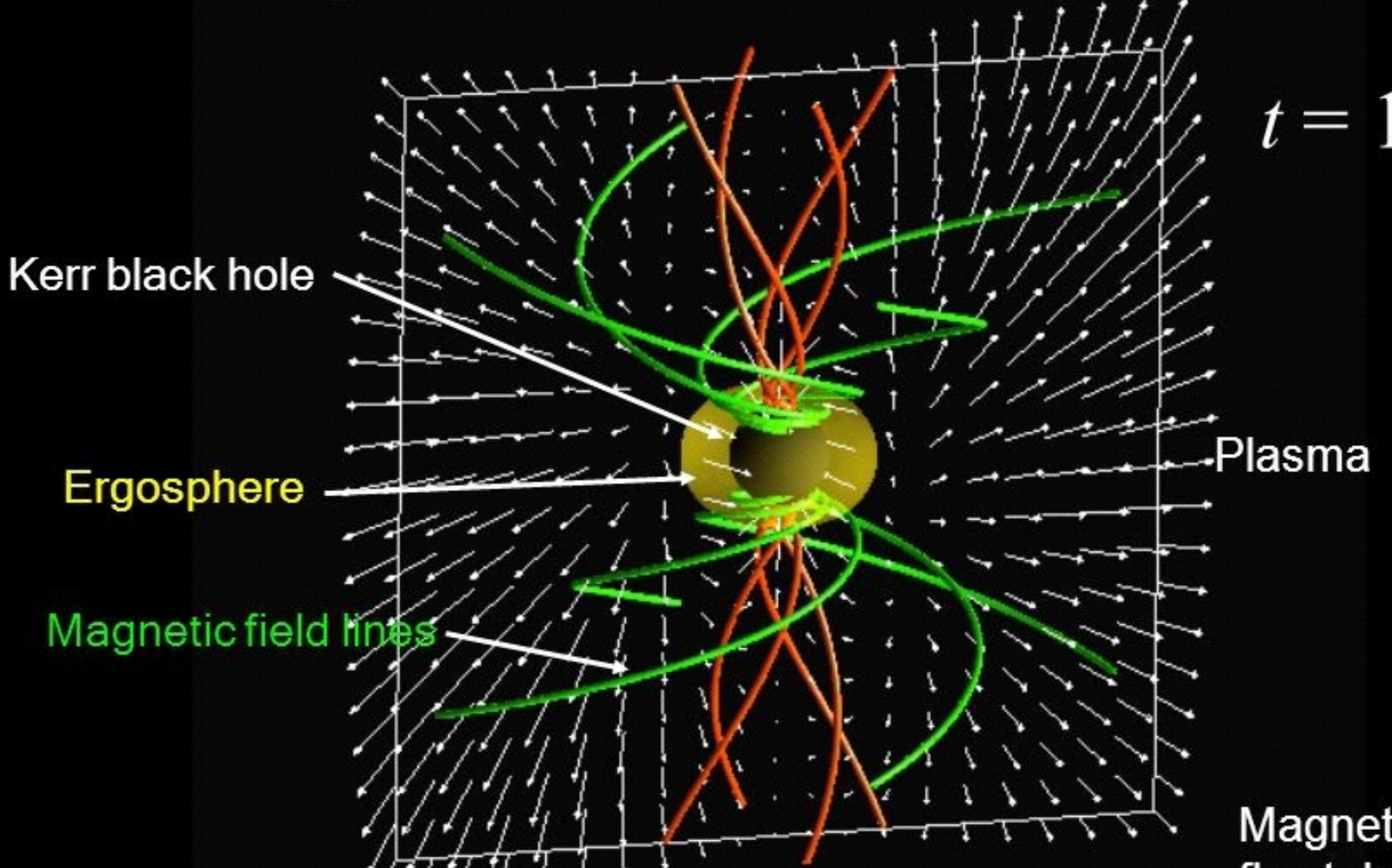

Magnetic field flux tube acts as propeller screw!

$$L_{\rm EM} \sim \frac{EB}{4\pi} c\, \pi R_{\rm g}^2 \sim B^2 c R_{\rm g}^2.$$

$$L \approx 10^{46} \left(\frac{B_{\rm n}}{10^4\ {\rm G}}\right)^2 \left(\frac{M}{10^9 M_\odot}\right)^2 a_*^2\ {\rm erg\,s^{-1}}.$$

Initial collimation of relativistic jets requires a "nozzle", external confining medium.

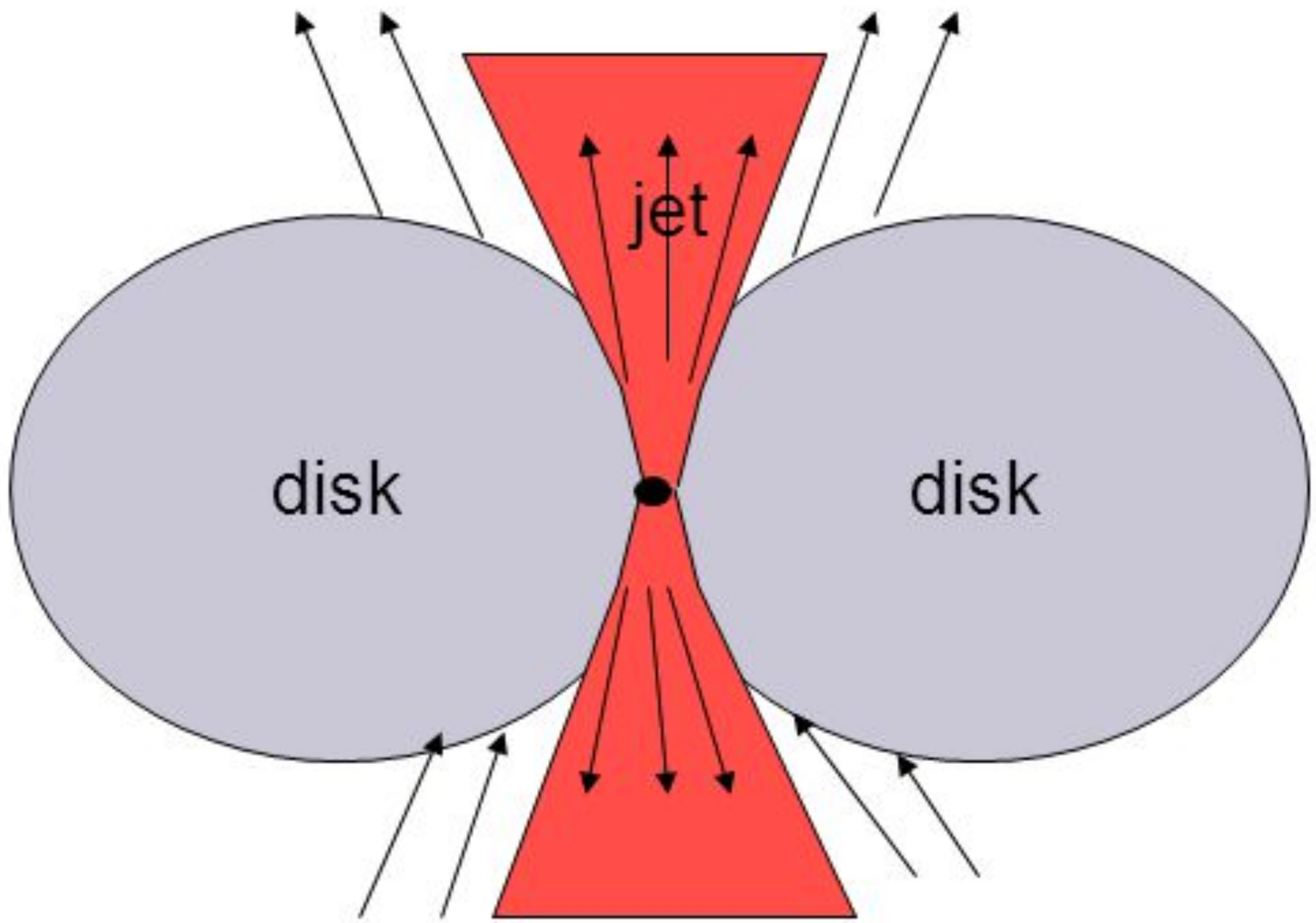

Suspects:

- Thick disk (torus)
- Disk corona
- Disk wind
- ISM

Mass load of jets

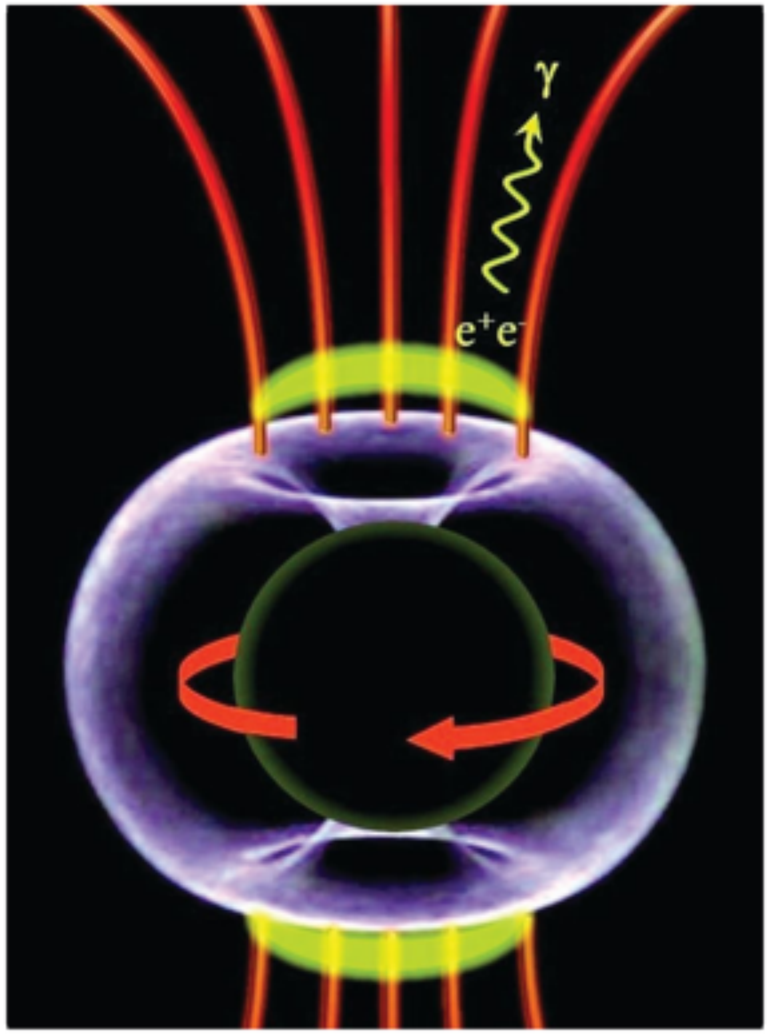

In the laboratory frame, ***the rotation of the magnetic field will induce an electric field***. If not screened, this field could in principle be tapped for the acceleration of particles. By Gauss' law, the induced electric field is supported by a local charge density corresponding to a particle number density (commonly referred to as the Goldreich–Julian [GJ] density well inside the light cylinder.

$$n_{\rm GJ} = \frac{\Omega B\cos\theta}{2\pi e c} = 0.1\eta^{-1}\left(\frac{B}{10^4{\rm G}}\right)\left(\frac{10^8\,{\rm M_\odot}}{M}\right)\cos\theta\ [\text{particles cm}^{-3}],$$

→ $|\vec{E}| \sim (\Omega_H r_H)B_p/c$ $\quad \Omega_H = a(c/2r_H)$ $\quad r_H = \frac{r_s}{2}(1+\sqrt{1-a^2}),$

$$\Phi \sim r_H|\vec{E}| = (a/2)r_H B_p$$

$$\Phi \sim 2\times 10^{19} a(1+\sqrt{1-a^2})\left(\frac{M}{10^8\,{\rm M_\odot}}\right)\left(\frac{B_p}{10^4{\rm G}}\right)[{\rm V}].$$

The charge density in the vicinity of accreting black holes may well be so high that a significant fraction of this potential is screened and thus no longer available for particle acceleration

$$\Phi_e \sim \Omega_H\left(\frac{h}{r_H}\right)^2 r_H^2 B_p/c = \left(\frac{h}{r_H}\right)^2\Phi.$$

$$\frac{dE}{dt} = Ze\Phi_e c/h,$$

Particles accelerated in the gap can trigger electromagnetic cascades outside the gap injecting pairs.

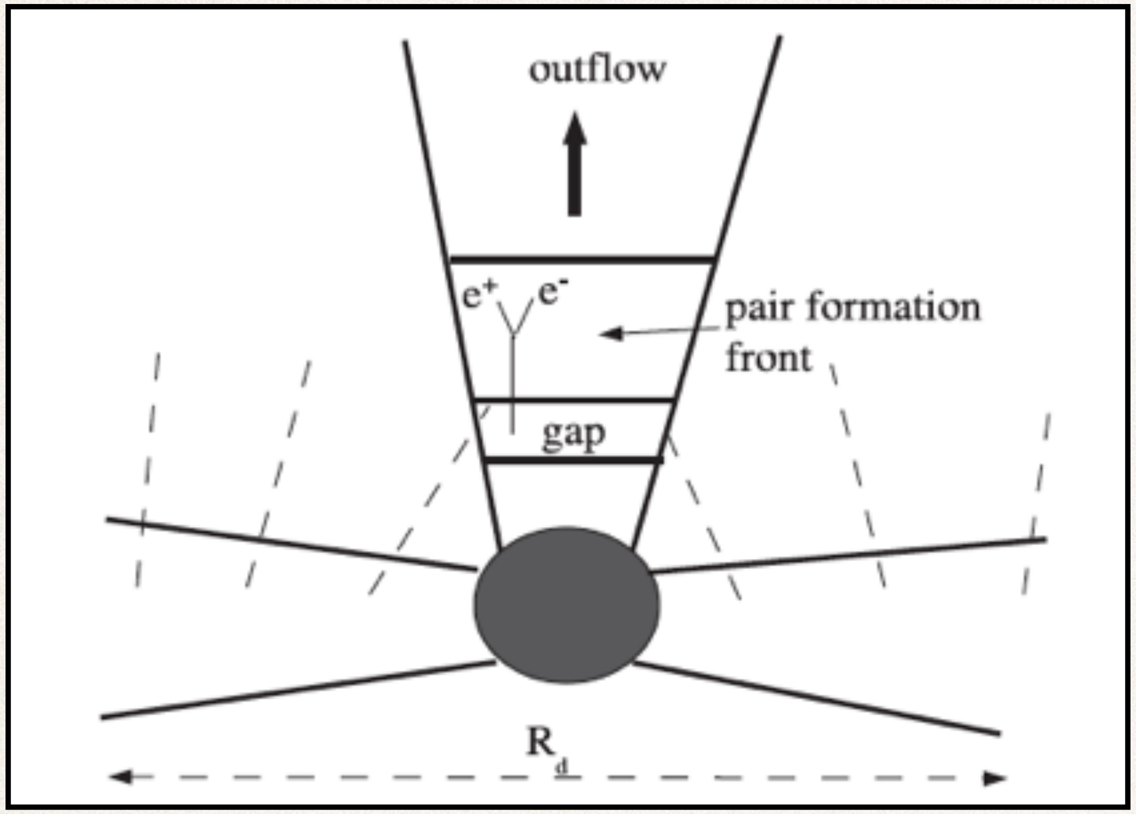

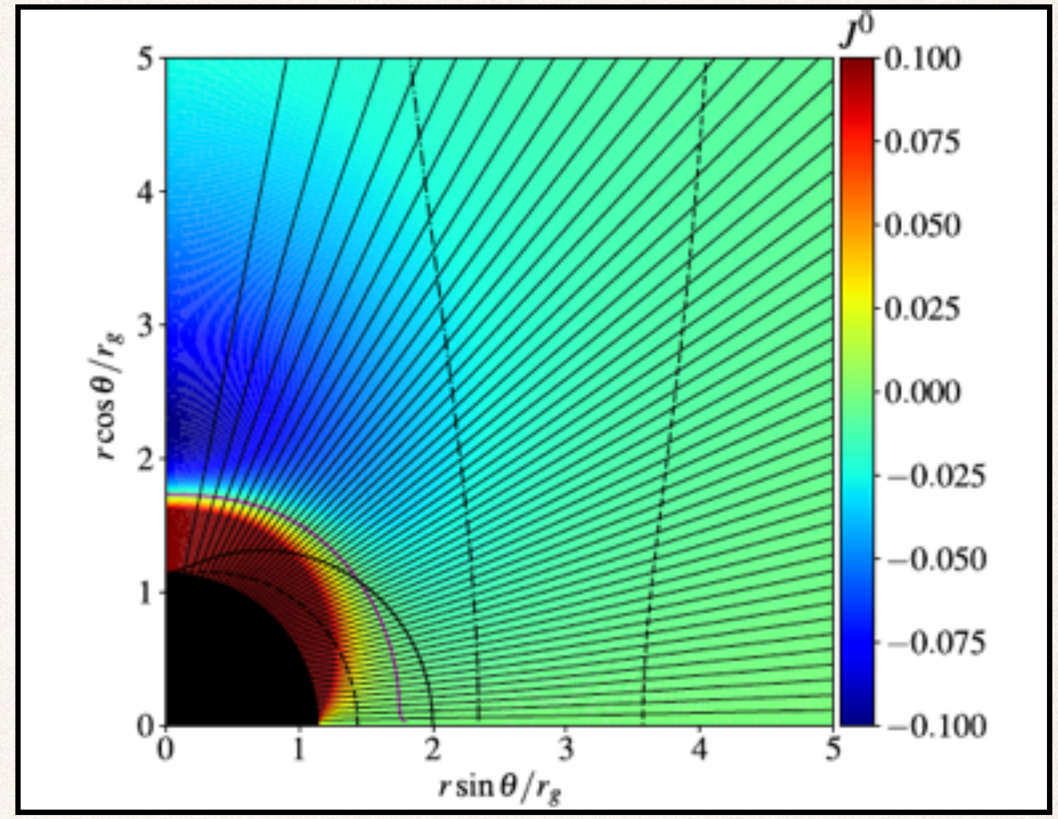

Neutrons produced in the disk by *pp* collisions can decay inside the jet injecting *p* and electrons.

$$p + p \rightarrow p + n + \pi^+ + a\pi^0 + b(\pi^+ + \pi)\,,$$
$$p + p \rightarrow n + n + 2\pi^+ + a\pi^0 + b(\pi^+ + \pi)\,,$$
$$p + \gamma \rightarrow n + \pi^+ + a\pi^0 + b(\pi^+ + \pi),$$

$$n \rightarrow p + e^- + \bar{\nu}_e\,.$$

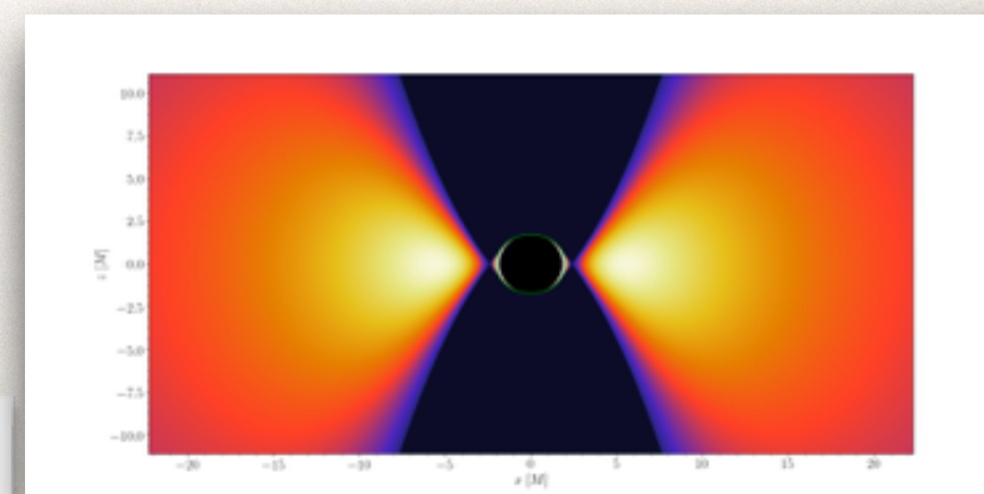

Additional load by entrainment of external medium

Evolution of magnetisation in the outflow

$$\sigma(r,z) = \frac{B(r,z)B(r_0, z_{\text{base}})}{8\pi c^2 \rho_{\text{base}}}$$

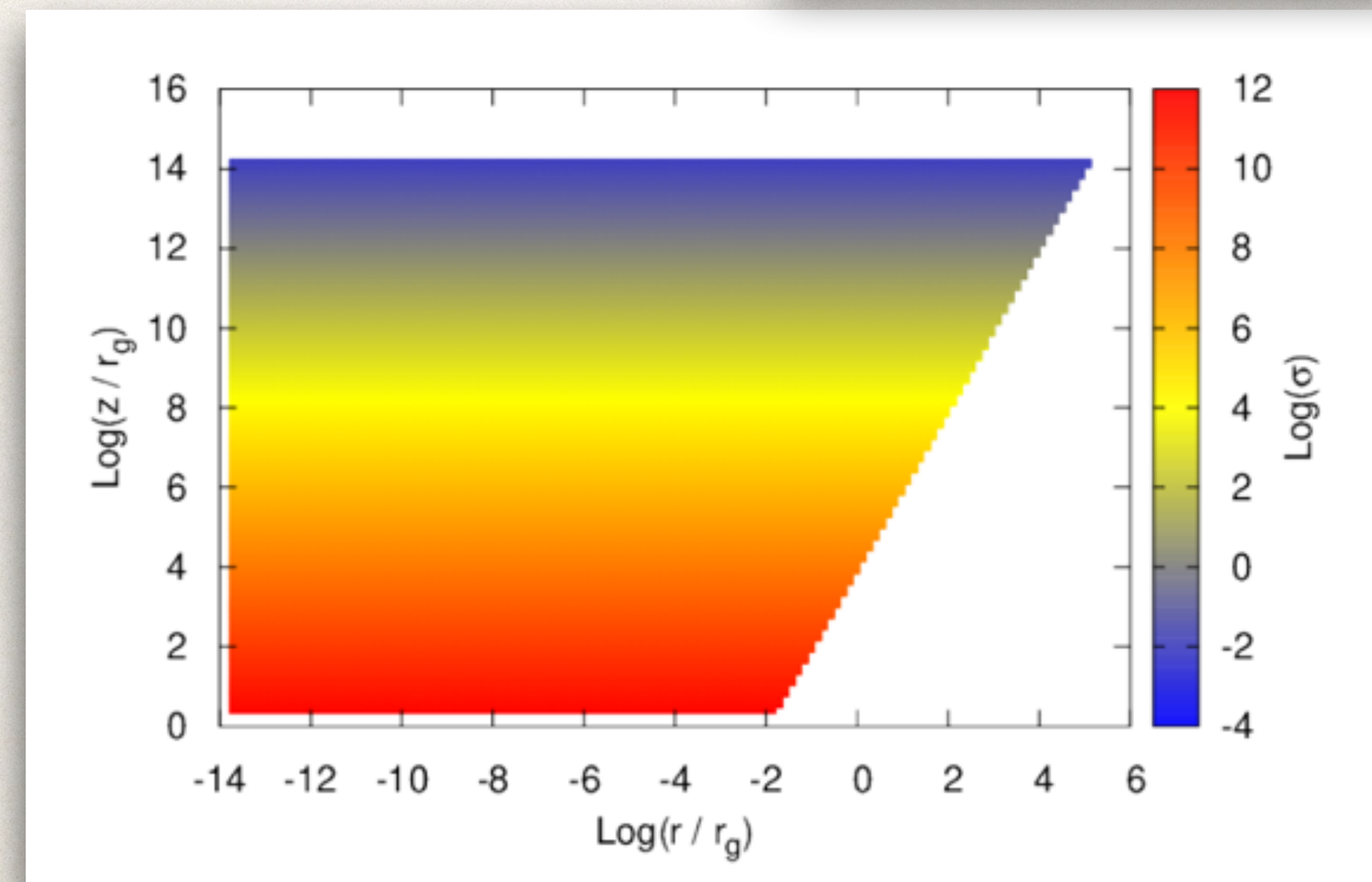

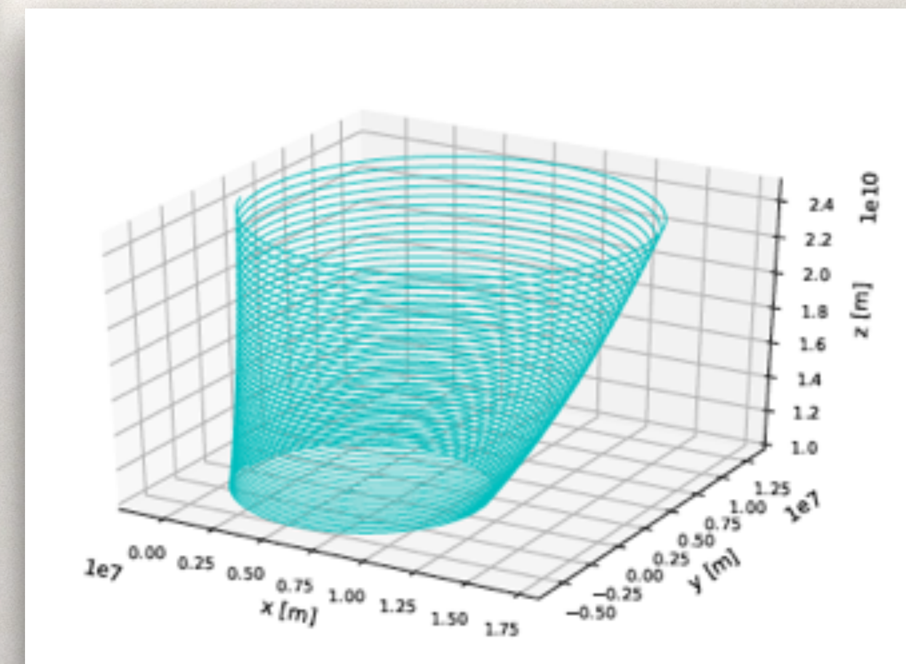

(b) $E = 10^{15}$ eV, $\alpha = 1$

Pelle, Romero, Pellizza 2019

Gamma-ray bursts: Collapsar

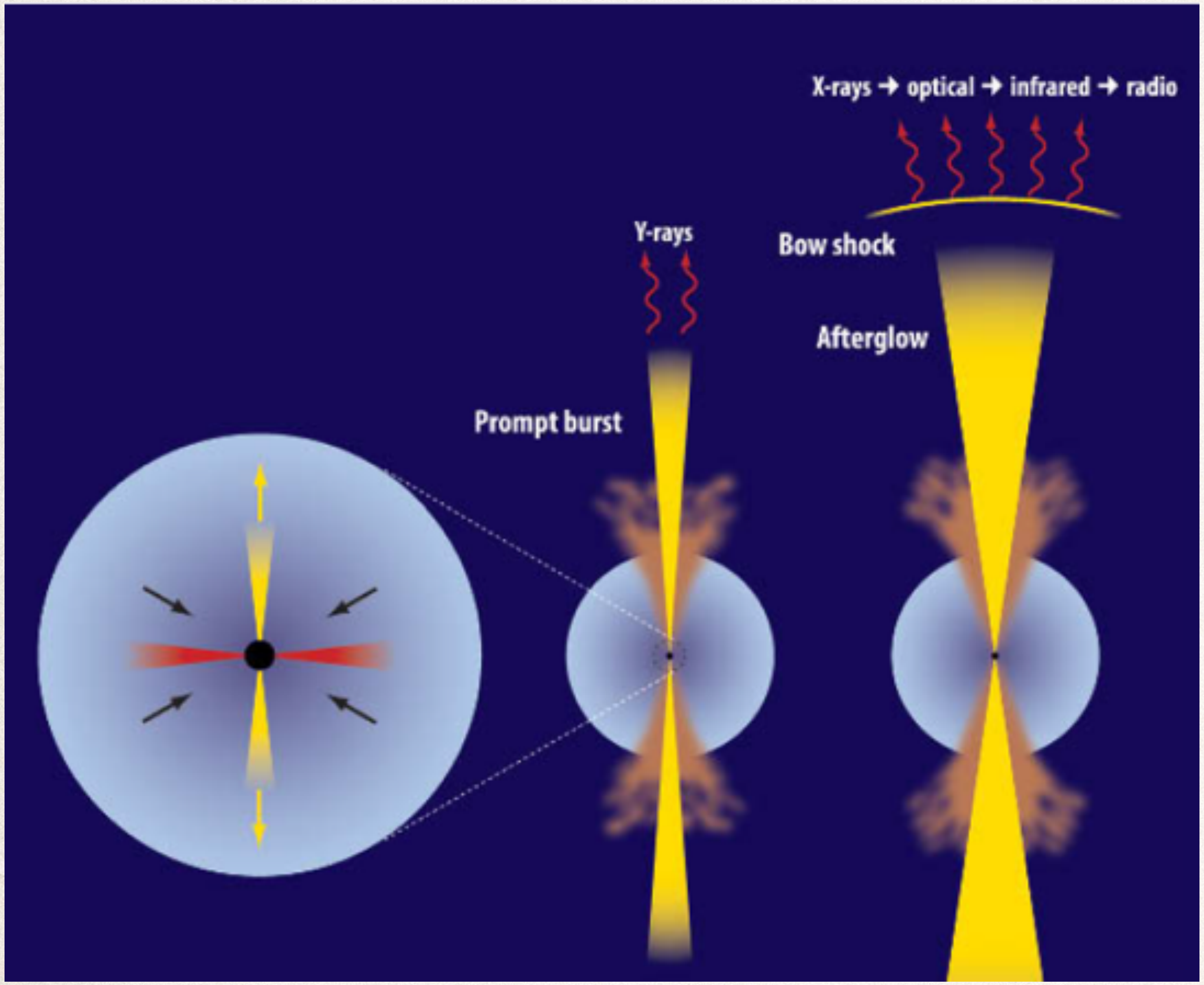

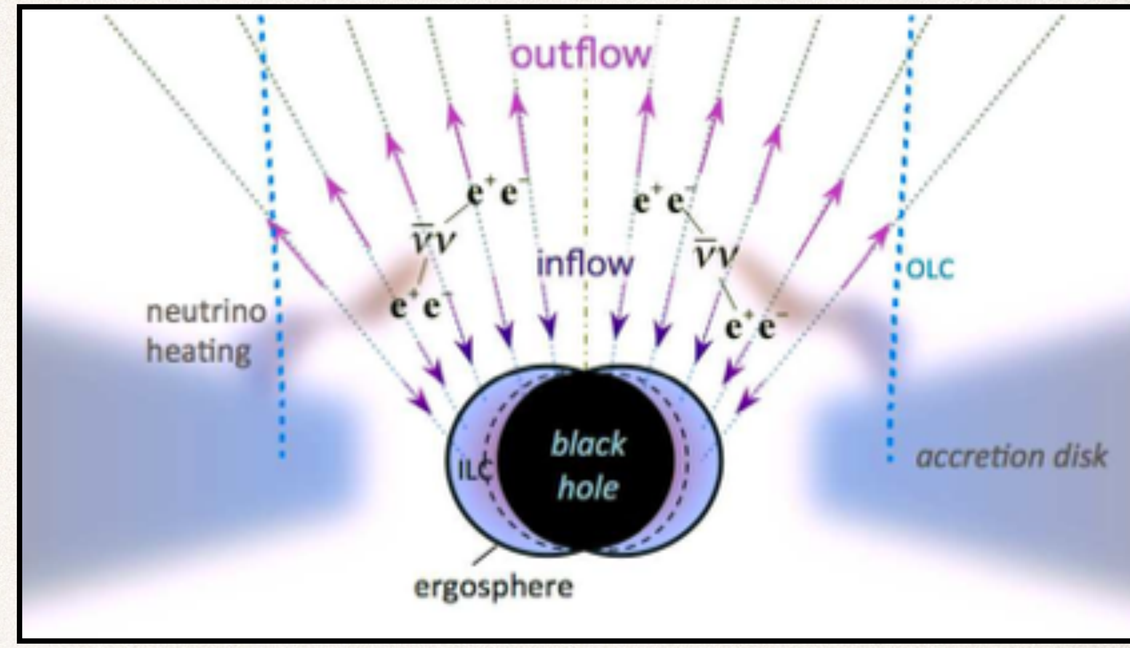

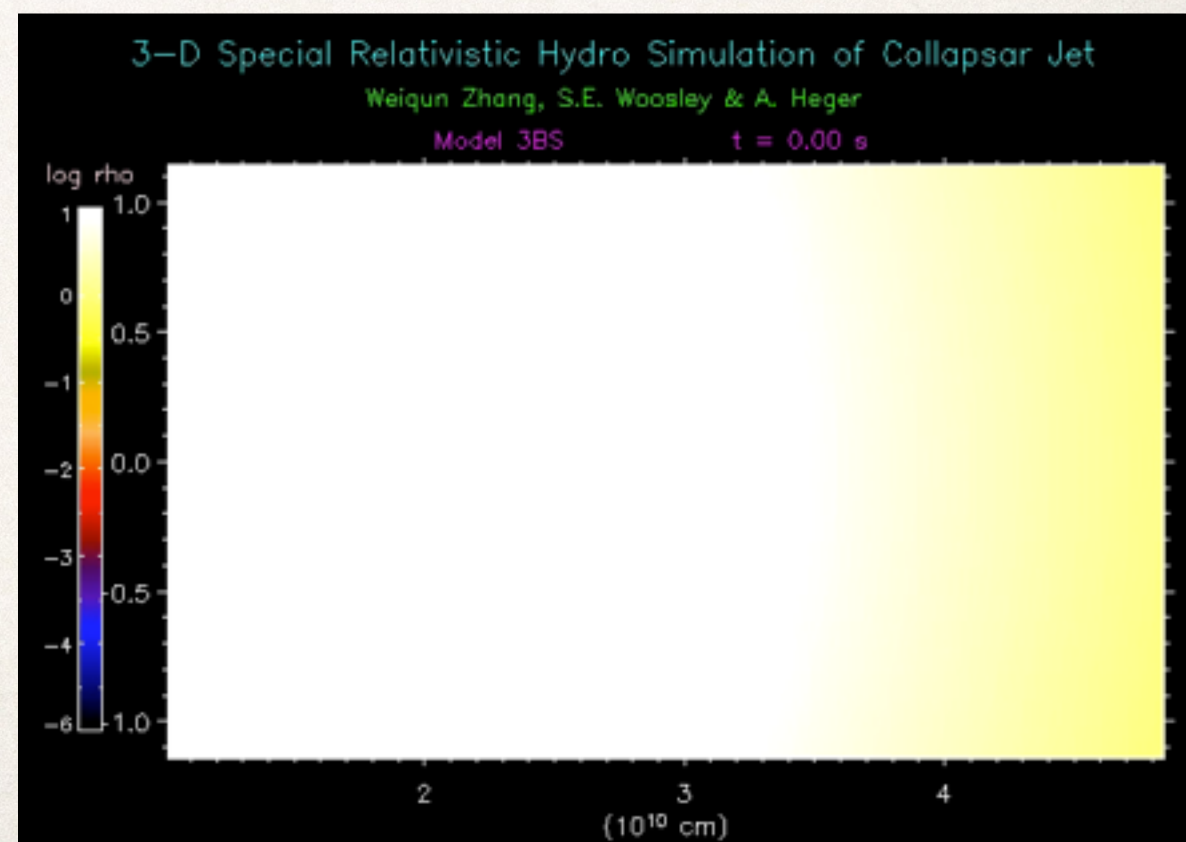

Pair load by neutrino annihilation

Neutron dragging?

Collapsar: jet interactions

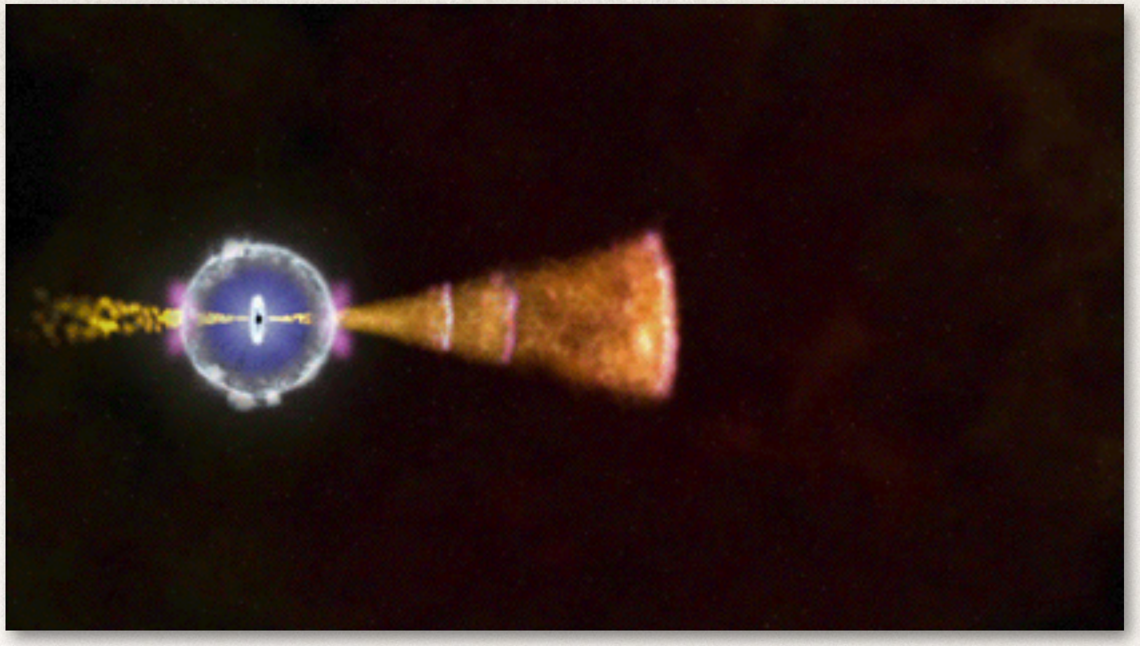

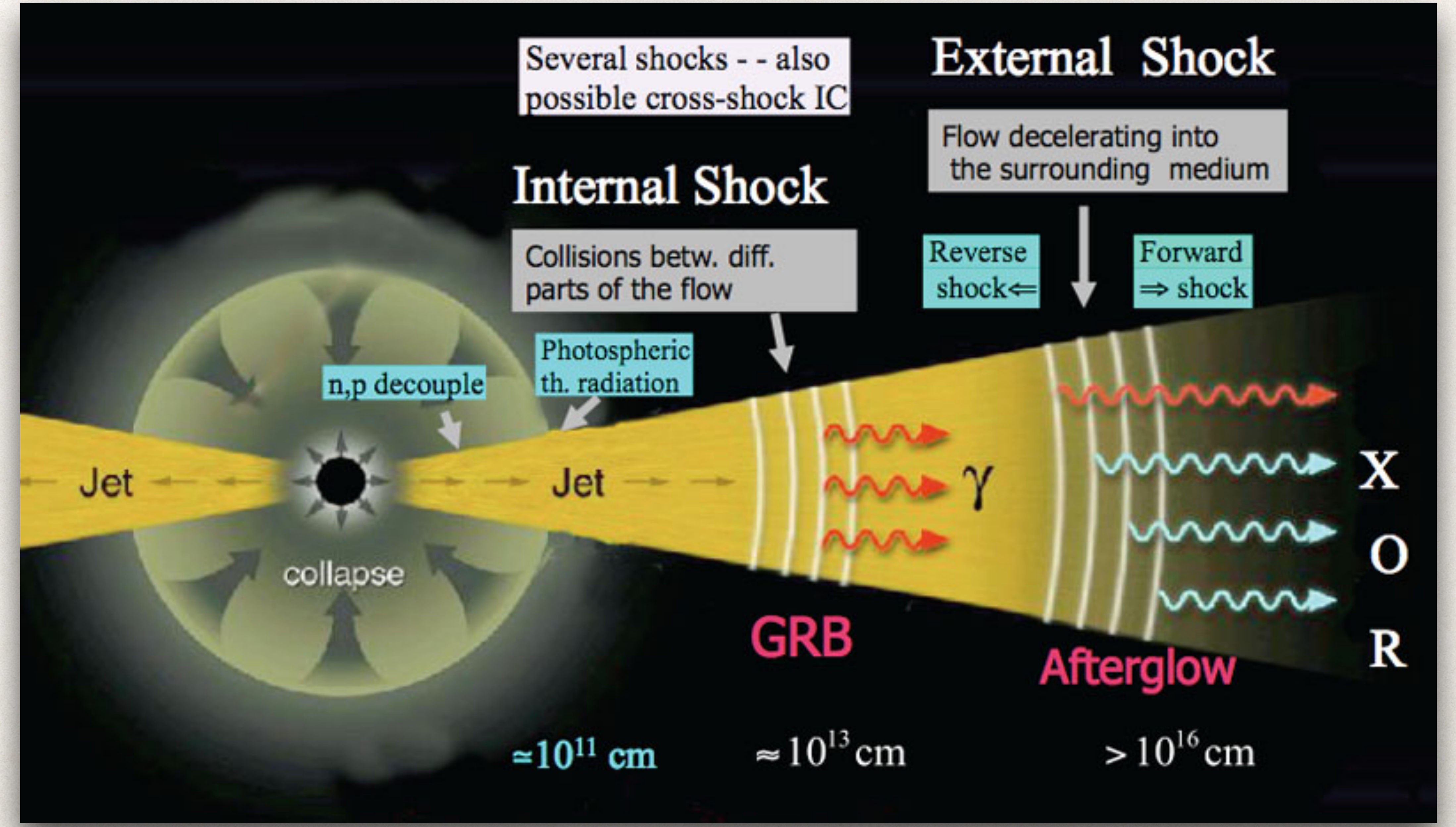

Short gamma-ray bursts: binary neutron star merger

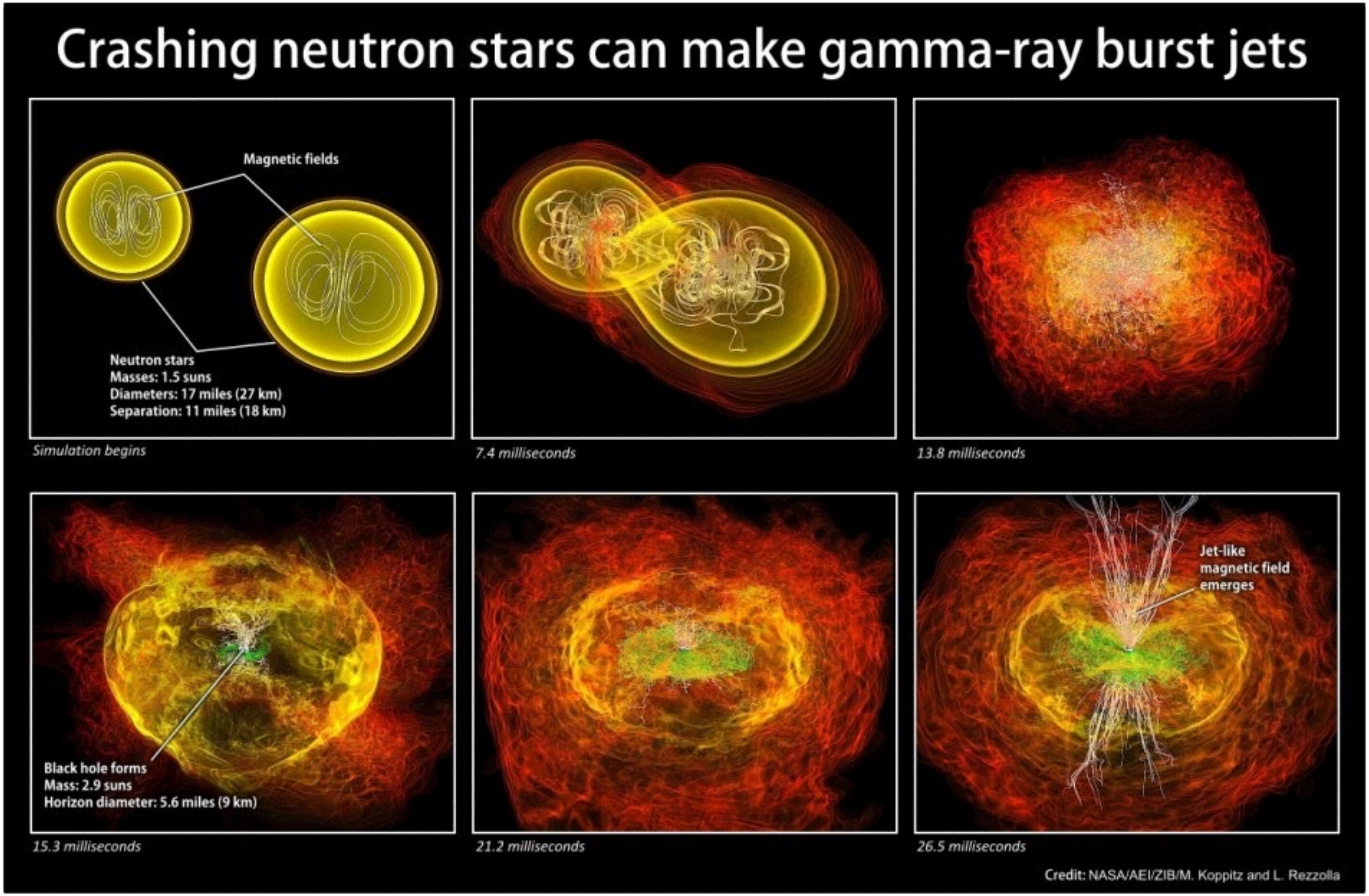

Neutrino cooled accretion disks

$$p + e^- \to n + \nu_e$$
$$p + \bar{\nu}_e \to n + e^+$$
$$p + e^- + \bar{\nu}_e \to n$$
$$n + e^+ \to p + \bar{\nu}_e$$
$$n \to p + e^- + \bar{\nu}_e$$
$$n + \nu_e \to p + e^-,$$

$$e^- + e^+ \to \nu_i + \bar{\nu}_i$$
$$n + n \to n + n + \nu_i + \bar{\nu}_i$$
$$\tilde{\gamma} \to \nu_e + \bar{\nu}_e.$$

$$p = p_{gas} + p_{rad} + p_e + p_\nu.$$

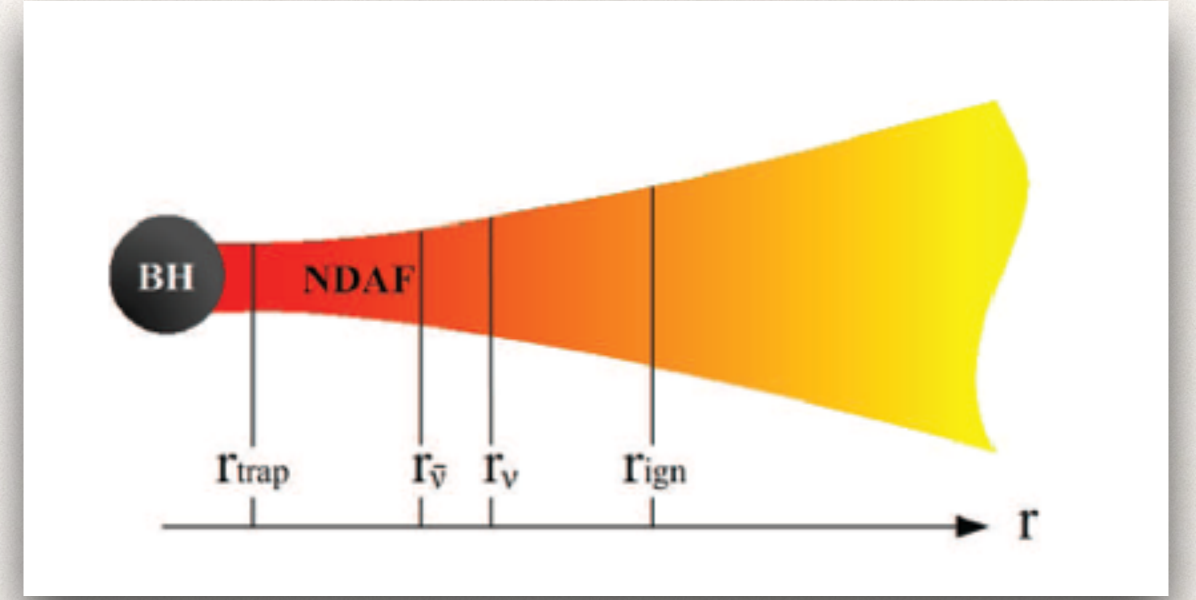

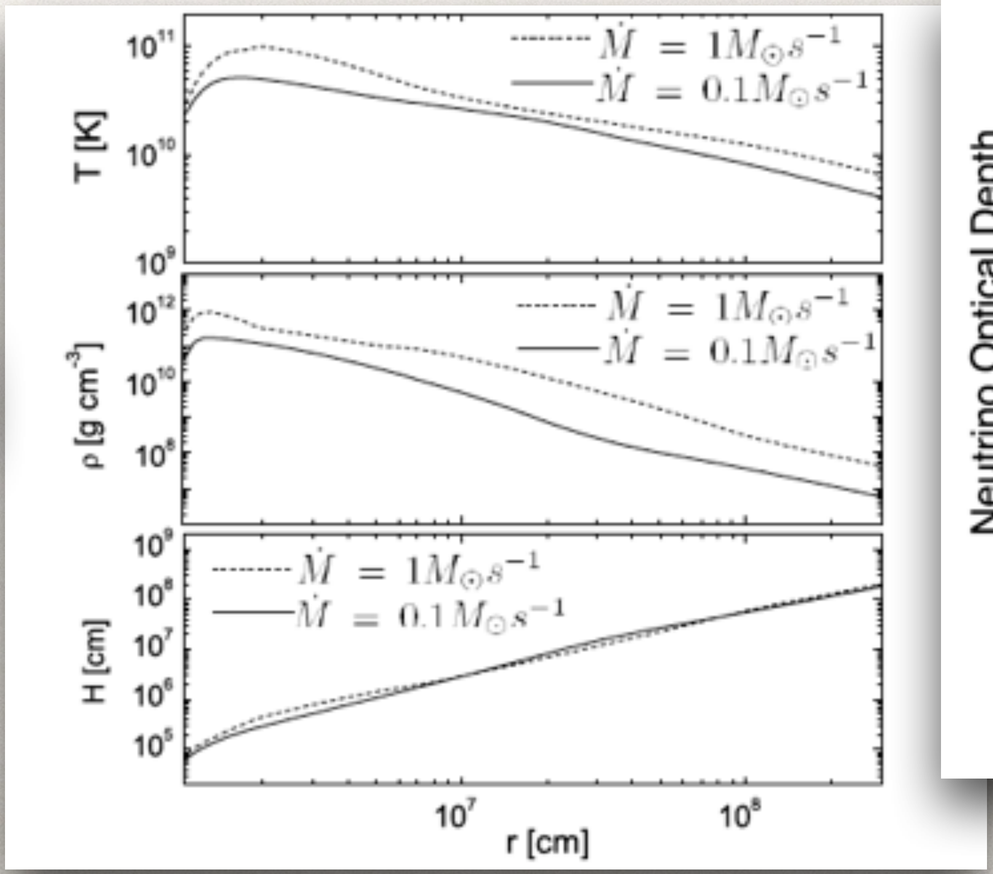

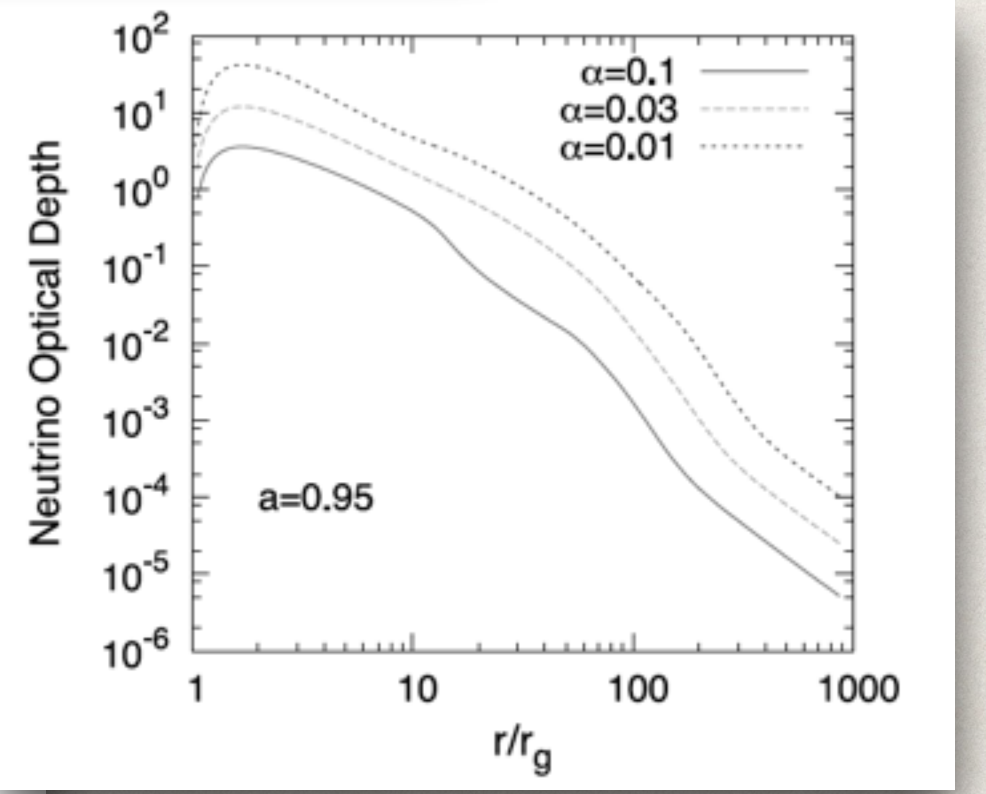

Simulations

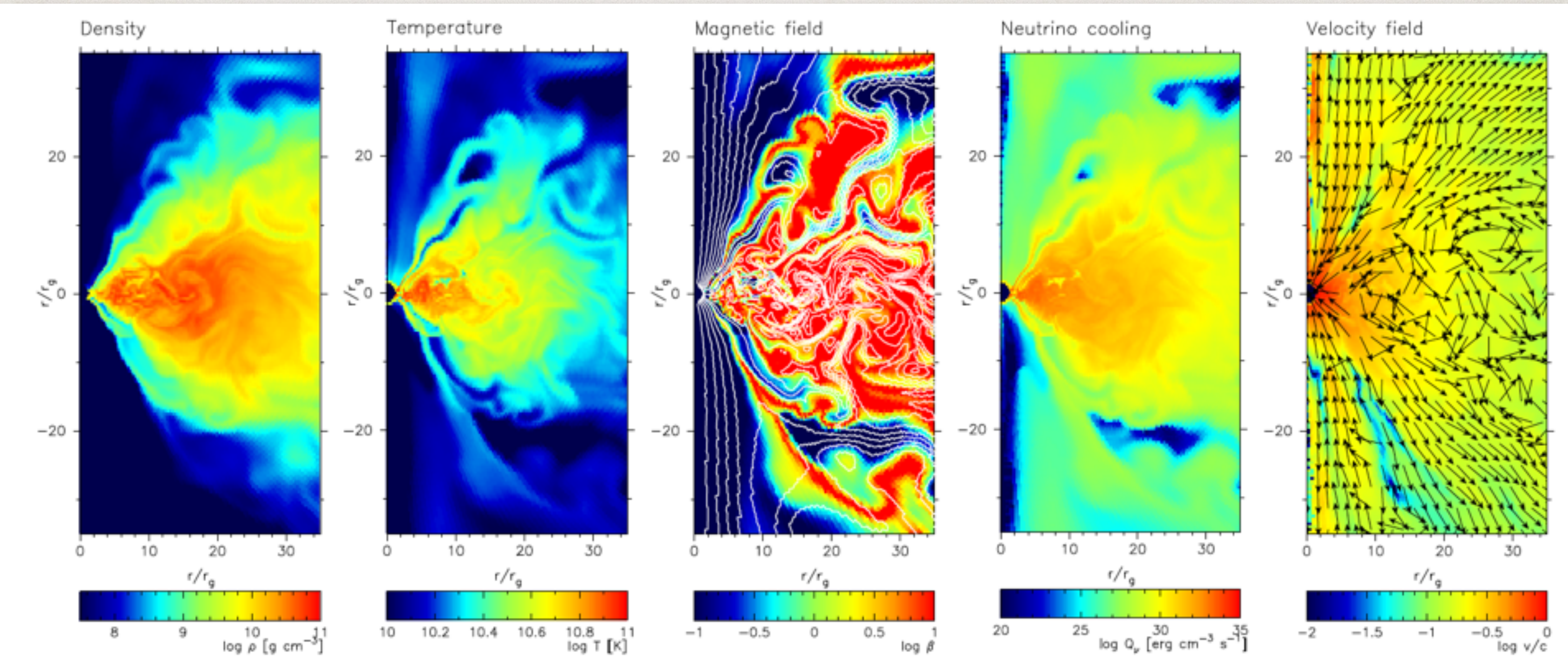

Parameters of the model: black-hole mass $M_{\rm BH} = 3\,M_\odot$, torus mass $M_{\rm t} = 0.1\,M_\odot$, and BH spin $a = 0.6$.

ß= $P_{\rm gas}/P_{\rm mag}$

Janiuk 2017

Neutrino cooled accretion disks

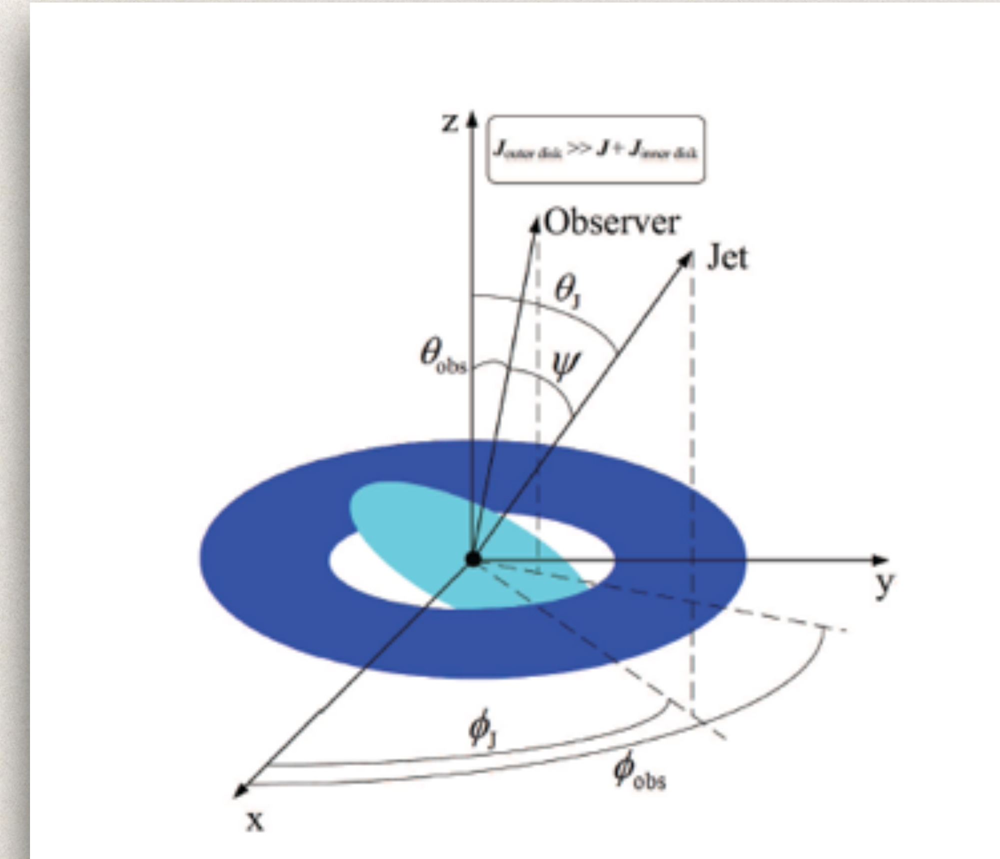

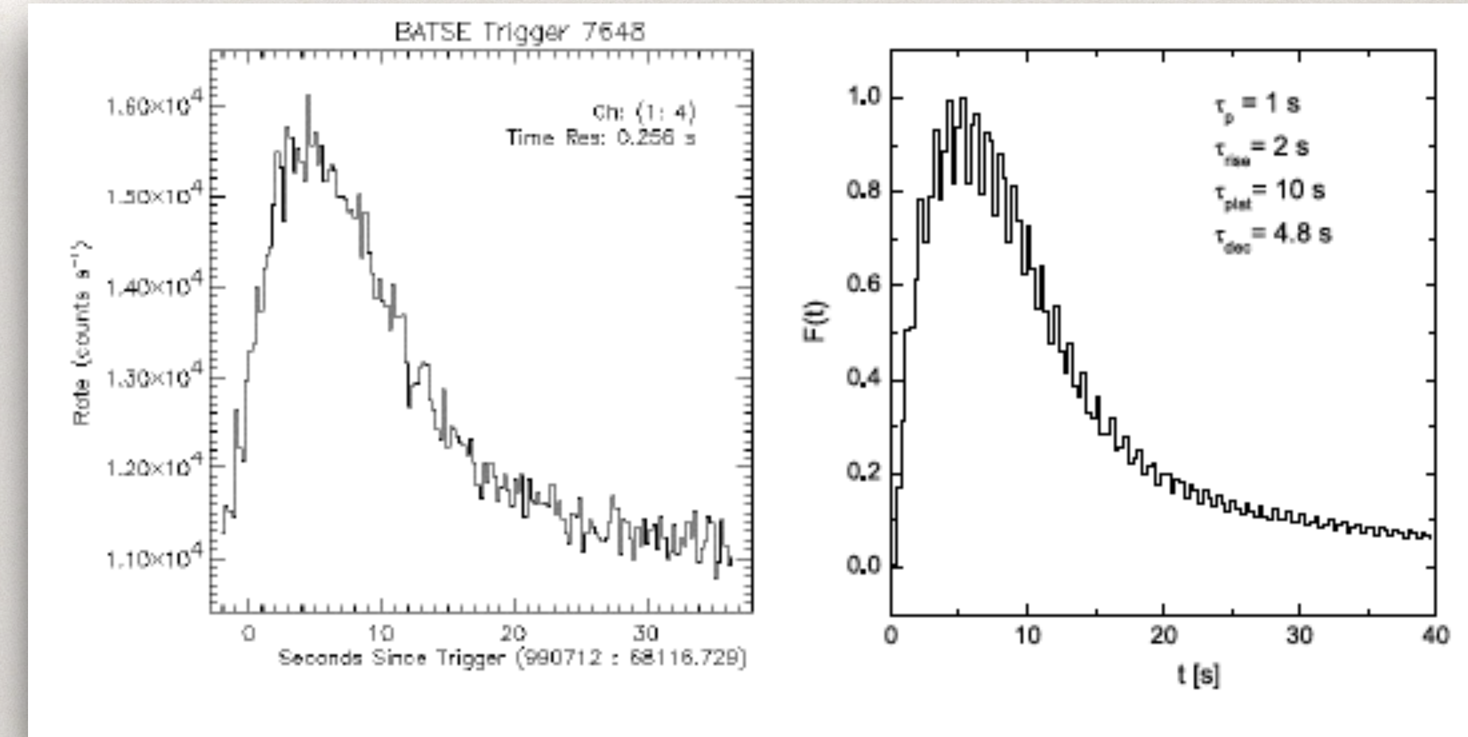

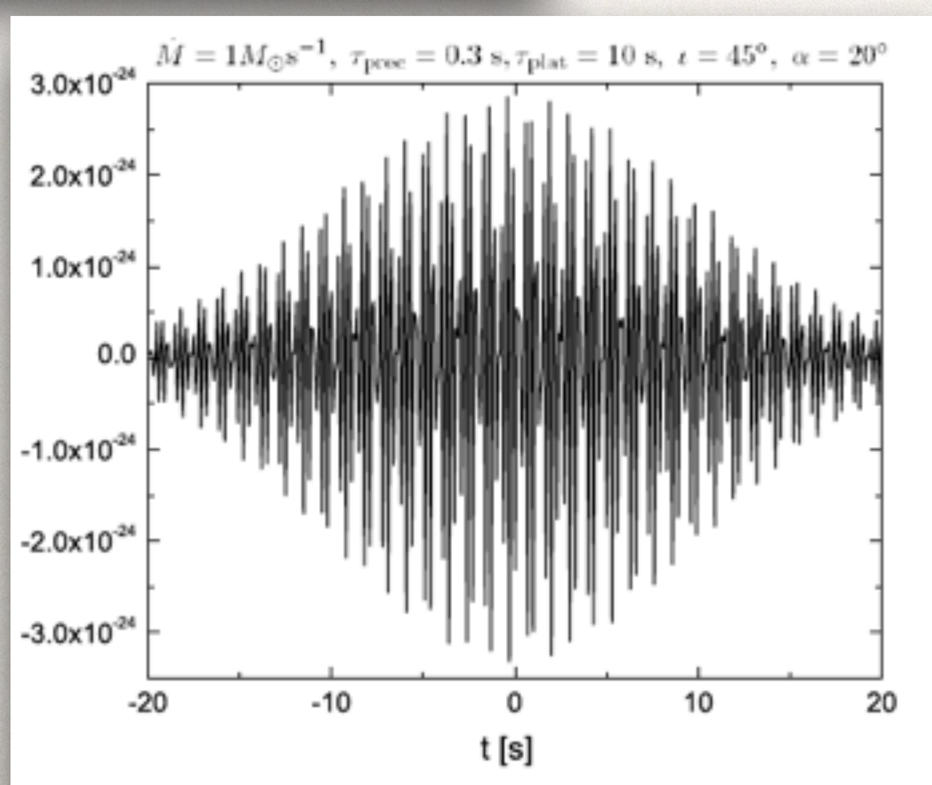

Depending on the viewing angle, these events can be detected with LIGO for d<100 Mpc (Romero et al. 2010).

Tidal effects

Some objects can approach the BH close enough to undergo tidal effects

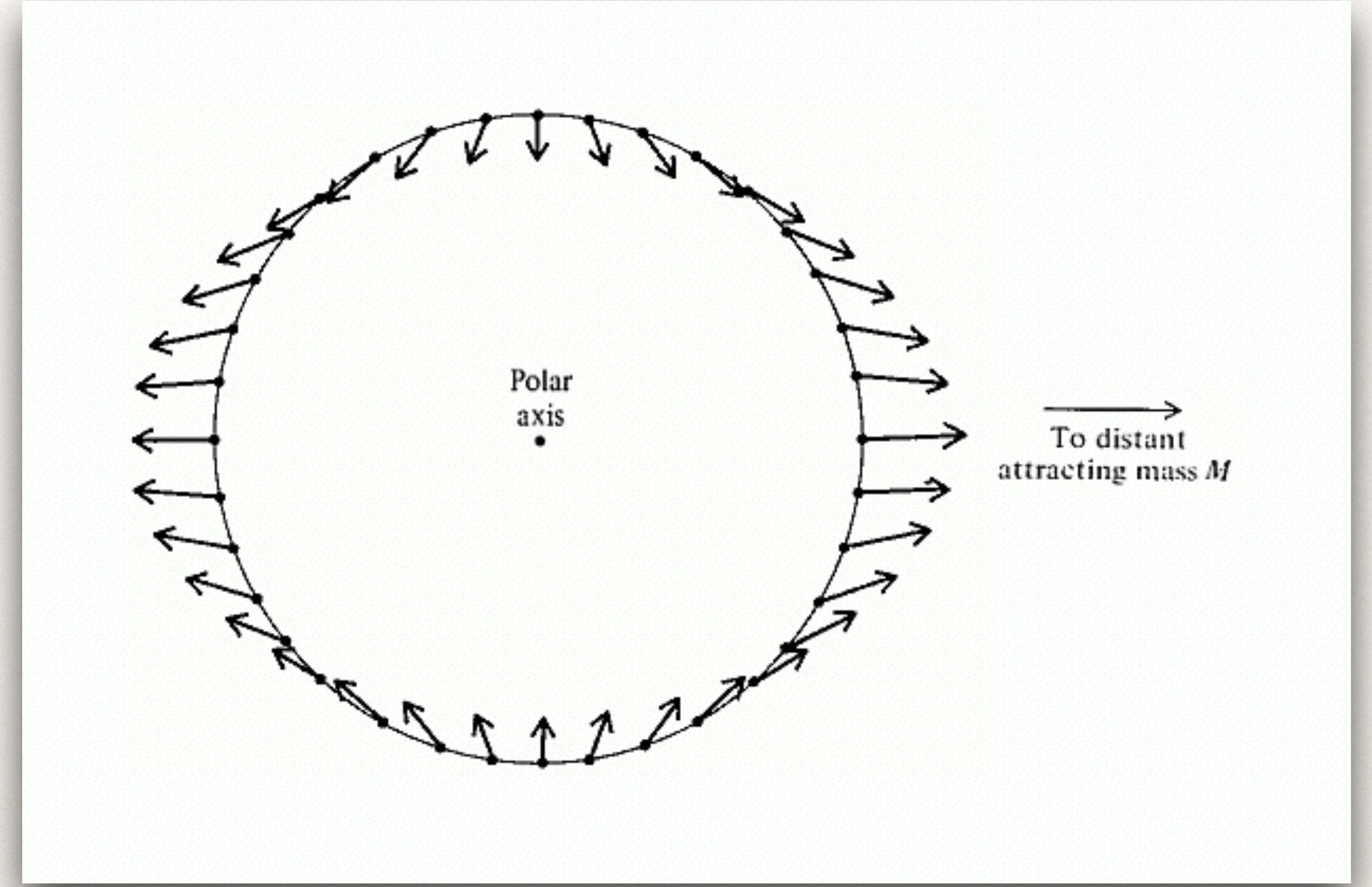

Differential acceleration

$$dg = \frac{2r_g}{r^3}c^2dr.$$

Sgr A*

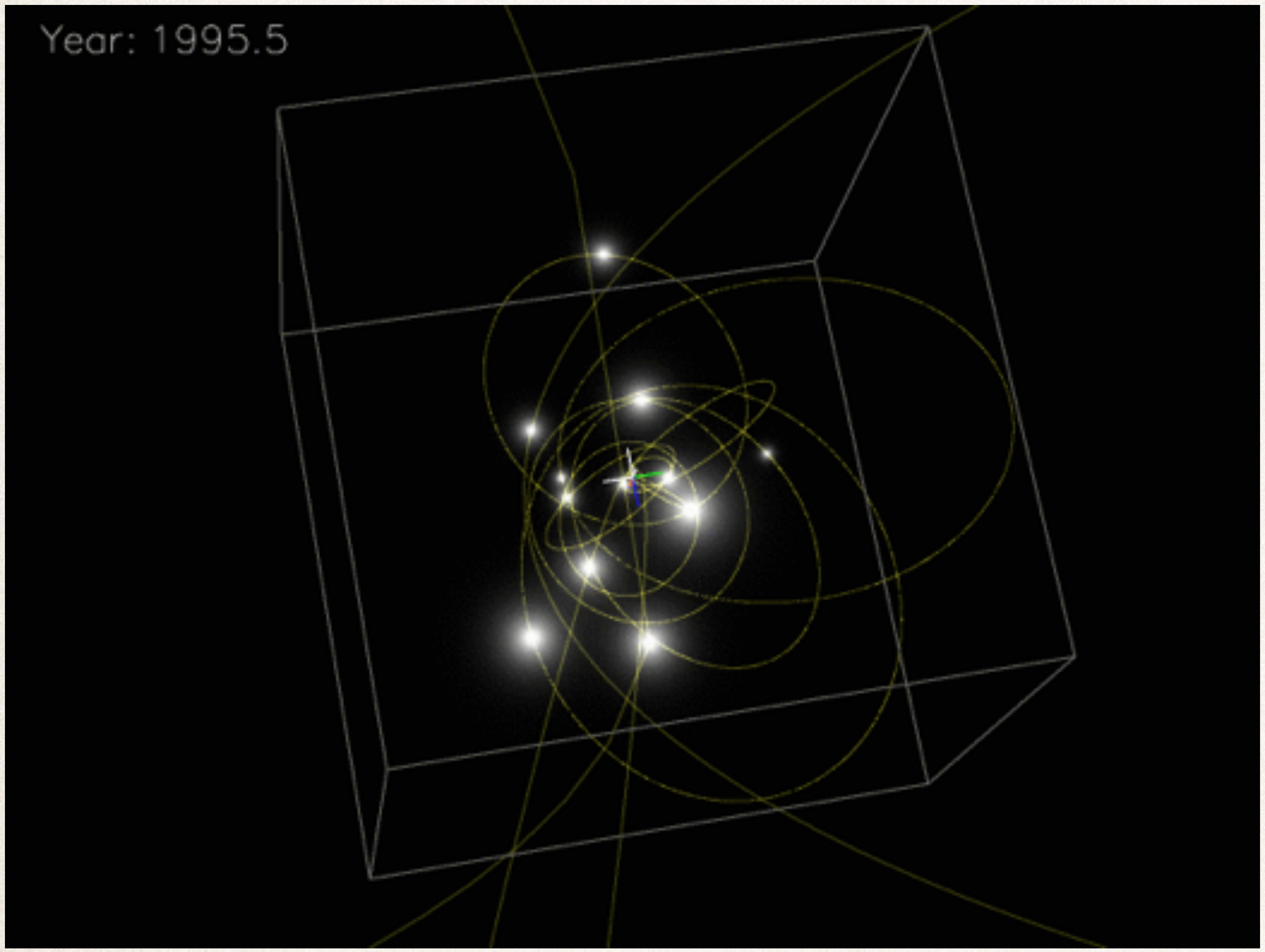

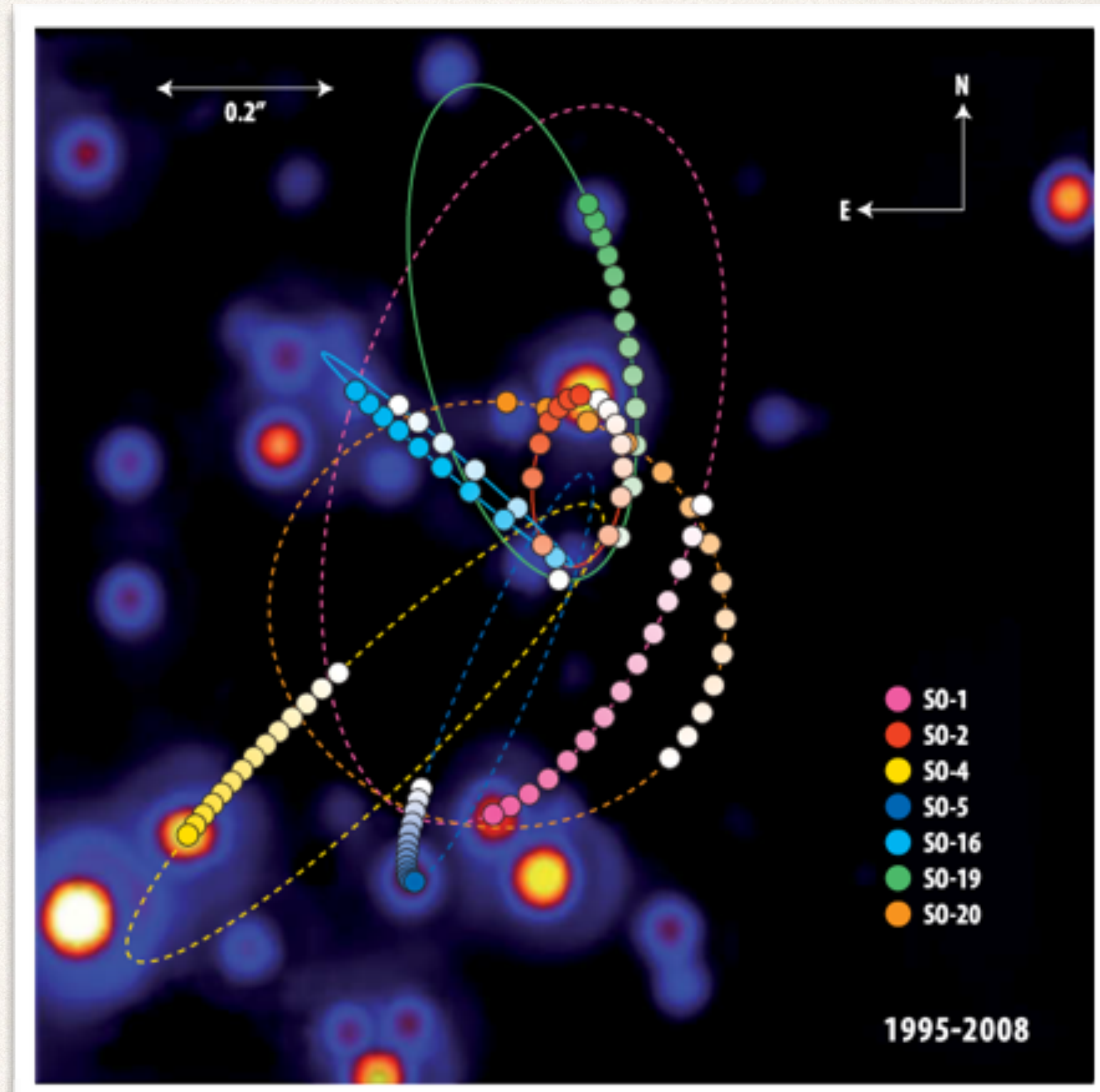

Gravitational capture: $$\sigma_{\text{non-rel}} = \pi b_{\text{cr}}^2 = 4\pi \frac{c^2 r_{\text{Schw}}^2}{v_\infty^2}.$$

Cloud G2

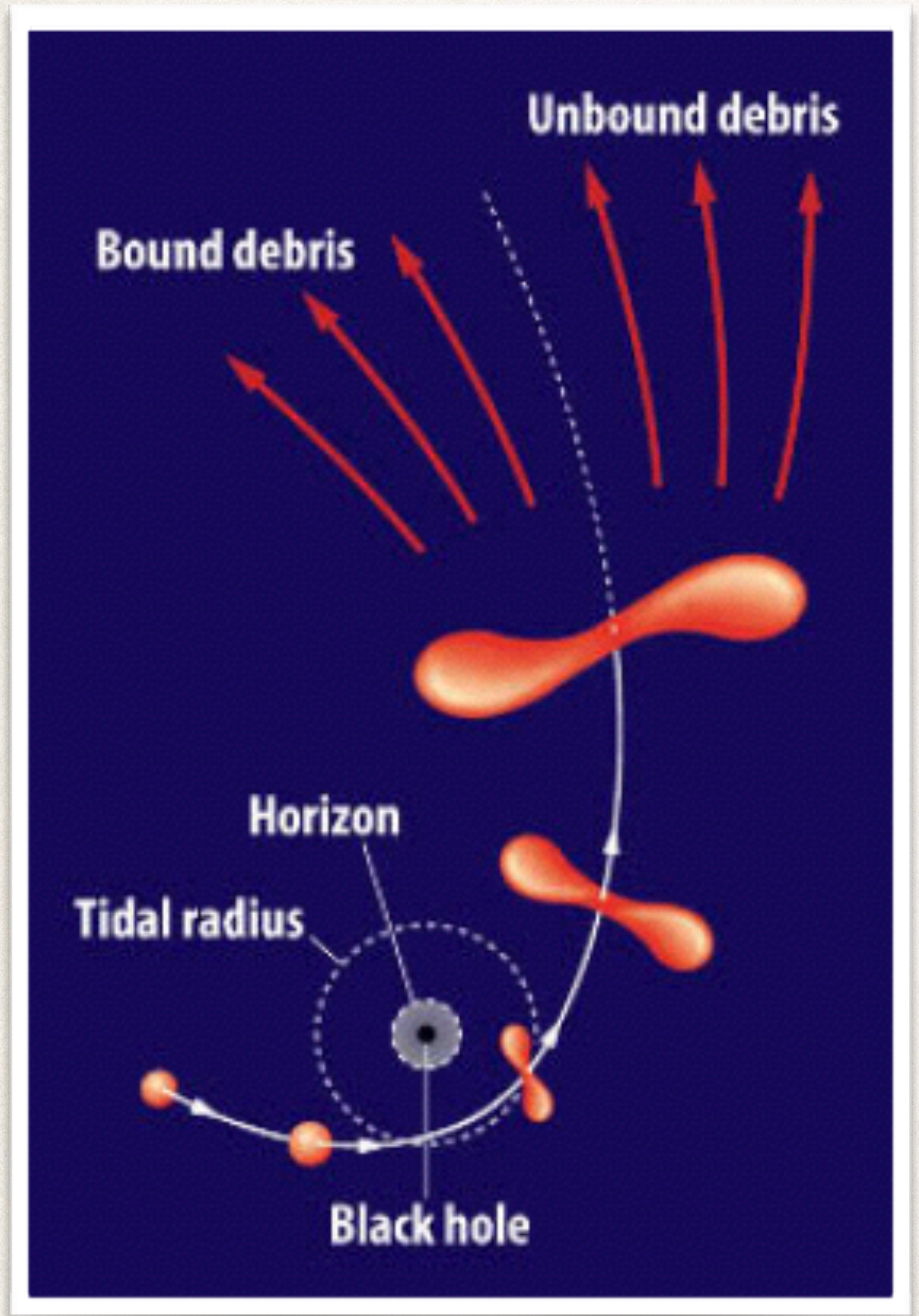

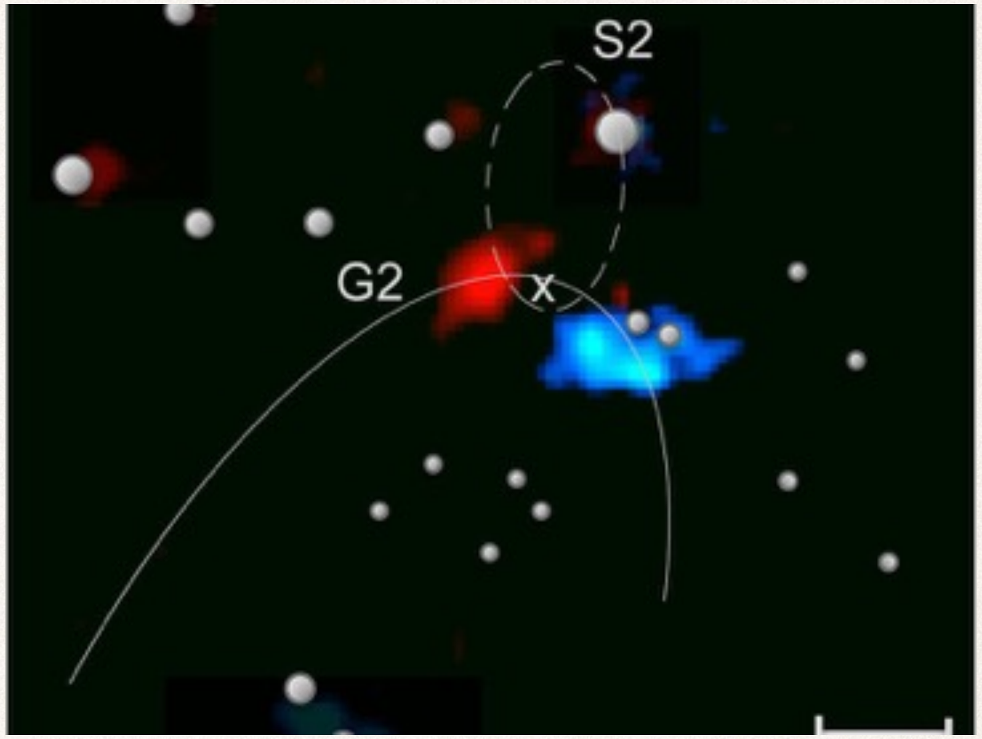

G2 was likely a light binary system, a protostar, or a clump in a stream.

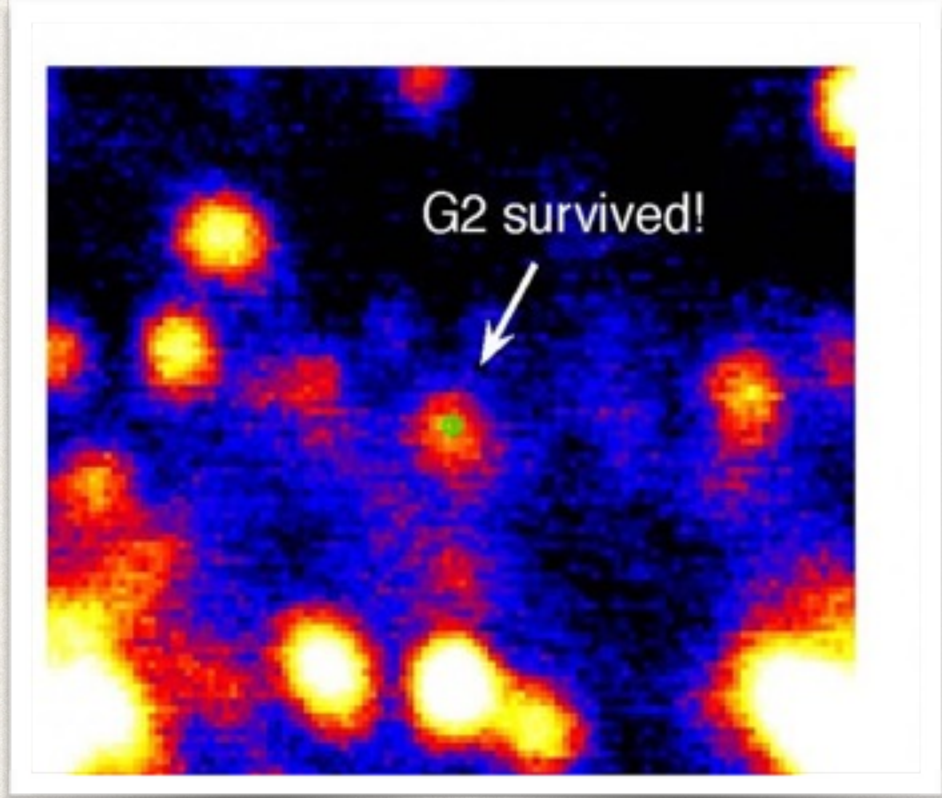

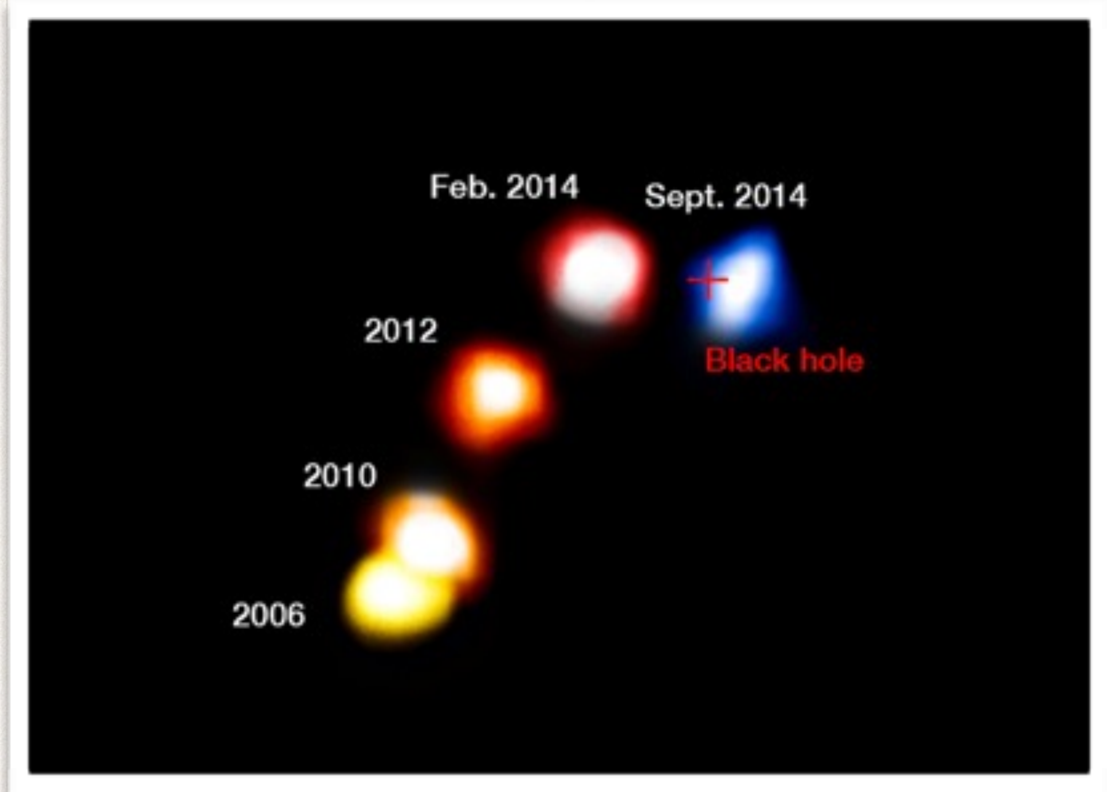

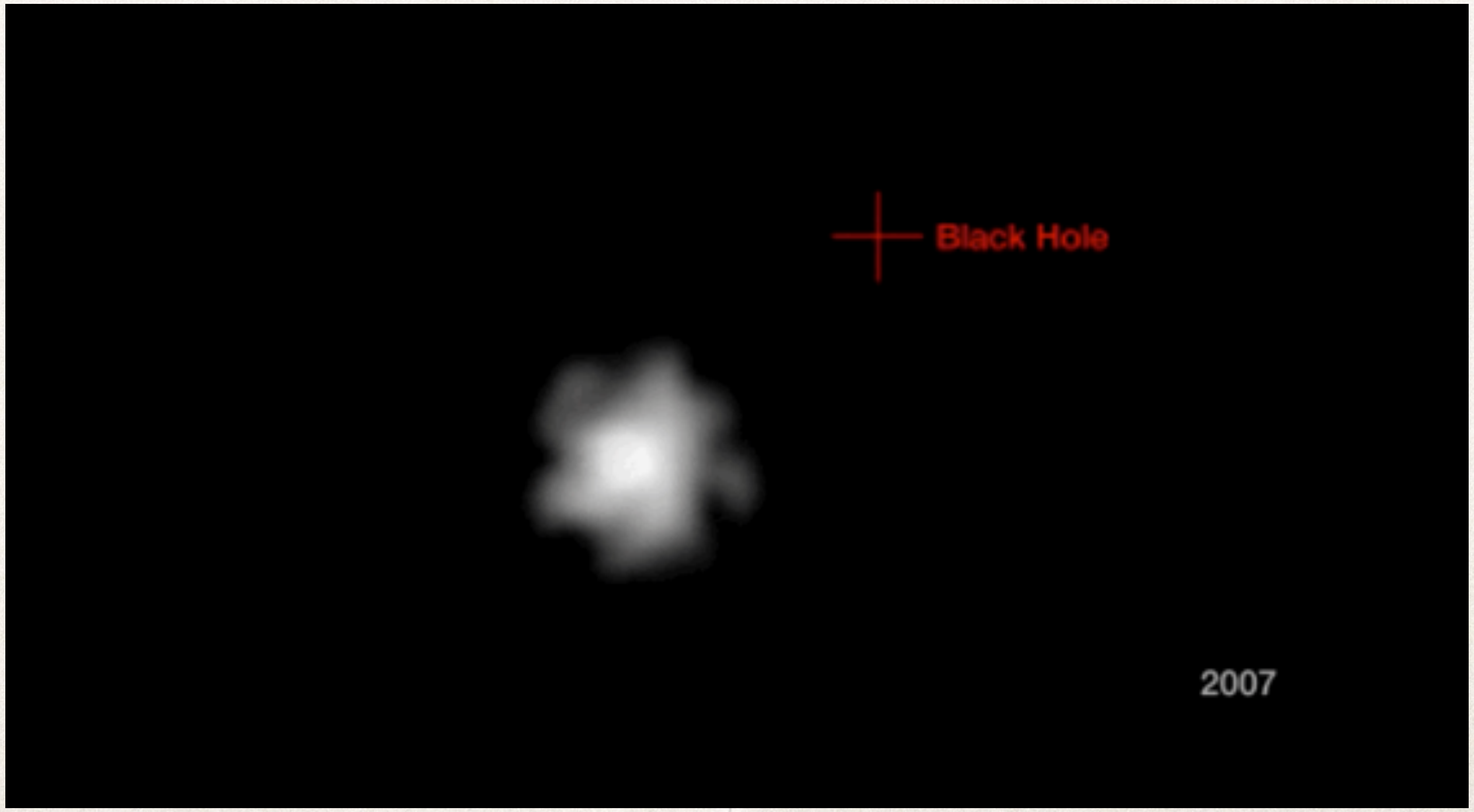

Other tidal disruption events (TDE)

- TDE rate: 10^{-4}–10^{-5}/yr/galaxy
- Several tens detected
- Formation of transient accretion disks and jets
- Both thermal and non-thermal emission
- Super-Eddington accretion rates
- Timescales from months in X-rays to years in radio

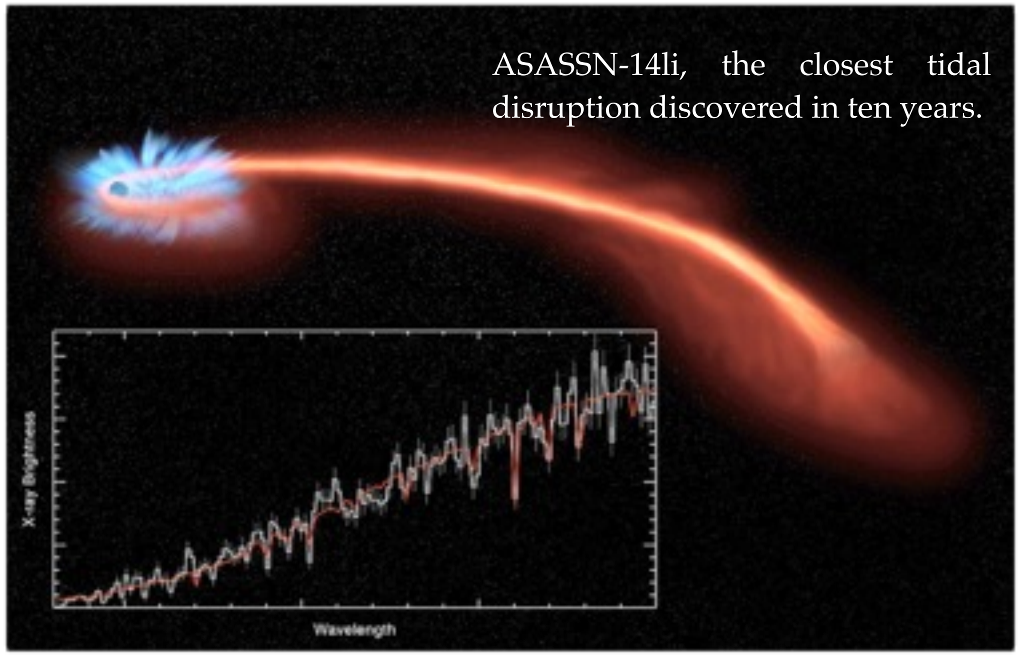

ASASSN-14li, the closest tidal disruption discovered in ten years.

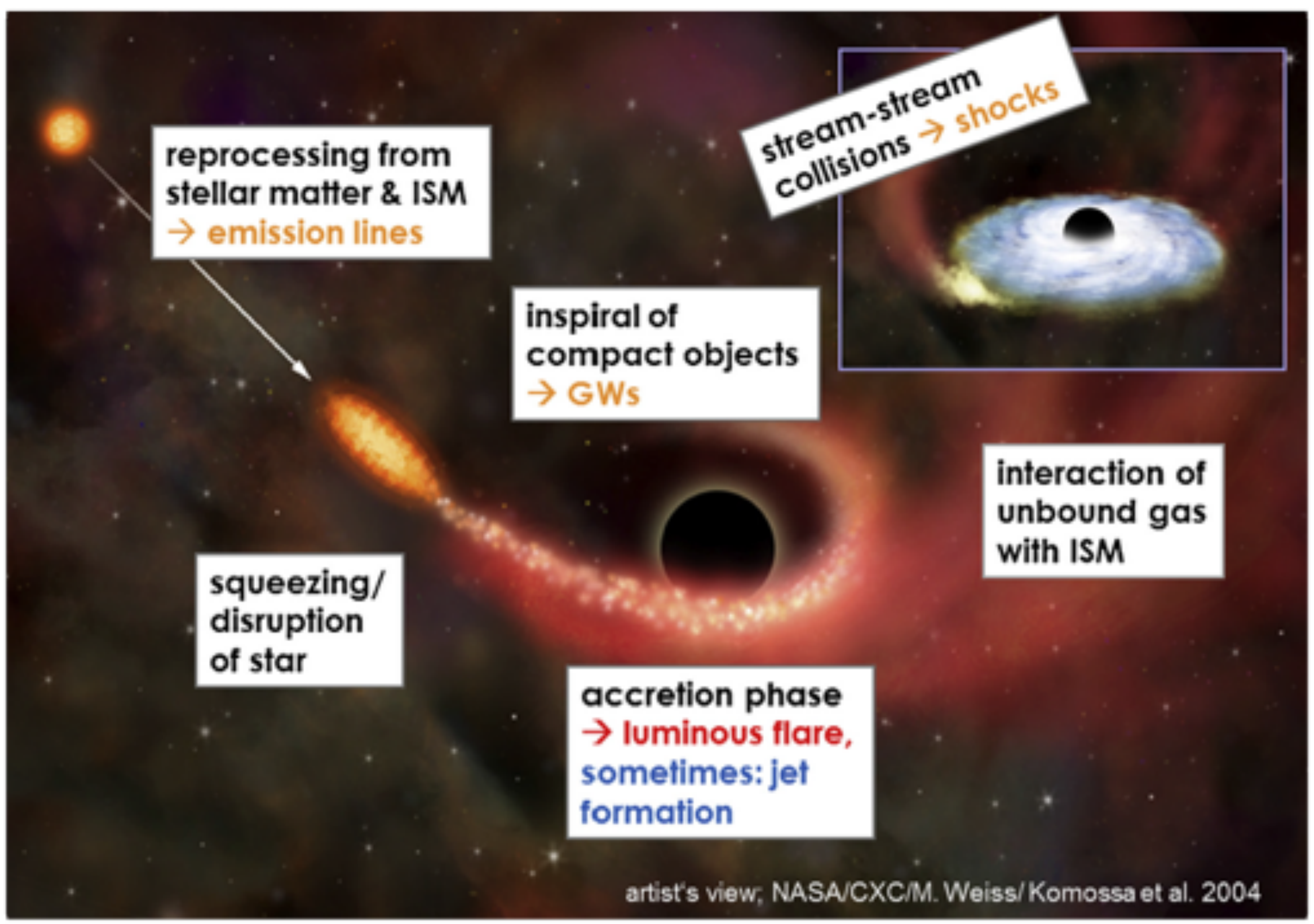

artist's view; NASA/CXC/M. Weiss/Komossa et al. 2004

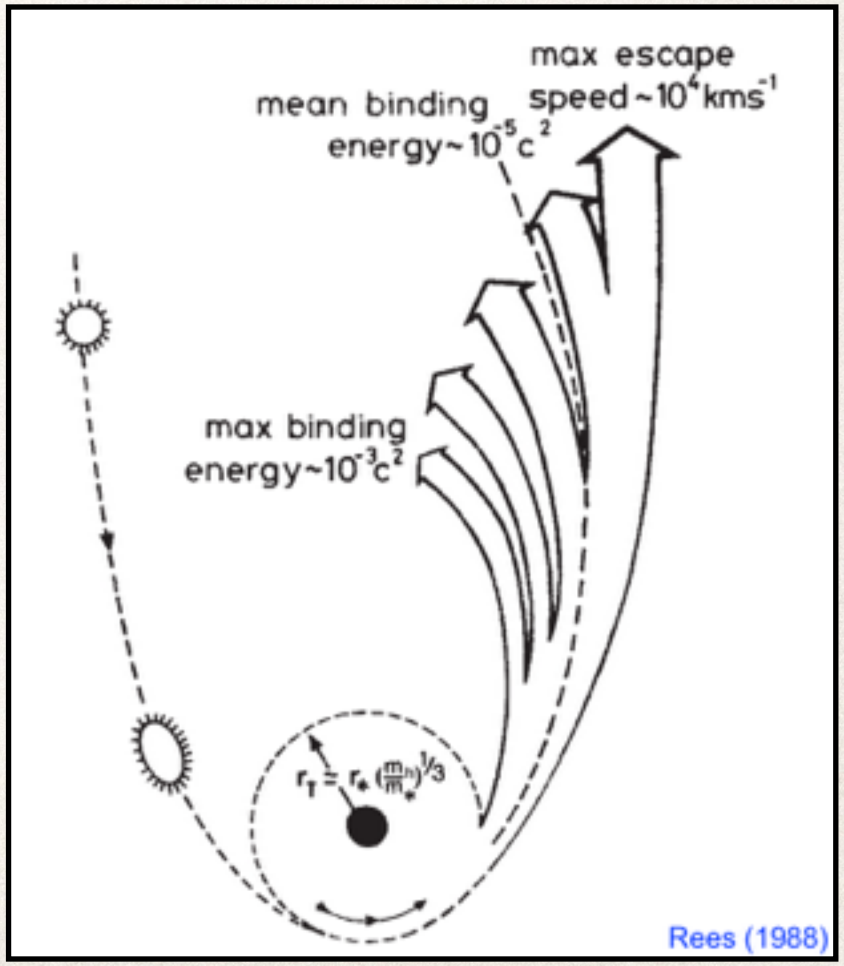

Rees (1988)

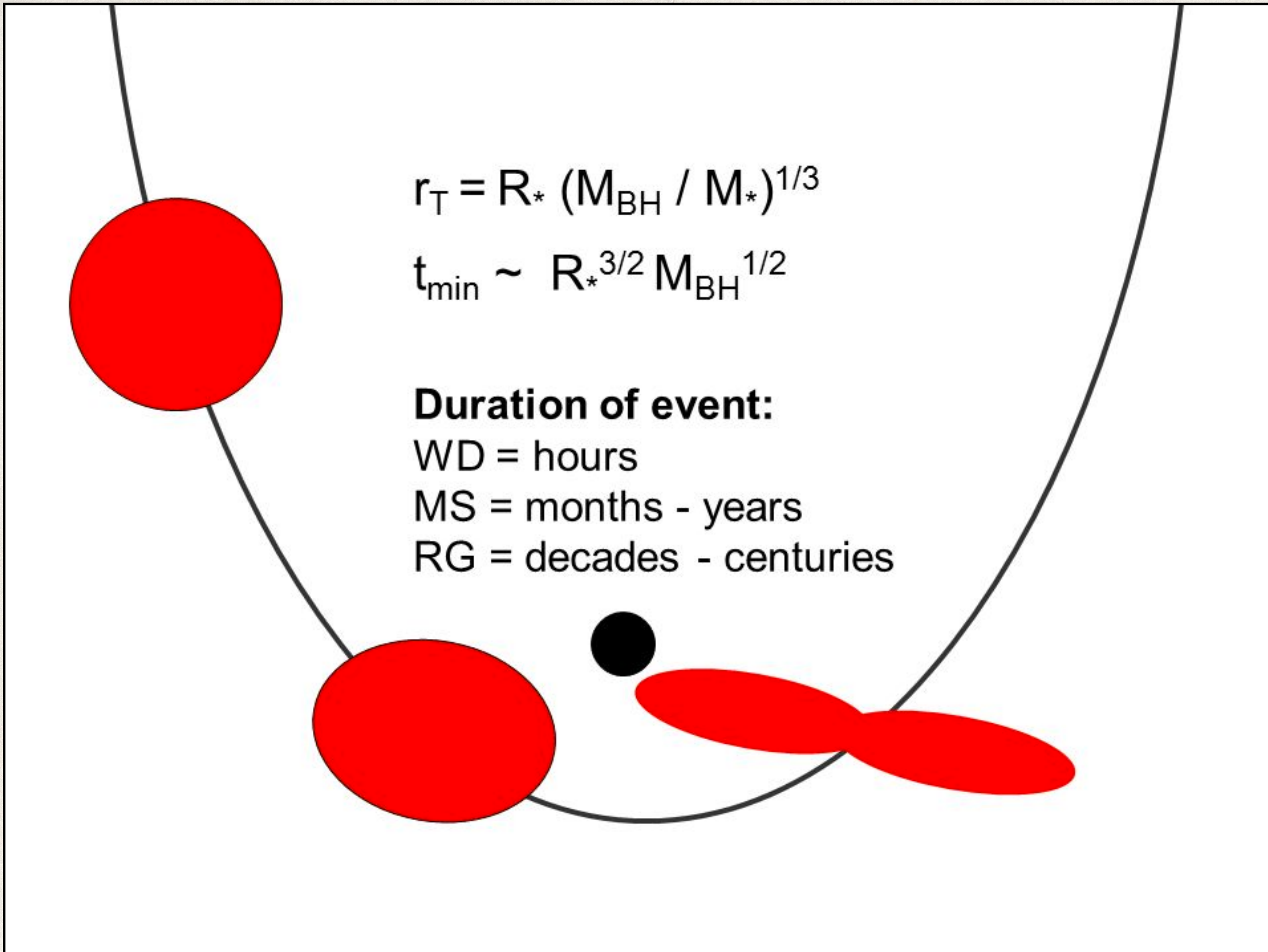
$r_T = R_* (M_{BH} / M_*)^{1/3}$
$t_{min} \sim R_*^{3/2} M_{BH}^{1/2}$
Duration of event:
WD = hours
MS = months - years
RG = decades - centuries

For more comprehensive treatments and discussions

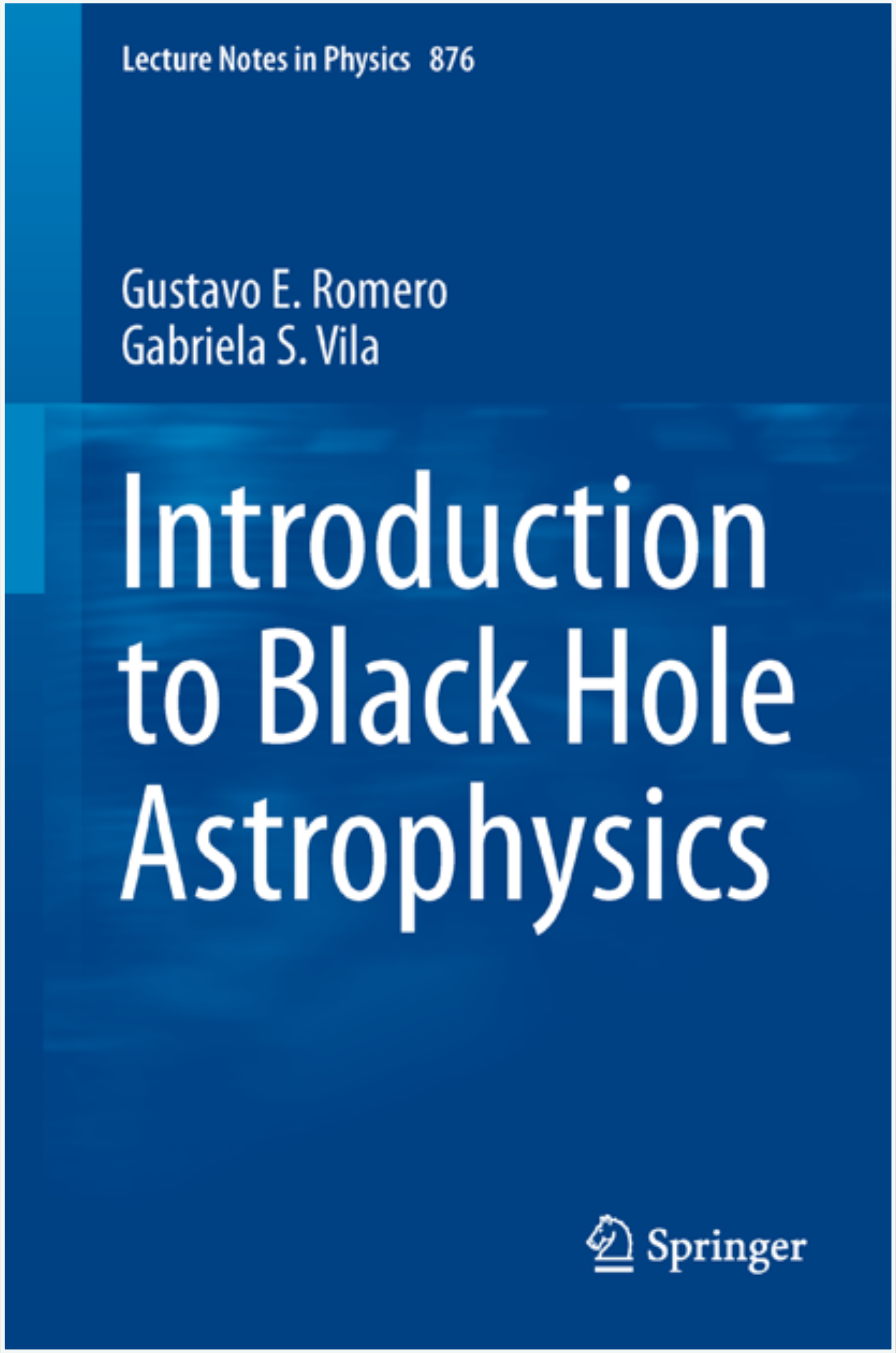

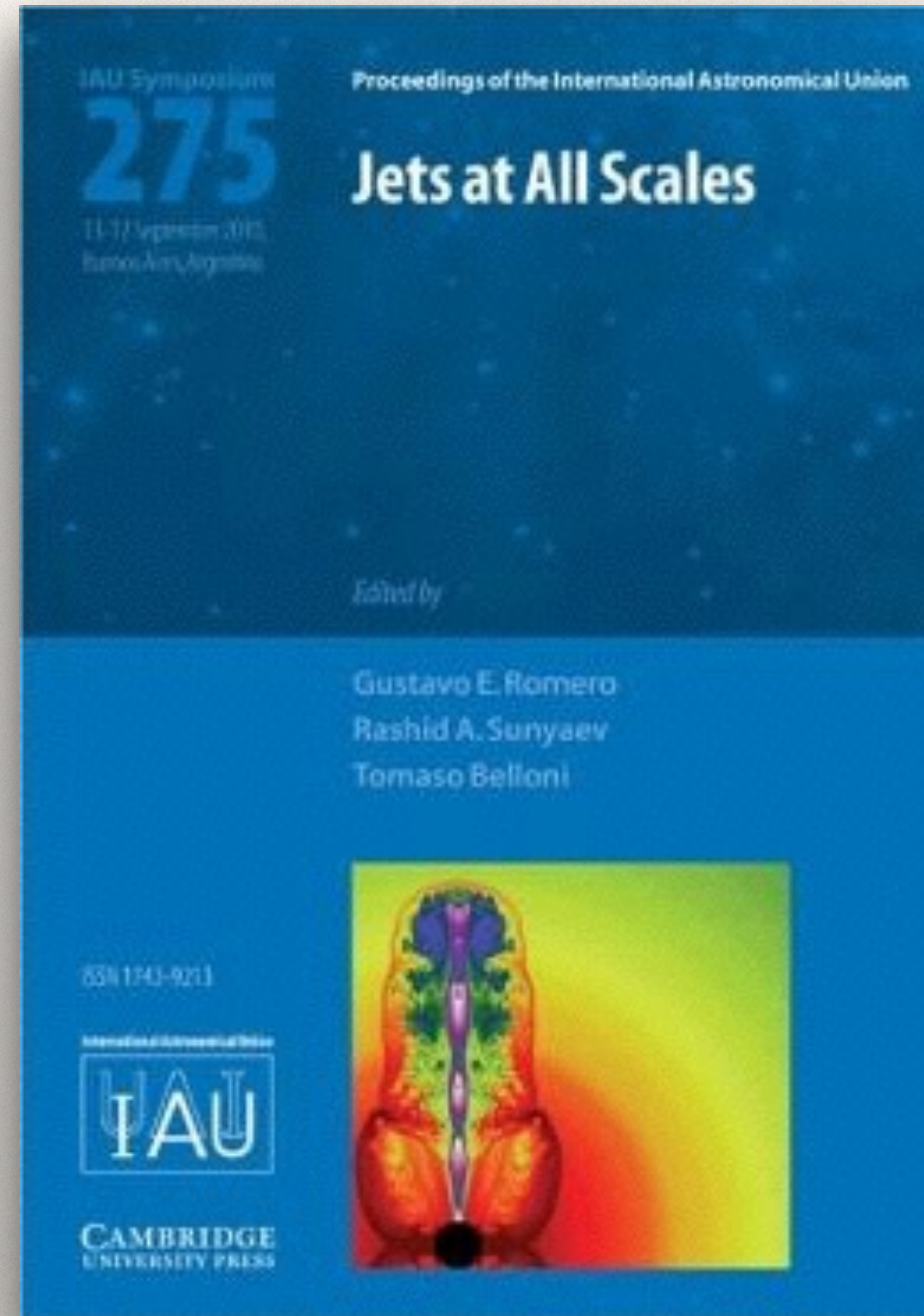

–*Thank you*

Gravitational waves from BH mergers

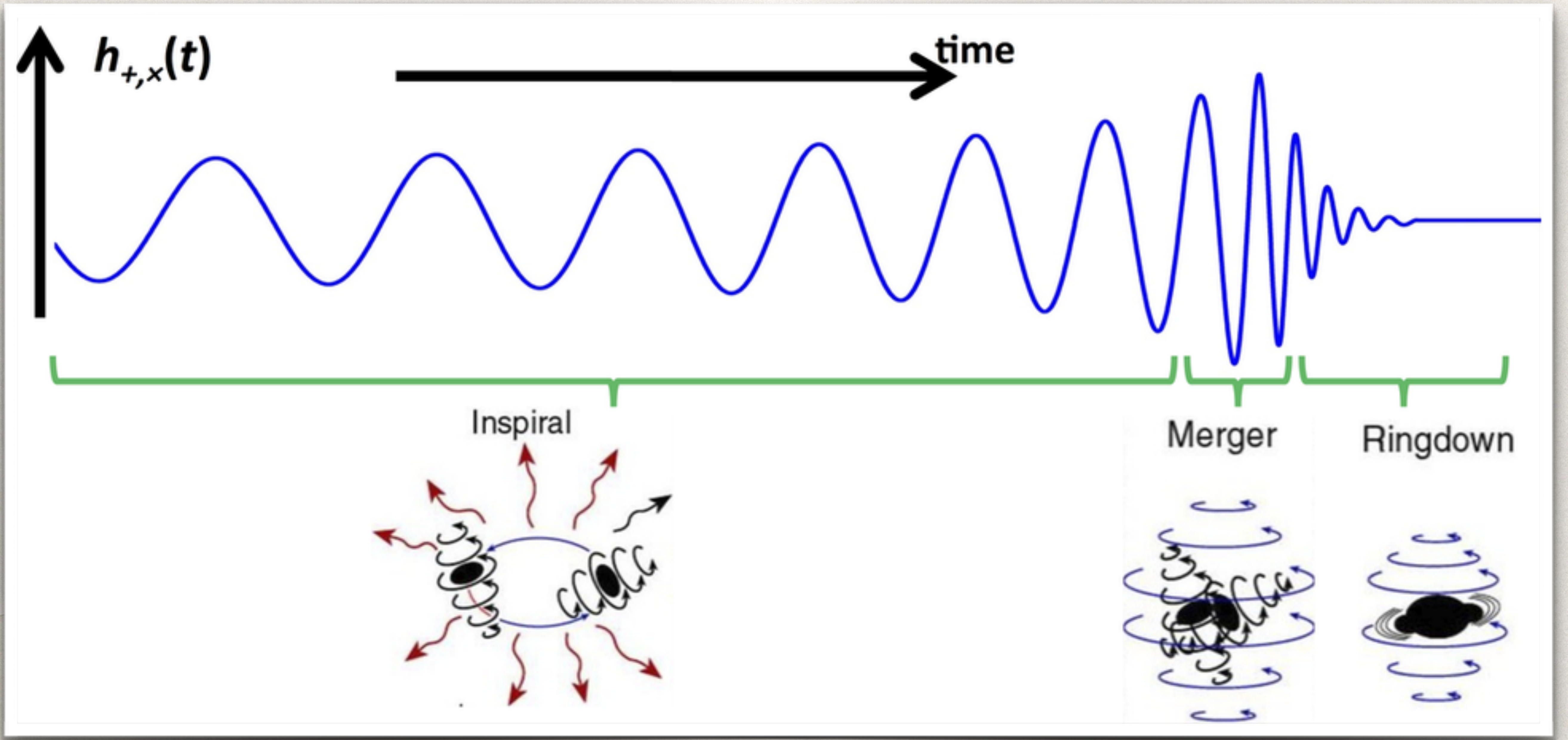

$$g_{\mu\nu} = \eta_{\mu\nu} + h_{\mu\nu}.$$

$$\Box^2 \overline{h}^{\mu\nu} = 0.$$

$$\overline{h}^{\mu\nu} = \Re[A^{\mu\nu} \exp{(ik_\alpha x^\alpha)}].$$

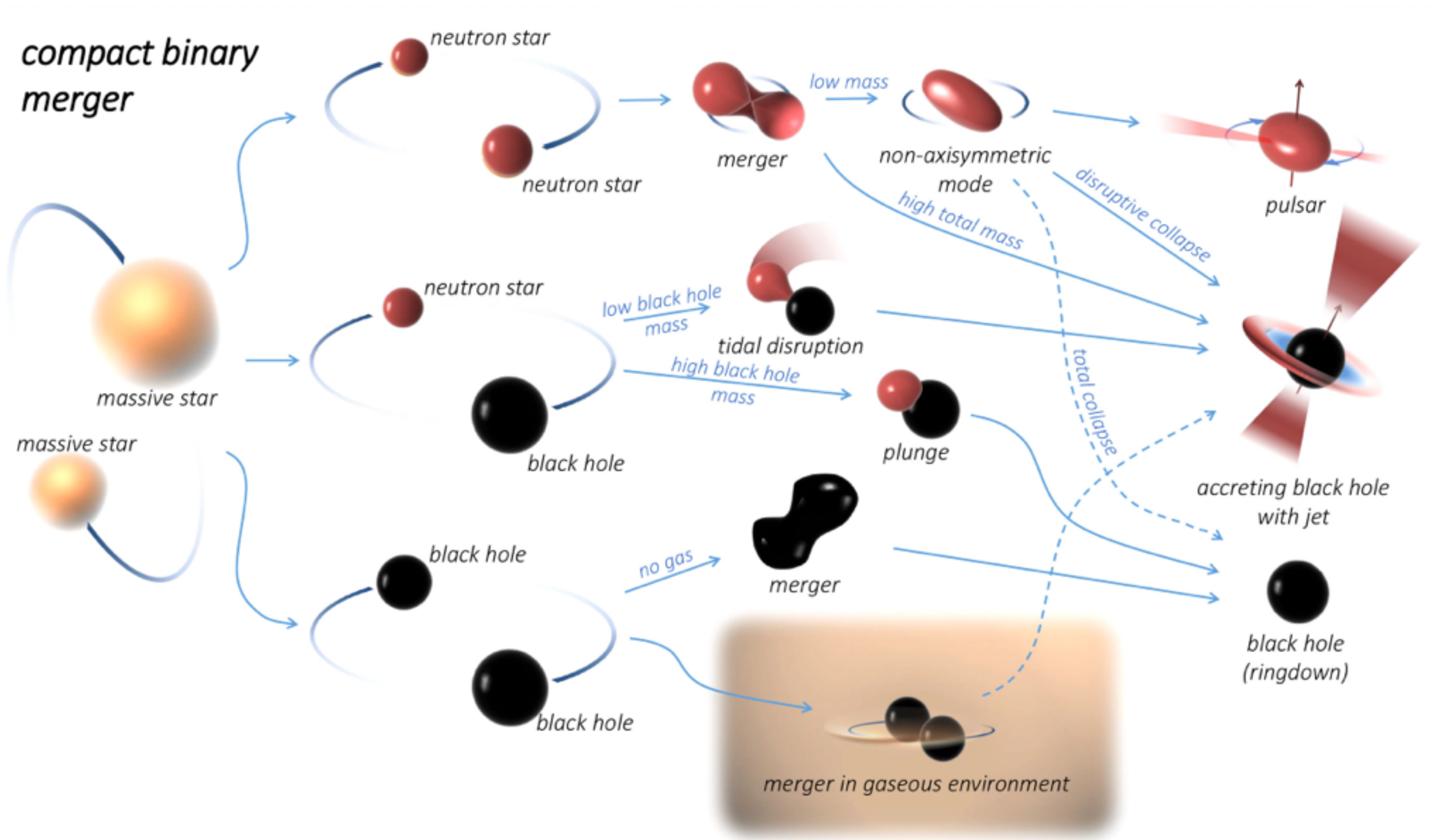
compact binary merger
neutron star
neutron star
merger
low mass
non-axisymmetric mode
pulsar
high total mass
disruptive collapse
massive star
neutron star
low black hole mass
tidal disruption
high black hole mass
total collapse
black hole
plunge
accreting black hole with jet
massive star
black hole
no gas
merger
black hole
black hole (ringdown)
merger in gaseous environment

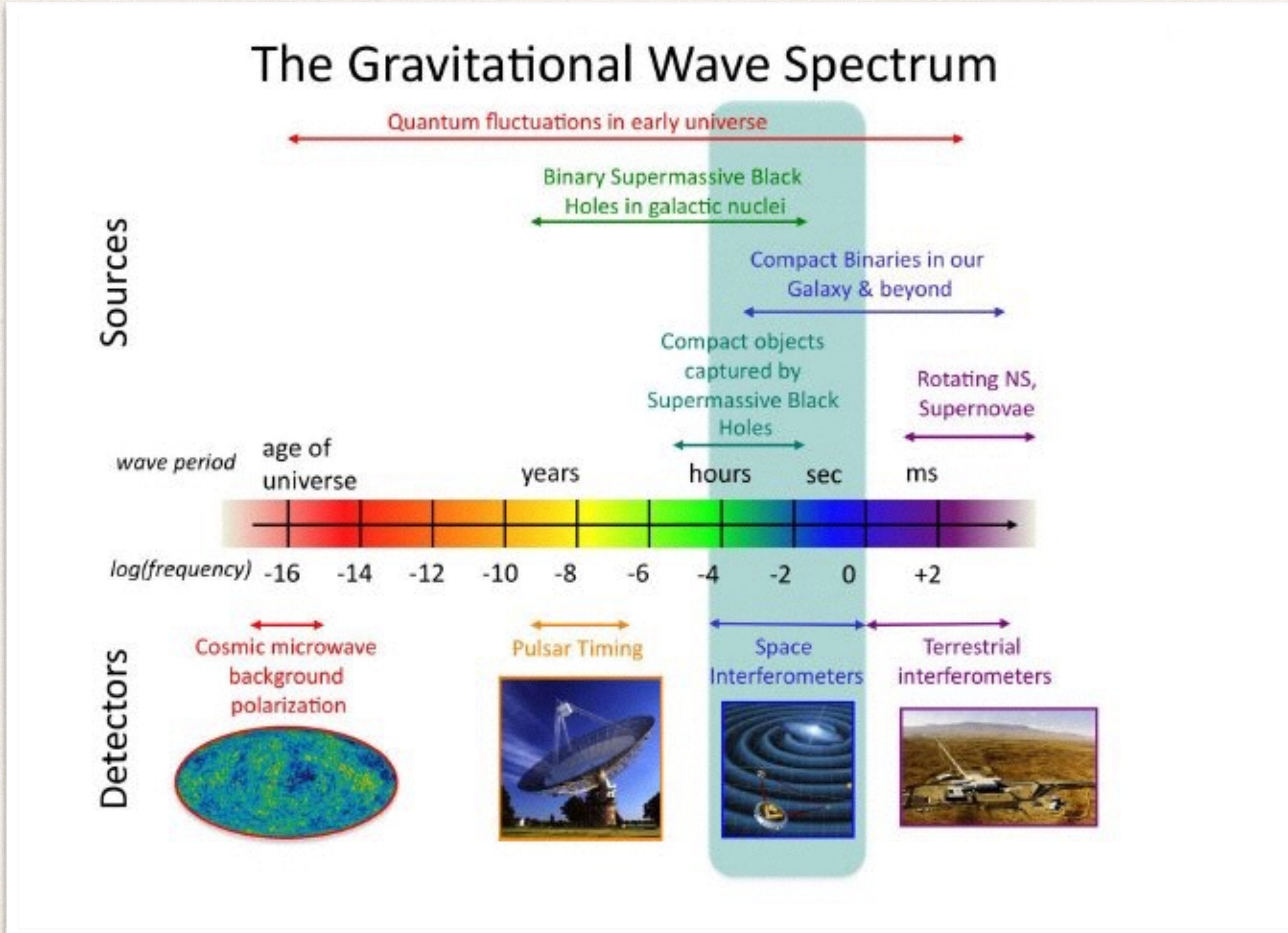
The Gravitational Wave Spectrum
Quantum fluctuations in early universe
Binary Supermassive Black Holes in galactic nuclei
Compact Binaries in our Galaxy & beyond
Compact objects captured by Supermassive Black Holes
Rotating NS, Supernovae
Sources
wave period
age of universe
years
hours
sec
ms
log(frequency)
-16
-14
-12
-10
-8
-6
-4
-2
0
+2
Detectors
Cosmic microwave background polarization
Pulsar Timing
Space Interferometers
Terrestrial interferometers

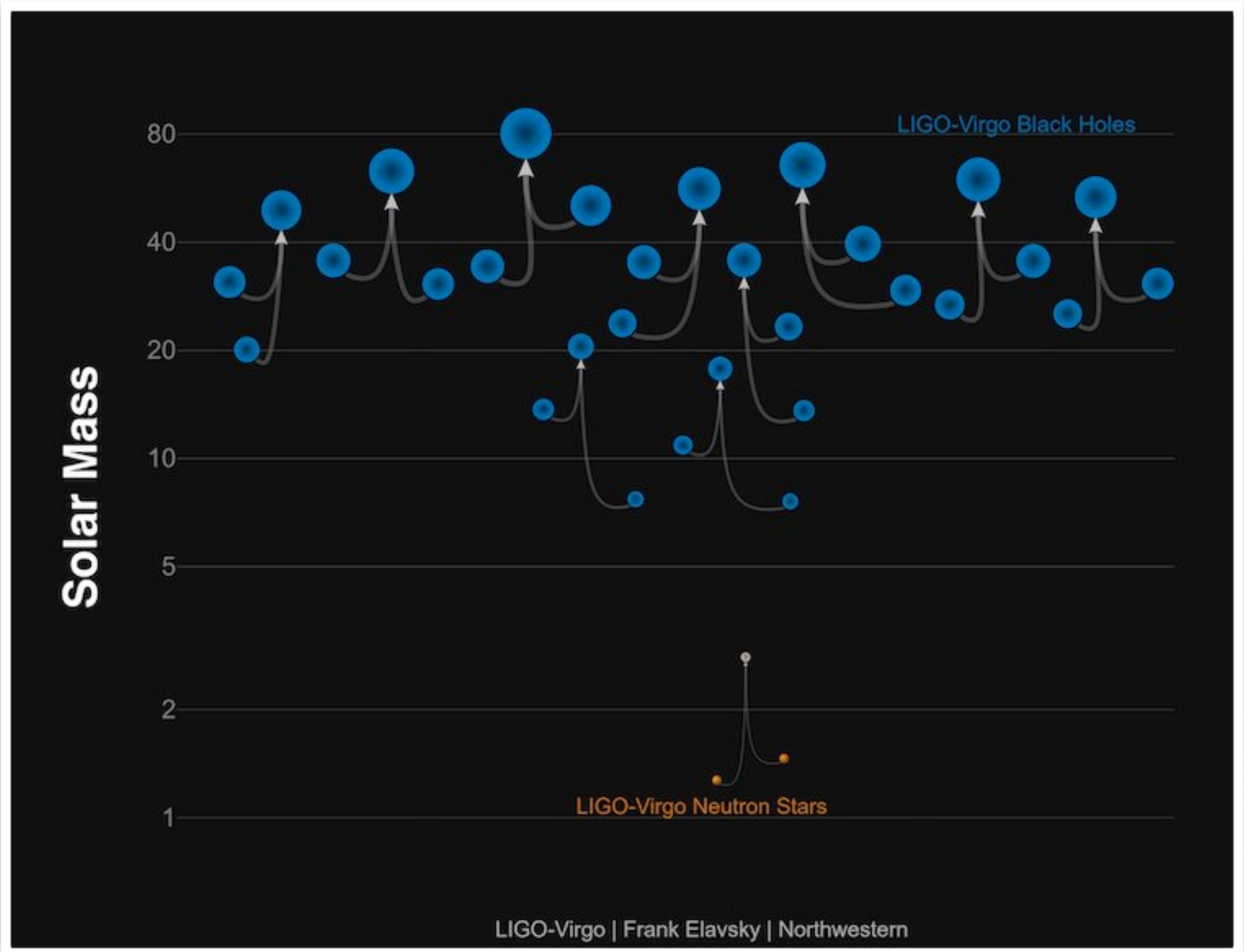

as for December 2018

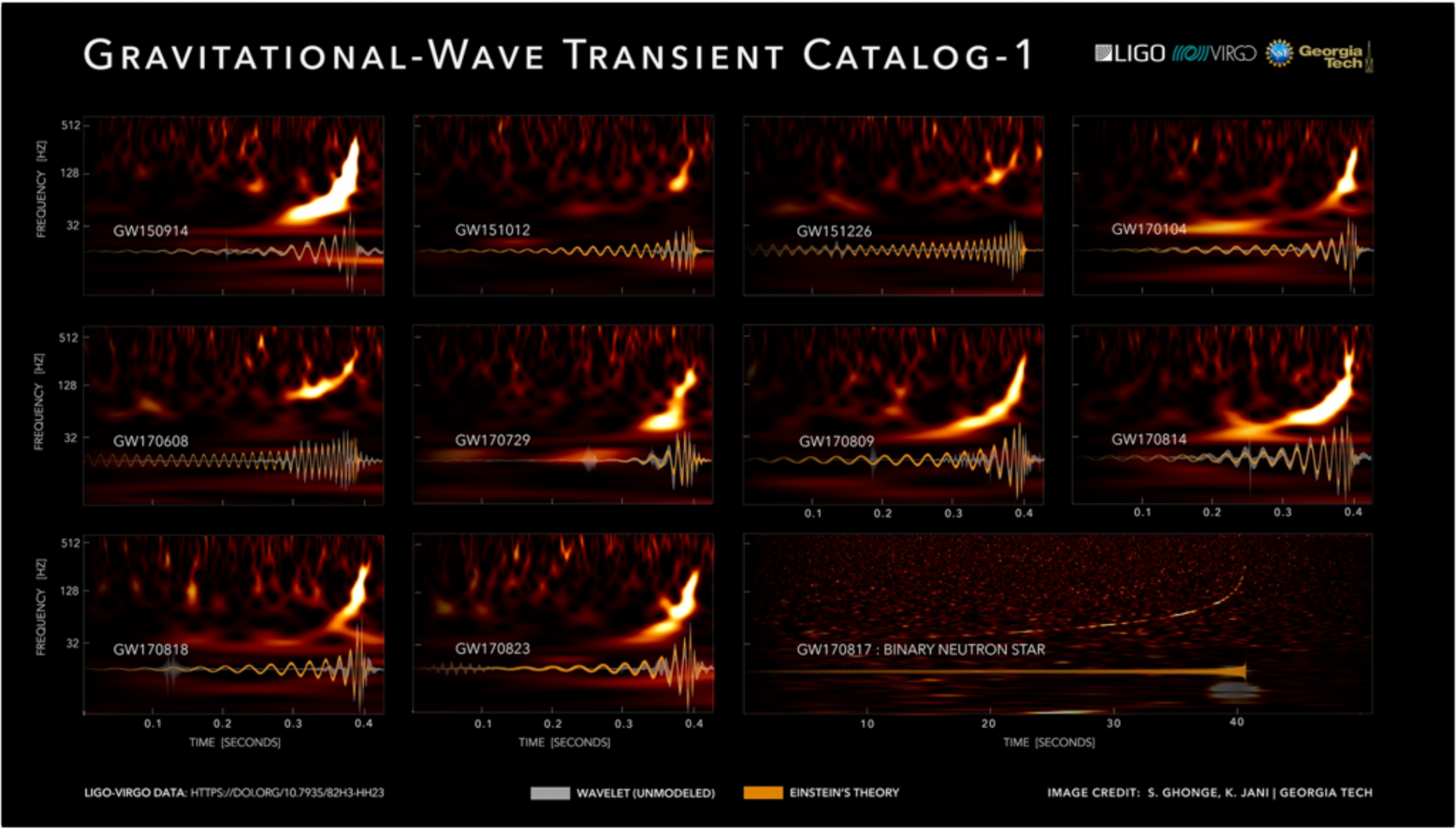
GRAVITATIONAL-WAVE TRANSIENT CATALOG-1
LIGO
VIRGO
Georgia Tech
FREQUENCY [HZ]
512
128
32
GW150914
GW151012
GW151226
GW170104
GW170608
GW170729
GW170809
GW170814
GW170818
GW170823
GW170817 : BINARY NEUTRON STAR
0.1
0.2
0.3
0.4
10
20
30
40
TIME [SECONDS]
LIGO-VIRGO DATA: HTTPS://DOI.ORG/10.7935/82H3-HH23
WAVELET (UNMODELED)
EINSTEIN'S THEORY
IMAGE CREDIT: S. GHONGE, K. JANI | GEORGIA TECH